

PUBLISHED VERSION

G. Aad ... P. Jackson ... L. Lee ... A. Petridis ... N. Soni ... M. J. White ... et al. (ATLAS Collaboration)
Search for charged Higgs bosons decaying via $H_{\pm} \rightarrow \tau \nu$ in $t\bar{t}$ events using pp collision data at $\sqrt{s} = 7\text{TeV}$ with the ATLAS detector
Journal of High Energy Physics, 2012; 2012(6):039-0-039-49

Copyright CERN, for the benefit of the ATLAS collaboration. This article is distributed under the terms of the Creative Commons Attribution License which permits any use, distribution and reproduction in any medium, provided the original author(s) and source are credited

Originally published at:

[http://doi.org/10.1007/JHEP06\(2012\)039](http://doi.org/10.1007/JHEP06(2012)039)

PERMISSIONS

<http://creativecommons.org/licenses/by/4.0/>



Attribution 4.0 International (CC BY 4.0)

This is a human-readable summary of (and not a substitute for) the [license](#).

[Disclaimer](#)



You are free to:

Share — copy and redistribute the material in any medium or format

Adapt — remix, transform, and build upon the material

for any purpose, even commercially.

The licensor cannot revoke these freedoms as long as you follow the license terms.

Under the following terms:



Attribution — You must give **appropriate credit**, provide a link to the license, and **indicate if changes were made**. You may do so in any reasonable manner, but not in any way that suggests the licensor endorses you or your use.

No additional restrictions — You may not apply legal terms or **technological measures** that legally restrict others from doing anything the license permits.

28 November 2016

<http://hdl.handle.net/2440/101804>

Search for charged Higgs bosons decaying via $H^\pm \rightarrow \tau\nu$ in $t\bar{t}$ events using pp collision data at $\sqrt{s} = 7$ TeV with the ATLAS detector

The ATLAS collaboration

E-mail: atlas.publications@cern.ch

ABSTRACT: The results of a search for charged Higgs bosons are presented. The analysis is based on 4.6 fb^{-1} of proton-proton collision data at $\sqrt{s} = 7$ TeV collected by the ATLAS experiment at the Large Hadron Collider, using top quark pair events with a τ lepton in the final state. The data are consistent with the expected background from Standard Model processes. Assuming that the branching ratio of the charged Higgs boson to a τ lepton and a neutrino is 100%, this leads to upper limits on the branching ratio of top quark decays to a b quark and a charged Higgs boson between 5% and 1% for charged Higgs boson masses ranging from 90 GeV to 160 GeV, respectively. In the context of the m_h^{max} scenario of the MSSM, $\tan\beta$ above 12–26, as well as between 1 and 2–6, can be excluded for charged Higgs boson masses between 90 GeV and 150 GeV.

KEYWORDS: Hadron-Hadron Scattering

Contents

1	Introduction	2
2	Data and simulated events	3
3	Physics object reconstruction	5
3.1	Electrons	5
3.2	Muons	5
3.3	Jets	5
3.4	τ jets	6
3.5	Removal of geometric overlaps between objects	6
3.6	Missing transverse momentum	6
4	Analysis of the lepton+jets channel	6
4.1	Event selection	7
4.2	Data-driven estimation of backgrounds with misidentified leptons	7
4.3	Reconstruction of discriminating variables after the selection cuts	8
5	Analysis of the τ+lepton channel	11
5.1	Event selection	11
5.2	Data-driven estimation of backgrounds with misidentified leptons	11
5.3	Backgrounds with electrons and jets misidentified as τ jets	11
5.4	Event yields and E_T^{miss} distribution after the selection cuts	12
6	Analysis of the τ+jets channel	13
6.1	Event selection	14
6.2	Data-driven estimation of the multi-jet background	15
6.3	Backgrounds with electrons and jets misidentified as τ jets	15
6.4	Data-driven estimation of backgrounds with correctly reconstructed τ jets	15
6.5	Event yields and m_T distribution after the selection cuts	17
7	Systematic uncertainties	19
7.1	Systematic uncertainties arising from the detector simulation	19
7.2	Systematic uncertainties arising from the generation of $t\bar{t}$ events	19
7.3	Systematic uncertainties arising from data-driven background estimates	19
8	Results	22
9	Conclusions	22
	The ATLAS collaboration	29

1 Introduction

Charged Higgs bosons (H^+ , H^-) are predicted by several non-minimal Higgs scenarios, such as Two Higgs Doublet Models (2HDM) [1] or models containing Higgs triplets [2–6]. As the Standard Model (SM) does not contain any elementary charged scalar particle, the observation of a charged Higgs boson¹ would clearly indicate new physics beyond the SM. For instance, supersymmetric models predict the existence of charged Higgs bosons. In a type-II 2HDM, such as the Higgs sector of the Minimal Supersymmetric extension of the Standard Model (MSSM) [7–11], the main H^+ production mode at the Large Hadron Collider (LHC) is through top quark decays $t \rightarrow bH^+$, for charged Higgs boson masses (m_{H^+}) smaller than the top quark mass (m_{top}). The dominant source of top quarks at the LHC is through $t\bar{t}$ production. The cross section for H^+ production from single top quark events is much smaller and is not considered here. For $\tan\beta > 2$, where $\tan\beta$ is the ratio of the vacuum expectation values of the two Higgs doublets, the charged Higgs boson decay via $H^+ \rightarrow \tau\nu$ is dominant and remains sizeable for $1 < \tan\beta < 2$ [12]. In this paper, $\mathcal{B}(H^+ \rightarrow \tau\nu) = 100\%$ is assumed, unless otherwise specified. Under this assumption, the combined LEP lower limit for the charged Higgs boson mass is about 90 GeV [13]. The Tevatron experiments placed upper limits on $\mathcal{B}(t \rightarrow bH^+)$ in the 15–20% range for $m_{H^+} < m_{\text{top}}$ [14, 15].

This paper describes a search for charged Higgs bosons with masses in the range 90–160 GeV, using $t\bar{t}$ events with a leptonically or hadronically decaying τ lepton in the final state, i.e. with the topology shown in figure 1. Charged Higgs bosons are searched for in a model-independent way, hence exclusion limits are given in terms of $\mathcal{B}(t \rightarrow bH^+)$, as well as in the m_h^{max} scenario [16] of the MSSM. The results are based on 4.6 fb^{-1} of data from pp collisions at $\sqrt{s} = 7 \text{ TeV}$, collected in 2011 with the ATLAS experiment [17] at the LHC. Three final states, which are expected to yield the highest sensitivity, are analysed:

- lepton+jets: $t\bar{t} \rightarrow b\bar{b}WH^+ \rightarrow b\bar{b}(q\bar{q}')(\tau_{\text{lep}}\nu)$, i.e. W decays hadronically and τ decays into an electron or a muon, with two neutrinos;
- τ +lepton: $t\bar{t} \rightarrow b\bar{b}WH^+ \rightarrow b\bar{b}(l\nu)(\tau_{\text{had}}\nu)$, i.e. W decays leptonically (with $l = e, \mu$) and τ decays hadronically;
- τ +jets: $t\bar{t} \rightarrow b\bar{b}WH^+ \rightarrow b\bar{b}(q\bar{q}')(\tau_{\text{had}}\nu)$, i.e. both W and τ decay hadronically.

In section 2, the data and simulated samples used in this analysis are described. In section 3, the reconstruction of physics objects in ATLAS is discussed. Sections 4–6 present results obtained in the lepton+jets, τ +lepton and τ +jets channels, respectively. Systematic uncertainties are discussed in section 7, before exclusion limits in terms of $\mathcal{B}(t \rightarrow bH^+)$ and $\tan\beta$ are presented in section 8. Finally, a summary is given in section 9.

¹In the following, charged Higgs bosons are denoted H^+ , with the charge-conjugate H^- always implied. Hence, τ denotes a positively charged τ lepton.

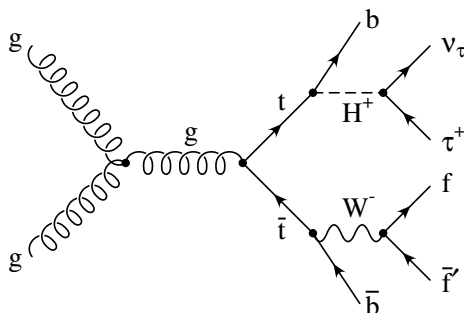


Figure 1. Example of a leading-order Feynman diagram for the production of $t\bar{t}$ events arising from gluon fusion, where a top quark decays to a charged Higgs boson, followed by the decay $H^+ \rightarrow \tau\nu$.

2 Data and simulated events

The ATLAS detector [17] consists of an inner tracking detector with a coverage in pseudorapidity² up to $|\eta| = 2.5$, surrounded by a thin 2 T superconducting solenoid, a calorimeter system extending up to $|\eta| = 4.9$ for the detection of electrons, photons and hadronic jets, and a large muon spectrometer extending up to $|\eta| = 2.7$ that measures the deflection of muon tracks in the field of three superconducting toroid magnets. A three-level trigger system is used. The first level trigger is implemented in hardware, using a subset of detector information to reduce the event rate to a design value of at most 75 kHz. This is followed by two software-based trigger levels, which together reduce the event rate to about 300 Hz.

Only data taken with all ATLAS sub-systems operational are used; this results in an integrated luminosity of 4.6 fb^{-1} for the 2011 data-taking period. The integrated luminosity has an uncertainty of 3.9%, measured as described in refs. [18, 19] and based on the whole 2011 dataset. Following basic data quality checks, further event cleaning is performed by demanding that no jet is consistent with having originated from instrumental effects, such as large noise signals in one or several channels of the hadronic end-cap calorimeter, coherent noise in the electromagnetic calorimeter, or non-collision backgrounds. In addition, events are discarded if the reconstructed vertex with the largest sum of squared track momenta has fewer than five associated tracks with transverse momenta $p_T > 400 \text{ MeV}$.

The background processes that enter this search include the SM pair production of top quarks $t\bar{t} \rightarrow b\bar{b}W^+W^-$, as well as the production of single top quark, W +jets, Z/γ^* +jets, diboson and multi-jet events. Data-driven methods are used in order to estimate the multi-jet background, as well as the backgrounds with intrinsic missing transverse momentum where electrons or jets are misidentified as hadronically decaying τ leptons. The modelling of SM $t\bar{t}$ and single top quark events is performed with MC@NLO [20], except for the

²ATLAS uses a right-handed coordinate system with its origin at the nominal interaction point (IP) in the centre of the detector and the z -axis along the beam pipe. The x -axis points from the IP to the centre of the LHC ring, and the y -axis points upwards. Cylindrical coordinates (r, ϕ) are used in the transverse plane, ϕ being the azimuthal angle around the beam pipe. The pseudorapidity is defined in terms of the polar angle θ as $\eta = -\ln \tan(\theta/2)$.

Process	Generator	Cross section [pb]	
SM $t\bar{t}$ with at least one lepton $\ell = e, \mu, \tau$	MC@NLO [20]	91	[26]
Single top quark t -channel (with ℓ)	AcerMC [21]	21	[27]
Single top quark s -channel (with ℓ)	MC@NLO [20]	1.5	[28]
Single top quark Wt -channel (inclusive)	MC@NLO [20]	16	[29]
$W \rightarrow \ell\nu$	ALPGEN [31]	3.1×10^4	[33]
$Z/\gamma^* \rightarrow \ell\ell$ with $m(\ell\ell) > 10$ GeV	ALPGEN [31]	1.5×10^4	[34]
WW	HERWIG [23]	17	[35]
ZZ	HERWIG [23]	1.3	[35]
WZ	HERWIG [23]	5.5	[35]
H^+ signal with $\mathcal{B}(t \rightarrow bH^+) = 5\%$	PYTHIA [25]	16	

Table 1. Cross sections for the simulated processes and generators used to model them.

t -channel single top quark production where AcerMC [21] is used. The top quark mass is set to 172.5 GeV and the set of parton distribution functions used is CT10 [22]. For the events generated with MC@NLO, the parton shower, hadronisation and underlying event are added using HERWIG [23] and JIMMY [24]. PYTHIA [25] is instead used for events generated with AcerMC. Inclusive cross sections are taken from the approximate next-to-next-to-leading-order (NNLO) predictions for $t\bar{t}$ production [26], for single top quark production in the t -channel and s -channel [27, 28], as well as for Wt production [29]. Overlaps between Wt and SM $t\bar{t}$ final states are removed [30]. Single vector boson (W and Z/γ^*) production is simulated with ALPGEN [31] interfaced to HERWIG and JIMMY, using CTEQ6.1 [32] parton distribution functions. The additional partons produced in the matrix element part of the event generation can be light partons or heavy quarks. In the latter case, dedicated samples with matrix elements for the production of massive $b\bar{b}$ or $c\bar{c}$ pairs are used. Diboson events (WW , WZ and ZZ) are generated using HERWIG. The cross sections are normalised to NNLO predictions for W and Z/γ^* production [33, 34] and to next-to-leading-order (NLO) predictions for diboson production [35].

The SM background samples are summarised in table 1. In addition, three types of signal samples are produced with PYTHIA for $90 \text{ GeV} < m_{H^+} < 160 \text{ GeV}$: $t\bar{t} \rightarrow b\bar{b}H^+W^-$, $t\bar{t} \rightarrow b\bar{b}H^-W^+$ and $t\bar{t} \rightarrow b\bar{b}H^+H^-$, where the charged Higgs bosons decay as $H^+ \rightarrow \tau\nu$. The cross section for each of these three processes depends only on the total $t\bar{t}$ production cross section (167 pb) and the branching ratio $\mathcal{B}(t \rightarrow bH^+)$. TAUOLA [36] is used for τ decays, and PHOTOS [37] is used for photon radiation from charged leptons.

The event generators are tuned in order to describe the ATLAS data. The parameter sets AUET2 [38] and AUET2B [39] are used for events for which hadronisation is simulated using HERWIG/JIMMY and PYTHIA, respectively. To take into account the presence of multiple interactions (around nine, on average) occurring in the same and neighbouring

bunch crossings (referred to as pile-up), simulated minimum bias events are added to the hard process in each generated event. Prior to the analysis, simulated events are reweighted in order to match the distribution of the average number of pile-up interactions in the data. All generated events are propagated through a detailed GEANT4 simulation [40, 41] of the ATLAS detector and are reconstructed with the same algorithms as the data.

3 Physics object reconstruction

3.1 Electrons

Electrons are reconstructed by matching clustered energy deposits in the electromagnetic calorimeter to tracks reconstructed in the inner detector. The electron candidates are required to meet quality requirements based on the expected shower shape [42], to have a transverse energy $E_T > 20$ GeV and to be in the fiducial volume of the detector, $|\eta| < 2.47$ (the transition region between the barrel and end-cap calorimeters, $1.37 < |\eta| < 1.52$, is excluded). Additionally, E_T and η -dependent calorimeter (tracking) isolation requirements are imposed in a cone with a radius³ $\Delta R = 0.2$ (0.3) around the electron position, excluding the electron object itself, with an efficiency of about 90% for true isolated electrons.

3.2 Muons

Muon candidates are required to contain matching inner detector and muon spectrometer tracks [43], as well as to have $p_T > 15$ GeV and $|\eta| < 2.5$. Only isolated muons are accepted by requiring that the transverse energy deposited in the calorimeters (the transverse momentum of the inner detector tracks) in a cone of radius $\Delta R = 0.2$ (0.3) around the muon amounts to less than 4 GeV (2.5 GeV). The energy and momentum of the muon are excluded from the cone when applying these isolation requirements.

3.3 Jets

Jets are reconstructed using the anti- k_t algorithm [44, 45] with a size parameter value of $R = 0.4$. The jet finder uses reconstructed three-dimensional, noise-suppressed clusters of calorimeter cells [46]. Jets are calibrated to the hadronic energy scale with correction factors based on simulation [47, 48]. A method that allows for the identification and selection of jets originating from the hard-scatter interaction through the use of tracking and vertexing information is used [49]. This is referred to as the “Jet Vertex Fraction” (JVF), defined as the fraction of the total momentum of the charged particle tracks associated to the jet which belongs to tracks that are also compatible with the primary vertex. By convention, jets with no associated tracks are assigned a JVF value of -1 in order to keep a high efficiency for jets at large values of η , outside the range of the inner tracking detectors. The jet selection based on this discriminant is shown to be insensitive to pile-up. A requirement of $|\text{JVF}| > 0.75$ is placed on all jets during event selection. In order to identify the jets initiated by b quarks, an algorithm is used that combines impact-parameter information

³ $\Delta R = \sqrt{(\Delta\eta)^2 + (\Delta\phi)^2}$, where $\Delta\eta$ is the difference in pseudorapidity of the two objects in question, and $\Delta\phi$ is the difference between their azimuthal angles.

with the explicit determination of a secondary vertex [50]. A working point is chosen that corresponds to an average efficiency of about 70% for b jets with $p_T > 20$ GeV in $t\bar{t}$ events and a light-quark jet rejection factor of about 130. Since the b -tagger relies on the inner tracking detectors, the acceptance region for jets is restricted to $|\eta| < 2.4$.

3.4 τ jets

In order to reconstruct hadronically decaying τ leptons, anti- k_t jets with either one or three associated tracks reconstructed in the inner detector and depositing $E_T > 10$ GeV in the calorimeter are considered as τ candidates [51]. Dedicated algorithms are used in order to reject electrons and muons. Hadronic τ decays are identified using a likelihood criterion designed to discriminate against quark- and gluon-initiated jets by using the shower shape and tracking variables as inputs. A working point with an efficiency of about 30% for hadronically decaying τ leptons with $p_T > 20$ GeV in $Z \rightarrow \tau\tau$ events is chosen, leading to a rejection factor of about 100–1000 for jets. The rejection factor depends on the p_T and η of the candidate and the number of associated tracks. The τ candidates are further required to have a visible transverse momentum of at least 20 GeV and to be within $|\eta| < 2.3$. The selected τ candidates are henceforth referred to as “ τ jets”.

3.5 Removal of geometric overlaps between objects

When candidates selected using the criteria above overlap geometrically, the following procedures are applied, in this order: muon candidates are rejected if they are found within $\Delta R < 0.4$ of any jet with $p_T > 25$ GeV; a τ jet is rejected if found within $\Delta R < 0.2$ of a selected muon or electron; jets are removed if they are within $\Delta R < 0.2$ of a selected τ object or electron.

3.6 Missing transverse momentum

The missing transverse momentum and its magnitude E_T^{miss} [52] are reconstructed from three-dimensional, noise-suppressed clusters of cells in the calorimeter and from muon tracks reconstructed in the muon spectrometer and the inner tracking detectors. Clusters of calorimeter cells belonging to jets (including τ jets) with $p_T > 20$ GeV are calibrated to the hadronic energy scale. Calorimeter cells not associated with any object are also taken into account and they are calibrated at the electromagnetic energy scale. In order to deal appropriately with the energy deposited by muons in the calorimeters, the contributions of muons to E_T^{miss} are calculated differently for isolated and non-isolated muons.

4 Analysis of the lepton+jets channel

This analysis relies on the detection of lepton+jets decays of $t\bar{t}$ events, where the charged lepton l (electron or muon) arises from $H^+ \rightarrow \tau_{\text{lep}}\nu$, while the jets arise from a hadronically decaying W boson, i.e. $t\bar{t} \rightarrow b\bar{b}WH^+ \rightarrow b\bar{b}(q\bar{q}')(\tau_{\text{lep}}\nu)$.

4.1 Event selection

The lepton+jets analysis uses events passing a single-lepton trigger with an E_T threshold of 20–22 GeV for electrons⁴ and a p_T threshold of 18 GeV for muons. These thresholds are low enough to guarantee that electrons and muons chosen for the analysis are in the plateau region of the trigger-efficiency curve. In addition, to select a sample of lepton+jets events enriched in $t\bar{t}$ candidates, the following requirements are applied:

- exactly one lepton having $E_T > 25$ GeV (electron) or $p_T > 20$ GeV (muon) and matched to the corresponding trigger object, with neither a second lepton nor a τ jet in the event;
- at least four jets having $p_T > 20$ GeV, with exactly two of them being b -tagged;
- $E_T^{\text{miss}} > 40$ GeV and, in order to discriminate between E_T^{miss} arising from isolated neutrinos and from poorly reconstructed leptons, this requirement is tightened to $E_T^{\text{miss}} \times |\sin \Delta\phi_{l,\text{miss}}| > 20$ GeV if the azimuthal angle $\Delta\phi_{l,\text{miss}}$ between the lepton and E_T^{miss} is smaller than $\pi/6$.

Having selected a lepton+jets sample enriched in $t\bar{t}$ candidates, jets must be assigned correctly to the decay products of each W boson (with a mass $m_W = 80.4$ GeV) and top quark. In particular, the hadronic side of the event is identified by selecting the combination of one b -tagged jet (b) and two untagged jets (j) that minimises:

$$\chi^2 = \frac{(m_{jbb} - m_{\text{top}})^2}{\sigma_{\text{top}}^2} + \frac{(m_{jj} - m_W)^2}{\sigma_W^2}, \quad (4.1)$$

where $\sigma_{\text{top}} = 17$ GeV and $\sigma_W = 10$ GeV are the widths of the reconstructed top quark and W boson mass distributions, as measured in simulated $t\bar{t}$ events. Using information about the correctly identified combinations in the generated events, the jet assignment efficiency is found to be 72%. Events with $\chi^2 > 5$ are rejected in order to select well-reconstructed hadronic top quark candidates.

4.2 Data-driven estimation of backgrounds with misidentified leptons

While the ATLAS lepton identification gives a very pure sample of candidates, there is a non-negligible contribution from non-isolated leptons arising from the semileptonic decay of hadrons containing b or c quarks, from the decay-in-flight of π^\pm or K mesons and, in the case of misidentified electron objects, from the reconstruction of π^0 mesons, photon conversions or shower fluctuations. All leptons coming from such mechanisms are referred to as *misidentified* leptons, as opposed to truly isolated leptons (e.g. from the prompt decay of W or Z bosons), which are referred to as *real* leptons. The data-driven estimation of the number of misidentified leptons passing the lepton selections of sections 3.1 and 3.2 is based on exploiting differences in the lepton identification between real and misidentified

⁴The electron trigger threshold was increased from 20 GeV to 22 GeV towards the end of data-taking in 2011.

electrons or muons. Two data samples are defined, which differ only in the lepton identification criteria. The *tight* sample contains mostly events with real leptons and uses the same lepton selection as in the analysis. The *loose* sample contains mostly events with misidentified leptons. This latter sample is obtained by loosening the isolation and identification requirements for the leptons. For loose electrons, the isolation requirements have an efficiency of about 98% for true isolated electrons, compared to 90% in the tight sample. For loose muons, the isolation requirement is removed. By construction, the tight sample is therefore a subset of the loose sample.

Let N_r^L and N_m^L (N_r^T and N_m^T) be the number of events containing real and misidentified leptons, respectively, passing a loose (tight) selection. The numbers of events containing one loose or tight lepton are given by:

$$N^L = N_m^L + N_r^L, \tag{4.2}$$

$$N^T = N_m^T + N_r^T. \tag{4.3}$$

Defining p_r and p_m as:

$$p_r = \frac{N_r^T}{N_r^L} \quad \text{and} \quad p_m = \frac{N_m^T}{N_m^L}, \tag{4.4}$$

the number of misidentified leptons passing the tight selection N_m^T can then be written as:

$$N_m^T = \frac{p_m}{p_r - p_m} (p_r N^L - N^T). \tag{4.5}$$

The main ingredients of this data-driven method are thus the relative efficiencies p_r and p_m for a real or a misidentified lepton, respectively, to be detected as a tight lepton. The lepton identification efficiency p_r is measured using a tag-and-probe method on $Z \rightarrow ll$ data events with a dilepton invariant mass between 86 GeV and 96 GeV, where one lepton is required to fulfill tight selection criteria. The rate at which the other lepton passes the same tight selection criteria defines p_r . The average values of the electron and muon identification efficiencies are 80% and 97%, respectively. On the other hand, a control sample with misidentified leptons is selected by considering events in the data with exactly one lepton passing the loose criteria. In order to select events dominated by multi-jet production, E_T^{miss} is required to be between 5 GeV and 20 GeV. Residual true leptons contribute at a level below 10% and are subtracted from this sample using simulation. After this subtraction, the rate at which a loose lepton passes tight selection criteria defines the misidentification rate p_m . The average values of the electron and muon misidentification probabilities are 18% and 29%, respectively. In the final parameterisation of p_r and p_m , dependencies on the pseudorapidity of the lepton, its distance ΔR to the nearest jet and the leading jet p_T are taken into account.

4.3 Reconstruction of discriminating variables after the selection cuts

The analysis uses two variables that discriminate between leptons produced in $\tau \rightarrow l\nu_l\nu_\tau$ and leptons coming directly from W boson decays. The first discriminating variable is the

invariant mass m_{bl} of the b jet and the charged lepton l coming from the same top quark candidate, or more conveniently, $\cos\theta_l^*$ defined as:

$$\cos\theta_l^* = \frac{2m_{bl}^2}{m_{\text{top}}^2 - m_W^2} - 1 \simeq \frac{4p^b \cdot p^l}{m_{\text{top}}^2 - m_W^2} - 1. \quad (4.6)$$

Both m_b^2 and m_l^2 are neglected, hence $m_{bl}^2 \simeq 2p^b \cdot p^l$, where p^b and p^l are the four-momenta of the b jet and of the charged lepton l , respectively. The presence of a charged Higgs boson in a leptonic top quark decay reduces the invariant product $p^b \cdot p^l$, when compared to W -mediated top quark decays, leading to $\cos\theta_l^*$ values closer to -1 .

The second discriminating variable is the transverse mass m_{T}^H [53], obtained by fulfilling the constraint $(p^{\text{miss}} + p^l + p^b)^2 = m_{\text{top}}^2$ on the leptonic side of lepton+jets $t\bar{t}$ events. More than one neutrino accounts for the invisible four-momentum p^{miss} and its transverse component $\vec{p}_{\text{T}}^{\text{miss}}$. By construction, m_{T}^H gives an event-by-event lower bound on the mass of the leptonically decaying charged (W or Higgs) boson produced in the top quark decay, and it can be written as:

$$(m_{\text{T}}^H)^2 = \left(\sqrt{m_{\text{top}}^2 + (\vec{p}_{\text{T}}^l + \vec{p}_{\text{T}}^b + \vec{p}_{\text{T}}^{\text{miss}})^2} - p_{\text{T}}^b \right)^2 - \left(p_{\text{T}}^l + p_{\text{T}}^{\text{miss}} \right)^2. \quad (4.7)$$

The $\cos\theta_l^*$ distribution measured in the data is shown in figure 2a, superimposed on the predicted background, determined with a data-driven method for the multi-jet background and simulation for the other SM backgrounds. In the presence of a charged Higgs boson in the top quark decays, with a branching ratio $\mathcal{B}(t \rightarrow bH^+)$, the contribution of $t\bar{t} \rightarrow b\bar{b}W^+W^-$ events in the background is scaled according to this branching ratio. A control region enriched in $t\bar{t} \rightarrow b\bar{b}W^+W^-$ events is defined by requiring $-0.2 < \cos\theta_l^* < 1$. In section 8, this sample is used to fit the branching ratio $\mathcal{B}(t \rightarrow bH^+)$ and the product of the cross section $\sigma_{b\bar{b}W^+W^-}$, the luminosity, the selection efficiency and acceptance for $t\bar{t} \rightarrow b\bar{b}W^+W^-$, simultaneously with the likelihood for the signal estimation. In turn, this ensures that the final results, and in particular the upper limit on $\mathcal{B}(t \rightarrow bH^+)$, are independent of the assumed theoretical production cross section for $t\bar{t}$. With a branching fraction $\mathcal{B}(t \rightarrow bH^+) = 5\%$, the signal contamination in the control region would range from 1.3% for $m_{H^+} = 90$ GeV to 0.4% for $m_{H^+} = 160$ GeV. The signal region is defined by requiring $\cos\theta_l^* < -0.6$ and $m_{\text{T}}^W < 60$ GeV, where:

$$m_{\text{T}}^W = \sqrt{2p_{\text{T}}^l E_{\text{T}}^{\text{miss}} (1 - \cos\Delta\phi_{l,\text{miss}})}. \quad (4.8)$$

This is done in order to suppress the background from events with a W boson decaying directly into electrons or muons. For events in the signal region, m_{T}^H , shown in figure 2b, is used as a discriminating variable to search for charged Higgs bosons. Table 2 lists the contributions to the signal region of the SM processes and of $t\bar{t}$ events with at least one decay $t \rightarrow bH^+$, assuming $m_{H^+} = 130$ GeV and $\mathcal{B}(t \rightarrow bH^+) = 5\%$. When including signal in the prediction, the simulated SM $t\bar{t}$ contribution is scaled according to this branching ratio. The data are consistent with the predicted SM background and no significant deformation of the m_{T}^H distribution is observed.

Sample	Event yield (lepton+jets)
$t\bar{t}$	840 \pm 20 \pm 150
Single top quark	28 \pm 2 $\begin{smallmatrix} +8 \\ -6 \end{smallmatrix}$
W +jets	14 \pm 3 $\begin{smallmatrix} +6 \\ -3 \end{smallmatrix}$
Z +jets	2.1 \pm 0.7 $\begin{smallmatrix} +1.2 \\ -0.4 \end{smallmatrix}$
Diboson	0.5 \pm 0.1 \pm 0.2
Misidentified leptons	55 \pm 10 \pm 20
All SM backgrounds	940 \pm 22 \pm 150
Data	933
$t \rightarrow bH^+$ (130 GeV)	120 \pm 4 \pm 25
Signal+background	990 \pm 21 \pm 140

Table 2. Expected event yields in the signal region of the lepton+jets final state, and comparison with 4.6 fb^{-1} of data. A cross section of 167 pb is assumed for the SM $t\bar{t}$ background. The numbers shown in the last two rows, for a hypothetical H^+ signal with $m_{H^+} = 130 \text{ GeV}$, are obtained with $\mathcal{B}(t \rightarrow bH^+) = 5\%$. Both statistical and systematic uncertainties are shown, in this order.

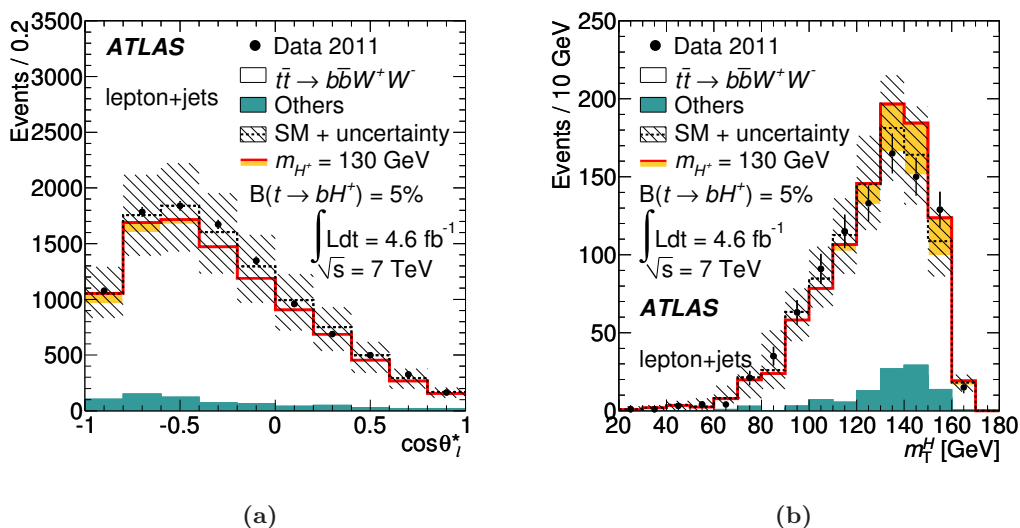


Figure 2. Distribution of (a) $\cos \theta_i^*$ and (b) m_T^H , in the signal region ($\cos \theta_i^* < -0.6$, $m_T^W < 60 \text{ GeV}$) for the latter. The dashed line corresponds to the SM-only hypothesis and the hatched area around it shows the total uncertainty for the SM backgrounds, where “Others” refers to the contribution of all SM processes except $t\bar{t} \rightarrow b\bar{b}W^+W^-$. The solid line shows the predicted contribution of signal+background in the presence of a 130 GeV charged Higgs boson, assuming $\mathcal{B}(t \rightarrow bH^+) = 5\%$ and $\mathcal{B}(H^+ \rightarrow \tau\nu) = 100\%$. The light area below the solid line corresponds to the contribution of the H^+ signal, stacked on top of the scaled $t\bar{t} \rightarrow b\bar{b}W^+W^-$ background and other SM processes.

5 Analysis of the τ +lepton channel

This analysis relies on the detection of τ +lepton decays of $t\bar{t}$ events, where the hadronically decaying τ lepton arises from $H^+ \rightarrow \tau_{\text{had}}\nu$, while an electron or muon comes from the decay of the W boson, i.e. $t\bar{t} \rightarrow b\bar{b}WH^+ \rightarrow b\bar{b}(l\nu)(\tau_{\text{had}}\nu)$.

5.1 Event selection

The τ +lepton analysis relies on the same single-lepton trigger signatures as the lepton+jets analysis presented in section 4. In order to select τ +lepton events, the following requirements are made:

- exactly one lepton, having $E_T > 25$ GeV (electron) or $p_T > 20$ GeV (muon) and matched to the corresponding trigger object, and no other electron or muon;
- exactly one τ jet having $p_T > 20$ GeV and an electric charge opposite to that of the lepton;
- at least two jets having $p_T > 20$ GeV, including at least one b -tagged jet;
- $\sum p_T > 100$ GeV in order to suppress multi-jet events, where $\sum p_T$ is the sum of the transverse momenta of all tracks associated with the primary vertex. Tracks entering the sum must pass quality cuts on the number of hits and have $p_T > 1$ GeV. As this variable is based on tracks from the primary vertex (as opposed to energy deposits in the calorimeter), it is robust against pile-up.

E_T^{miss} is used as the discriminating variable to distinguish between SM $t\bar{t}$ events and those where top quark decays are mediated by a charged Higgs boson, in which case the neutrinos are likely to carry away more energy.

5.2 Data-driven estimation of backgrounds with misidentified leptons

The estimation of the backgrounds with misidentified leptons uses the data-driven method described in section 4.2. When implementing the method, the dependence of real and misidentification rates on the b -tagged jet multiplicity are taken into account, as well as the requirement for one τ jet (instead of a τ jet veto).

5.3 Backgrounds with electrons and jets misidentified as τ jets

The background with electrons misidentified as τ jets is estimated using a $Z \rightarrow ee$ control region in the data [51], where one electron is reconstructed as a τ jet. The measured misidentification probabilities, which have an average value of 0.2%, are then applied to all simulated events in the τ +lepton analysis. Simulation studies show that this application is valid, as the misidentification probabilities for $Z \rightarrow ee$ and $t\bar{t}$ events are similar.

A data-driven method applied to a control sample enriched in W +jets events is used to measure the probability for a jet to be misidentified as a hadronically decaying τ lepton. This measured probability is used to predict the yield of background events due to jet $\rightarrow \tau$ misidentification. Like jets from the hard process in the dominant $t\bar{t}$ background, jets in the

control sample originate predominantly from quarks instead of gluons. The main difference between $t\bar{t}$ and W +jets events is the different fraction of b jets, which is smaller in W +jets events. However, the probability for a b jet to be misidentified as a τ jet is smaller than the corresponding probability for a light-quark jet, because the average track multiplicity is higher for b jets. Moreover, the visible mass measurement used in the τ identification provides further discrimination between b jets and τ jets. Differences in jet composition (e.g. the ratio of gluons to quarks) between $t\bar{t}$ and W +jets, assessed using simulation, are taken into account as systematic uncertainties. These also cover the dependence of the probability on whether a b jet or a light-quark jet is misidentified as a τ jet. Events in the control region are required to pass the same single-lepton trigger, data quality and lepton requirements as in the τ +lepton event selection. Additionally, a τ candidate and $E_T^{\text{miss}} > 40$ GeV are required, and events with b -tagged jets are vetoed. Simulated events with a true τ contribute at a level below 0.5% and are subtracted. The τ candidates are required to have $p_T > 20$ GeV, $|\eta| < 2.3$, and cannot be within $\Delta R = 0.2$ of any electron or muon. They are also not required to pass τ identification. The jet $\rightarrow \tau$ misidentification probability is defined as the number of objects passing the full τ identification divided by the number prior to requiring identification. This misidentification probability is evaluated separately for τ candidates with one or three associated tracks (the corresponding average values are about 7% and 2%, respectively) and, in addition, it is measured as a function of both p_T and η .

In order to predict the background for the charged Higgs boson search, the measured jet $\rightarrow \tau$ misidentification probability is applied to simulated $t\bar{t}$, single top quark, W +jets, Z/γ^* +jets and diboson events, all of which are required to pass the full event selection except for the τ identification. For these events, τ candidates not overlapping with a true τ lepton or a true electron, but otherwise fulfilling the same requirements as in the denominator of the misidentification probability, are identified. Each of them is considered separately to be potentially misidentified as a τ jet. In order to avoid counting the same object twice, each jet that corresponds to a τ candidate is removed from the event. The number of reconstructed jets and the number of b -tagged jets are adjusted accordingly. If, after taking this into consideration, the event passes the τ +lepton selection, it is counted as a background event with a weight given by the misidentification probability corresponding to the p_T and η of the τ candidate. The predicted numbers of events from this data-driven method and from simulation are shown in table 3. The backgrounds arising from the jet $\rightarrow \tau$ misidentification are not well modelled in simulation, which is why they are estimated using data-driven methods.

5.4 Event yields and E_T^{miss} distribution after the selection cuts

Table 4 shows the expected number of background events for the SM-only hypothesis and the observation in the data. The total number of predicted events (signal+background) in the presence of a 130 GeV charged Higgs boson with $\mathcal{B}(t \rightarrow bH^+) = 5\%$ is also shown. The τ +lepton analysis relies on the theoretical $t\bar{t}$ production cross section $\sigma_{t\bar{t}} = 167_{-18}^{+17}$ pb [26] for the background estimation. In the presence of a charged Higgs boson in the top quark decays, with a branching ratio $\mathcal{B}(t \rightarrow bH^+)$, the contributions of $t\bar{t} \rightarrow b\bar{b}W^+W^-$ events in the backgrounds with true or misidentified τ jets are scaled according to this branching

Sample	Data-driven method [events]	Simulation [events]
$t\bar{t}$	900 ± 15	877 ± 6
W +jets	150 ± 3	145 ± 9
Single top quark	81 ± 1	61 ± 2
Z/γ^* +jets	44 ± 1	69 ± 4
Diboson	6 ± 1	8 ± 1

Table 3. Application of the misidentification probability obtained from W +jets events in the data, for the τ +lepton channel. The predictions of the background contributions based on data-driven misidentification probabilities and on simulation are given, with statistical uncertainties only. In both cases, all top quarks are assumed to decay via $t \rightarrow bW$.

Sample	Event yield (τ +lepton)	
	$\tau + e$	$\tau + \mu$
True τ +lepton	$430 \pm 14 \pm 59$	$570 \pm 15 \pm 75$
Misidentified jet $\rightarrow \tau$	$510 \pm 23 \pm 86$	$660 \pm 26 \pm 110$
Misidentified $e \rightarrow \tau$	$33 \pm 4 \pm 5$	$34 \pm 4 \pm 6$
Misidentified leptons	$39 \pm 10 \pm 20$	$90 \pm 10 \pm 34$
All SM backgrounds	$1010 \pm 30 \pm 110$	$1360 \pm 30 \pm 140$
Data	880	1219
$t \rightarrow bH^+$ (130 GeV)	$220 \pm 6 \pm 29$	$310 \pm 7 \pm 39$
Signal+background	$1160 \pm 30 \pm 100$	$1570 \pm 30 \pm 130$

Table 4. Expected event yields after all selection cuts in the τ +lepton channel and comparison with 4.6 fb^{-1} of data. The numbers in the last two rows, obtained for a hypothetical H^+ signal with $m_{H^+} = 130 \text{ GeV}$, are obtained with $\mathcal{B}(t \rightarrow bH^+) = 5\%$. All other rows assume $\mathcal{B}(t \rightarrow bW) = 100\%$. Both statistical and systematic uncertainties are shown, in this order.

ratio. The background with correctly reconstructed τ jets is obtained with simulation. The data are found to be consistent with the expectation for the background-only hypothesis. The E_T^{miss} distributions for the $\tau + e$ and $\tau + \mu$ channels, after all selection cuts are applied, are shown in figure 3.

6 Analysis of the τ +jets channel

The analysis presented here relies on the detection of τ +jets decays of $t\bar{t}$ events, where the hadronically decaying τ lepton arises from $H^+ \rightarrow \tau_{\text{had}}\nu$, while the jets come from a hadronically decaying W boson, i.e. $t\bar{t} \rightarrow b\bar{b}WH^+ \rightarrow b\bar{b}(q\bar{q}')(\tau_{\text{had}}\nu)$.

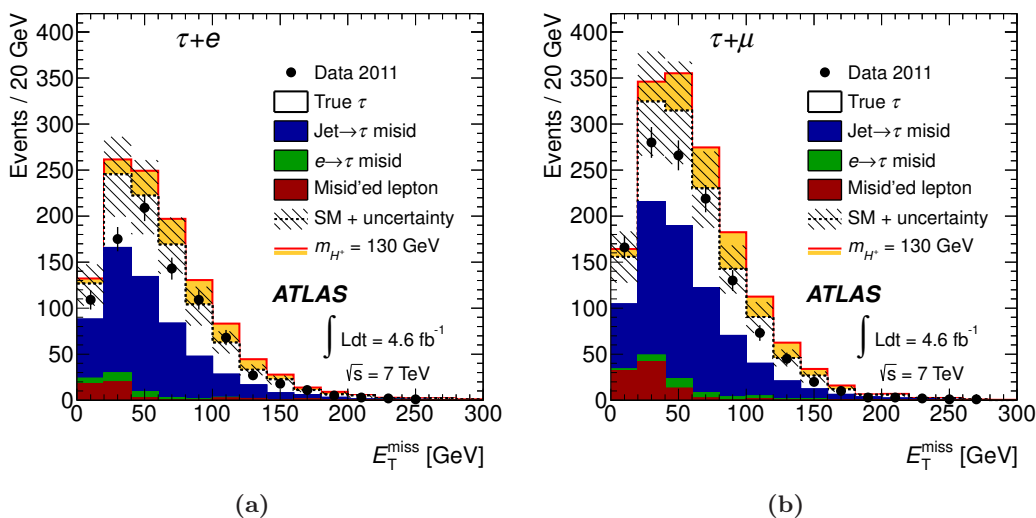


Figure 3. E_T^{miss} distribution after all selection cuts in the τ +lepton channel, for (a) τ +electron and (b) τ +muon final states. The dashed line corresponds to the SM-only hypothesis and the hatched area around it shows the total uncertainty for the SM backgrounds. The solid line shows the predicted contribution of signal+background in the presence of a 130 GeV charged Higgs boson with $\mathcal{B}(t \rightarrow bH^+) = 5\%$ and $\mathcal{B}(H^+ \rightarrow \tau\nu) = 100\%$. The contributions of $t\bar{t} \rightarrow b\bar{b}W^+W^-$ events in the backgrounds with true or misidentified τ jets are scaled down accordingly.

6.1 Event selection

The τ +jets analysis uses events passing a $\tau + E_T^{\text{miss}}$ trigger with a threshold of 29 GeV on the τ object and 35 GeV on calorimeter-based E_T^{miss} . The following requirements are applied, in this order:

- at least four jets (excluding τ jets) having $p_T > 20$ GeV, of which at least one is b -tagged;
- exactly one τ jet with $p_T^\tau > 40$ GeV, found within $|\eta| < 2.3$ and matched to a τ trigger object;
- neither a second τ jet with $p_T^\tau > 20$ GeV, nor any electrons with $E_T > 20$ GeV, nor any muons with $p_T > 15$ GeV;
- $E_T^{\text{miss}} > 65$ GeV;
- to reject events in which a large reconstructed E_T^{miss} is due to the limited resolution of the energy measurement, the following ratio based on the $\sum p_T$ definition of section 5 must satisfy:

$$\frac{E_T^{\text{miss}}}{0.5 \text{ GeV}^{1/2} \cdot \sqrt{\sum p_T}} > 13;$$

- a topology consistent with a top quark decay: the combination of one b -tagged jet (b) and two untagged jets (j) with the highest p_T^{jjb} must satisfy $m_{jjb} \in [120, 240]$ GeV.

For the selected events, the transverse mass m_T is defined as:

$$m_T = \sqrt{2p_T^\tau E_T^{\text{miss}}(1 - \cos \Delta\phi_{\tau, \text{miss}})}, \quad (6.1)$$

where $\Delta\phi_{\tau, \text{miss}}$ is the azimuthal angle between the τ jet and the direction of the missing momentum. This discriminating variable is related to the W boson mass in the $W \rightarrow \tau\nu$ background case and to the H^+ mass for the signal hypothesis.

6.2 Data-driven estimation of the multi-jet background

The multi-jet background is estimated by fitting its E_T^{miss} shape (and the E_T^{miss} shape of other backgrounds) to data. In order to study this shape in a data-driven way, a control region is defined where the τ identification and b -tagging requirements are modified, i.e. τ candidates must pass a loose τ identification but fail the tight τ identification used in the signal selection, and the event is required not to contain any b -tagged jet. Hence, the requirement on $m_{j\bar{j}b}$ is also removed. Assuming that the shapes of the E_T^{miss} and m_T distributions are the same in the control and signal regions, the E_T^{miss} shape for the multi-jet background is measured in the control region, after subtracting the simulated background contributions from other processes. These other processes amount to less than 1% of the observed events in the control region. The E_T^{miss} shapes obtained with the τ +jets selection of section 6.1 or in the control region are compared just before the E_T^{miss} requirement in the baseline selection in figure 4a. The differences between the two distributions are accounted for as systematic uncertainties. For the baseline selection, the E_T^{miss} distribution measured in the data is then fit using two shapes: the multi-jet model and the sum of other processes (dominated by $t\bar{t}$ and W +jets), for which the shape and the relative normalisation are taken from simulation, as shown in figure 4b. The ratio between the numbers of multi-jet background events in the control and signal regions enters the likelihood function for the signal estimation (see section 8) as a nuisance parameter while the shape of the multi-jet background is measured in the same region after additionally requiring $E_T^{\text{miss}} > 65$ GeV.

6.3 Backgrounds with electrons and jets misidentified as τ jets

The methods described in section 5.3 are used to estimate the probability for electrons or jets to be misidentified as τ jets. The estimated contribution to the background from the jet $\rightarrow \tau$ misidentification after the τ +jets selection is given in table 5. The backgrounds arising from the jet $\rightarrow \tau$ misidentification are not expected to be well modelled in simulation, which is why they are estimated using data-driven methods.

6.4 Data-driven estimation of backgrounds with correctly reconstructed τ jets

An embedding method [54] is used to estimate the backgrounds that contain correctly reconstructed τ jets. The method consists of selecting a control sample of $t\bar{t}$ -like μ +jets events and replacing the detector signature of the muon by a simulated hadronic τ decay. These new hybrid events are then used for the background prediction. In order to select this control sample from the data, the following event selection is applied:

- event triggered by a single-muon trigger with a p_T threshold of 18 GeV;

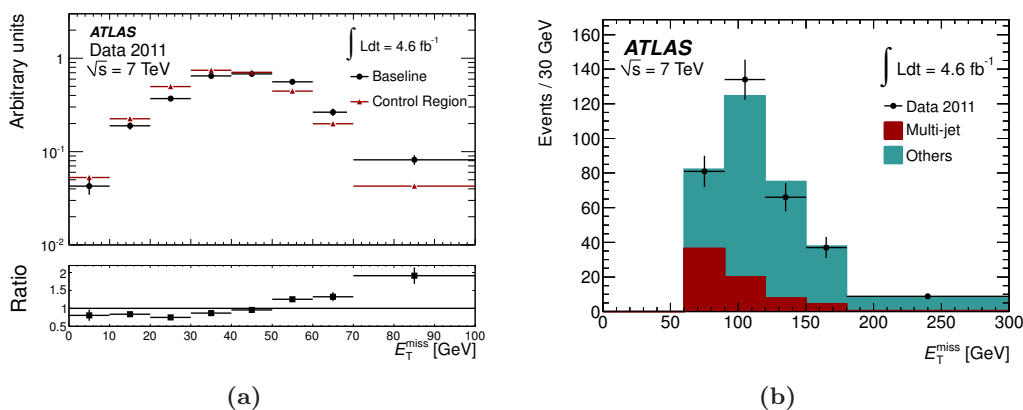


Figure 4. (a) Shape of E_T^{miss} in a control region of the data or using the baseline selection, after subtracting the expectation from $t\bar{t}$, W +jets, and single top quark processes estimated from simulation. The distributions are compared just before the E_T^{miss} requirement in the baseline selection of section 6.1, with the exception that, in the control region, the τ selection and the b -tagging requirements are modified, see text. (b) Fit of the E_T^{miss} template to data, in the signal region. Only statistical uncertainties are shown.

Sample	Data-driven method [events]	Simulation [events]
$t\bar{t}$	33 ± 1	37 ± 1
W +jets	2.5 ± 0.1	3.9 ± 1.5
Single top quark	1.3 ± 0.1	2.0 ± 0.3

Table 5. Application of the misidentification probability obtained from a control region in the data enriched in W +jets events, for the τ +jets channel. The predictions of the background contributions based on data-driven misidentification probabilities and on simulation are given, with statistical uncertainties only. In both cases, all top quarks decay via $t \rightarrow bW$.

- exactly one isolated muon with $p_T > 25$ GeV, no isolated electron with $E_T > 20$ GeV;
- at least four jets with $p_T > 20$ GeV, at least one of which is b -tagged;
- $E_T^{\text{miss}} > 35$ GeV.

This selection is looser than the selection defined in section 6.1 in order not to bias the control sample. The impurity from the background with muons produced in τ decays and non-isolated muons (dominantly $b\bar{b}$ and $c\bar{c}$ events) is about 10%. However, this contribution is greatly reduced as these events are much less likely to pass the τ +jets selection, in particular the p_T^τ requirement.

The shape of the m_T distribution for the backgrounds with true τ jets is taken from the distribution obtained with the embedded events, after having applied the τ +jets event selection. The normalisation is then derived from the number of embedded events:

$$N_\tau = N_{\text{embedded}} \cdot (1 - c_{\tau \rightarrow \mu}) \frac{\epsilon^{\tau + E_T^{\text{miss}} - \text{trigger}}}{\epsilon^{\mu - \text{ID}, \text{trigger}}} \cdot \mathcal{B}(\tau \rightarrow \text{hadrons} + \nu), \quad (6.2)$$

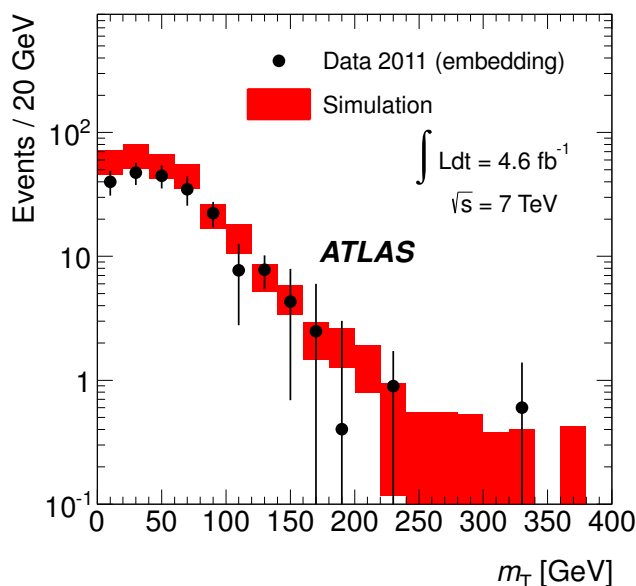


Figure 5. Comparison of the m_T distribution for correctly reconstructed τ jets, predicted by the embedding method and simulation. Combined statistical and systematic uncertainties (as described in section 7) are shown.

where N_τ is the estimated number of events with correctly reconstructed τ jets, N_{embedded} is the number of embedded events in the signal region, $c_{\tau \rightarrow \mu}$ is the fraction of events in which the selected muon is a decay product of a τ lepton (taken from simulation), $\epsilon^{\tau + E_T^{\text{miss}} - \text{trigger}}$ is the $\tau + E_T^{\text{miss}}$ trigger efficiency (as a function of p_T^τ and E_T^{miss} , derived from data), $\epsilon^{\mu - \text{ID, trigger}}$ is the muon trigger and identification efficiency (as a function of p_T and η , derived from data) and $\mathcal{B}(\tau \rightarrow \text{hadrons} + \nu)$ is the branching ratio of the τ lepton decays involving hadrons. The m_T distribution for correctly reconstructed τ jets, as predicted by the embedding method, is shown in figure 5 and compared to simulation.

6.5 Event yields and m_T distribution after the selection cuts

Table 6 shows the expected number of background events for the SM-only hypothesis and the observation in the data. The total number of predicted events (signal+background) in the presence of a 130 GeV charged Higgs boson with $\mathcal{B}(t \rightarrow bH^+) = 5\%$ is also shown. The number of events with a correctly reconstructed τ jet is derived from the number of embedded events and does not depend on the cross section of the $t\bar{t} \rightarrow b\bar{b}W^+W^-$ process. On the other hand, the τ +jets analysis relies on the theoretical inclusive $t\bar{t}$ production cross section $\sigma_{t\bar{t}} = 167_{-18}^{+17}$ pb [26] for the estimation of the background with electrons or jets misidentified as τ jets. In the presence of a charged Higgs boson in the top quark decays, with a branching ratio $\mathcal{B}(t \rightarrow bH^+)$, the contributions of $t\bar{t} \rightarrow b\bar{b}W^+W^-$ events in these backgrounds are scaled according to this branching ratio. The data are found to be consistent with the estimation of the SM background. The m_T distribution for the τ +jets channel, after all selection cuts are applied, is shown in figure 6.

Sample	Event yield (τ +jets)
True τ (embedding method)	$210 \pm 10 \pm 44$
Misidentified jet $\rightarrow \tau$	$36 \pm 6 \pm 10$
Misidentified $e \rightarrow \tau$	$3 \pm 1 \pm 1$
Multi-jet processes	$74 \pm 3 \pm 47$
All SM backgrounds	$330 \pm 12 \pm 65$
Data	355
$t \rightarrow bH^+$ (130 GeV)	$220 \pm 6 \pm 56$
Signal+background	$540 \pm 13 \pm 85$

Table 6. Expected event yields after all selection cuts in the τ +jets channel and comparison with 4.6 fb^{-1} of data. The numbers in the last two rows, obtained for a hypothetical H^+ signal with $m_{H^+} = 130 \text{ GeV}$, are obtained with $\mathcal{B}(t \rightarrow bH^+) = 5\%$. The rows for the backgrounds with misidentified objects assume $\mathcal{B}(t \rightarrow bW) = 100\%$. Both statistical and systematic uncertainties are shown, in this order.

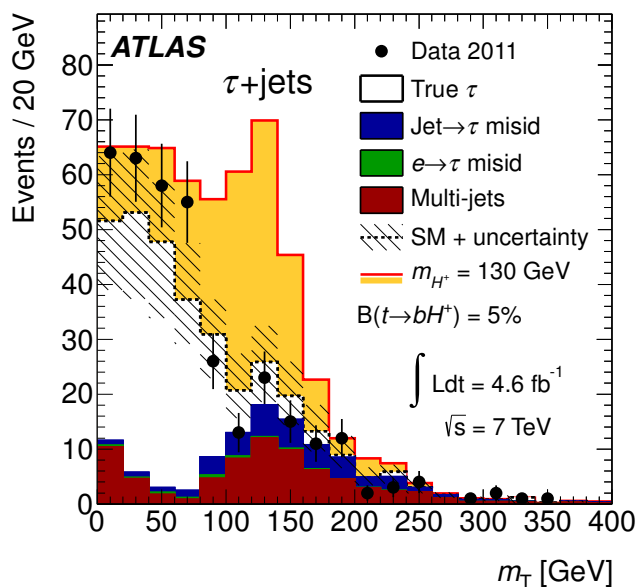


Figure 6. Distribution of m_T after all selection cuts in the τ +jets channel. The dashed line corresponds to the SM-only hypothesis and the hatched area around it shows the total uncertainty for the SM backgrounds. The solid line shows the predicted contribution of signal+background in the presence of a charged Higgs boson with $m_{H^+} = 130 \text{ GeV}$, assuming $\mathcal{B}(t \rightarrow bH^+) = 5\%$ and $\mathcal{B}(H^+ \rightarrow \tau\nu) = 100\%$. The contributions of $t\bar{t} \rightarrow b\bar{b}W^+W^-$ events in the backgrounds with misidentified objects are scaled down accordingly.

7 Systematic uncertainties

7.1 Systematic uncertainties arising from the detector simulation

Systematic uncertainties arising from the simulation of pile-up and object reconstruction are considered. The latter arise from the simulation of the trigger, from the reconstruction and identification efficiencies, as well as from the energy/momentum scale and resolution for the objects described in section 3. To assess the impact of most sources of systematic uncertainty, the selection cuts for each analysis are re-applied after shifting a particular parameter by its ± 1 standard deviation uncertainty. The systematic uncertainties related to the electrons and muons are discussed in, respectively, ref. [42] and refs. [43, 55]. For the jets, see ref. [48] and, in particular, ref. [50] for the b -tagging calibration. The systematic uncertainties related to τ jets are discussed in ref. [51]. Finally, for the reconstruction of E_T^{miss} , see ref. [52]. All studies of systematic uncertainties have been updated with the full dataset collected in 2011. The dominant instrumental systematic uncertainties arise from the jet energy resolution (10–30%, depending on p_T and η), the jet energy scale (up to 14%, depending on p_T and η , to which a pile-up term of 2–7% and a b jet term of 2.5% are added in quadrature), as well as the b -tagging efficiency (5–17%, depending on p_T and η) and misidentification probability (12–21%, depending on p_T and η). In comparison, the systematic uncertainties arising from the reconstruction and identification of electrons and muons are small. All instrumental systematic uncertainties are also propagated to the reconstructed E_T^{miss} .

7.2 Systematic uncertainties arising from the generation of $t\bar{t}$ events

In order to estimate the systematic uncertainties arising from the $t\bar{t}$ generation and the parton shower model, the acceptance is computed for $t\bar{t}$ events produced with MC@NLO interfaced to HERWIG/JIMMY and POWHEG [56] interfaced to PYTHIA. For the signal samples, which are generated with PYTHIA (i.e. without higher-order corrections), no alternative generator is available. Instead, the systematic uncertainty for the signal samples is set to the relative difference in acceptance between $t\bar{t}$ events generated with MC@NLO interfaced to HERWIG/JIMMY and with AcerMC, which is also a leading-order generator, interfaced to PYTHIA. The systematic uncertainties arising from initial and final state radiation are computed using $t\bar{t}$ samples generated with AcerMC interfaced to PYTHIA, where initial and final state radiation parameters are set to a range of values not excluded by the experimental data [57]. The largest relative differences with respect to the reference sample after full event selections are used as systematic uncertainties. The systematic uncertainties arising from the modelling of the $t\bar{t}$ event generation and the parton shower, as well as initial and final state radiation, are summarised in table 7 for each analysis.

7.3 Systematic uncertainties arising from data-driven background estimates

The systematic uncertainties arising from the data-driven methods used to estimate the various backgrounds are summarised in table 8, for each of the three channels considered in the analysis.

Source of uncertainty	Normalisation uncertainty
lepton+jets:	
Generator and parton shower ($b\bar{b}WH^+$, signal region)	10%
Generator and parton shower ($b\bar{b}W^+W^-$, signal region)	8%
Generator and parton shower ($b\bar{b}WH^+$, control region)	7%
Generator and parton shower ($b\bar{b}W^+W^-$, control region)	6%
Initial and final state radiation (signal region)	8%
Initial and final state radiation (control region)	13%
τ +lepton:	
Generator and parton shower ($b\bar{b}WH^+$)	2%
Generator and parton shower ($b\bar{b}W^+W^-$)	5%
Initial and final state radiation	13%
τ +jets:	
Generator and parton shower ($b\bar{b}WH^+$)	5%
Generator and parton shower ($b\bar{b}W^+W^-$)	5%
Initial and final state radiation	19%

Table 7. Systematic uncertainties arising from the modelling of $t\bar{t} \rightarrow b\bar{b}W^+W^-$ and $t\bar{t} \rightarrow b\bar{b}WH^+$ events and the parton shower, as well as from initial and final state radiation.

For backgrounds with misidentified leptons, discussed in sections 4.2 and 5.2, the main systematic uncertainties arise from the simulated samples used for subtracting true leptons in the determination of the misidentification probabilities. These are sensitive to the instrumental systematic uncertainties and to the sample dependence (misidentification probabilities are calculated in a control region dominated by gluon-initiated events, but later used in a data sample with a higher fraction of quark-initiated events).

The dominant systematic uncertainties in the estimation of the multi-jet background in the τ +jets channel, described in section 6.2, are the statistical uncertainty of the fit due to the limited size of the data control sample and uncertainties due to potential differences of the E_T^{miss} shape in the signal and control regions. The dominant systematic uncertainties in estimating the contribution of events with electrons misidentified as τ jets in sections 5.3 and 6.3 arise from the subtraction of the multi-jet and electroweak backgrounds in the control region enriched with $Z \rightarrow ee$ events and from potential correlations in the selections of the tag and probe electrons. For the estimation of backgrounds with jets misidentified as hadronically decaying τ leptons, also discussed in sections 5.3 and 6.3, the dominant systematic uncertainties on the misidentification probability are the statistical uncertainty due to the limited control sample size and uncertainties due to the difference of the jet composition (gluon- or quark-initiated) in the control and signal regions, which is estimated

Source of uncertainty	Normalisation uncertainty	Shape uncertainty
lepton+jets: lepton misidentification		
Choice of control region	6%	-
Z mass window	4%	-
Jet energy scale	16%	-
Jet energy resolution	7%	-
Sample composition	31%	-
τ +lepton: jet \rightarrow τ misidentification		
Statistics in control region	2%	-
Jet composition	11%	-
Object-related systematics	23%	3%
τ +lepton: $e \rightarrow \tau$ misidentification		
Misidentification probability	20%	-
τ +lepton: lepton misidentification		
Choice of control region	4%	-
Z mass window	5%	-
Jet energy scale	14%	-
Jet energy resolution	4%	-
Sample composition	39%	-
τ +jets: true τ		
Embedding parameters	6%	3%
Muon isolation	7%	2%
Parameters in normalisation	16%	-
τ identification	5%	-
τ energy scale	6%	1%
τ +jets: jet $\rightarrow \tau$ misidentification		
Statistics in control region	2%	-
Jet composition	12%	-
Purity in control region	6%	1%
Object-related systematics	21%	2%
τ +jets: $e \rightarrow \tau$ misidentification		
Misidentification probability	22%	-
τ +jets: multi-jet estimate		
Fit-related uncertainties	32%	-
E_T^{miss} -shape in control region	16%	-

Table 8. Dominant systematic uncertainties on the data-driven estimates. The shape uncertainty given is the relative shift of the mean value of the final discriminant distribution. A “-” in the second column indicates negligible shape uncertainties.

using simulation. Other uncertainties come from the impurities arising from multi-jet background events and from true hadronic τ decays in the control sample. The systematic uncertainties affecting the estimation of the background from correctly reconstructed τ jets in the τ +jets channel, discussed in section 6.4, consist of the potential bias introduced by the embedding method itself, uncertainties from the trigger efficiency measurement, uncertainties associated to simulated τ jets (τ energy scale and identification efficiency) and uncertainties on the normalisation, which are dominated by the statistical uncertainty of the selected control sample and the $\tau + E_T^{\text{miss}}$ trigger efficiency uncertainties.

8 Results

In order to test the compatibility of the data with background-only and signal+background hypotheses, a profile likelihood ratio [58] is used with m_T^H (lepton+jets), E_T^{miss} (τ +lepton) and m_T (τ +jets) as the discriminating variables. The statistical analysis is based on a binned likelihood function for these distributions. The systematic uncertainties in shape and normalisation are incorporated via nuisance parameters, and the one-sided profile likelihood ratio, \tilde{q}_μ , is used as a test statistic. No significant deviation from the SM prediction is observed in any of the investigated final states in 4.6 fb^{-1} of data. Exclusion limits are set on the branching fraction $\mathcal{B}(t \rightarrow bH^+)$ and, in the context of the m_h^{max} scenario of the MSSM, on $\tan \beta$, by rejecting the signal hypothesis at the 95% confidence level (CL) using the CL_s procedure [59]. These limits are based on the asymptotic distribution of the test statistic [58]. The combined limit is derived from the product of the individual likelihoods, and systematic uncertainties are treated as correlated where appropriate. The exclusion limits for the individual channels, as well as the combined limit, are shown in figure 7 in terms of $\mathcal{B}(t \rightarrow bH^+)$ with the assumption $\mathcal{B}(H^+ \rightarrow \tau\nu) = 100\%$. In figure 8, the combined limit on $\mathcal{B}(t \rightarrow bH^+) \times \mathcal{B}(H^+ \rightarrow \tau\nu)$ is interpreted in the context of the m_h^{max} scenario of the MSSM. The following relative theoretical uncertainties on $\mathcal{B}(t \rightarrow bH^+)$ are considered [60, 61]: 5% for one-loop electroweak corrections missing from the calculations, 2% for missing two-loop QCD corrections, and about 1% (depending on $\tan \beta$) for Δ_b -induced uncertainties, where Δ_b is a correction factor to the running b quark mass [62]. These uncertainties are added linearly, as recommended by the LHC Higgs cross section working group [61].

9 Conclusions

Charged Higgs bosons have been searched for in $t\bar{t}$ events, in the decay mode $t \rightarrow bH^+$ followed by $H^+ \rightarrow \tau\nu$. For this purpose, a total of 4.6 fb^{-1} of pp collision data at $\sqrt{s} = 7 \text{ TeV}$, recorded in 2011 with the ATLAS experiment, is used. Three final states are considered, which are characterised by the presence of a leptonic or hadronic τ decay, E_T^{miss} , b jets, and a leptonically or hadronically decaying W boson. Data-driven methods and simulation are employed to estimate the number of background events. The observed data are found to be in agreement with the SM predictions. Assuming $\mathcal{B}(H^+ \rightarrow \tau\nu) = 100\%$, upper limits at the 95% confidence level have been set on the branching ratio $\mathcal{B}(t \rightarrow bH^+)$ between 5% ($m_{H^+} = 90 \text{ GeV}$) and 1% ($m_{H^+} = 160 \text{ GeV}$). This result constitutes a significant

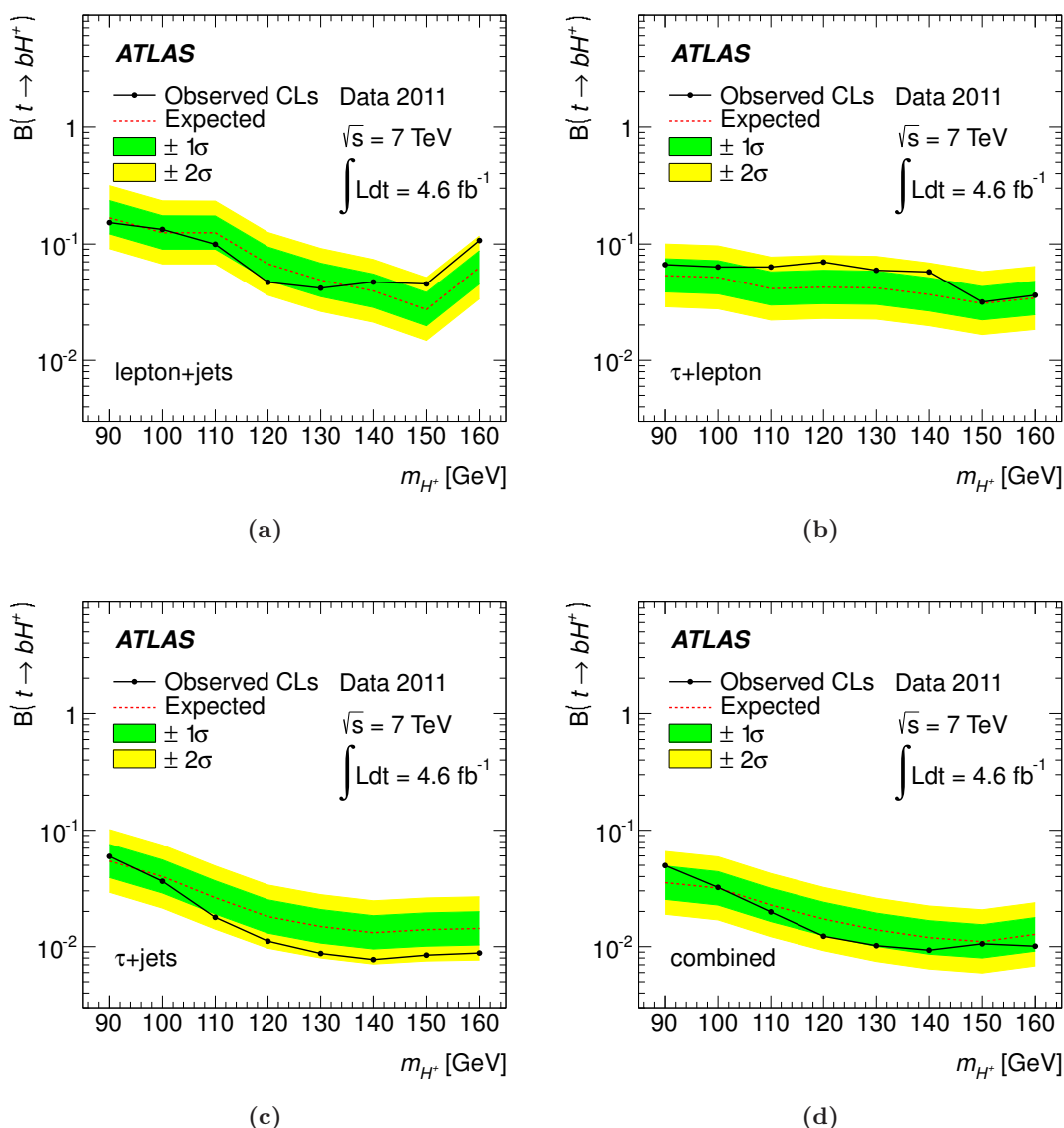


Figure 7. Expected and observed 95% CL exclusion limits on $\mathcal{B}(t \rightarrow bH^+)$ for charged Higgs boson production from top quark decays as a function of m_{H^+} , assuming $\mathcal{B}(H^+ \rightarrow \tau\nu) = 100\%$. Shown are the results for: (a) lepton+jets channel; (b) τ +lepton channel; (c) τ +jets channel; (d) combination.

improvement compared to existing limits provided by the Tevatron experiments [14, 15] over the whole investigated mass range, but in particular for m_{H^+} close to the top quark mass. Interpreted in the context of the m_h^{\max} scenario of the MSSM, $\tan\beta$ above 12–26, as well as between 1 and 2–6, can be excluded in the mass range $90 \text{ GeV} < m_{H^+} < 150 \text{ GeV}$.

Acknowledgments

We thank CERN for the very successful operation of the LHC, as well as the support staff from our institutions without whom ATLAS could not be operated efficiently.

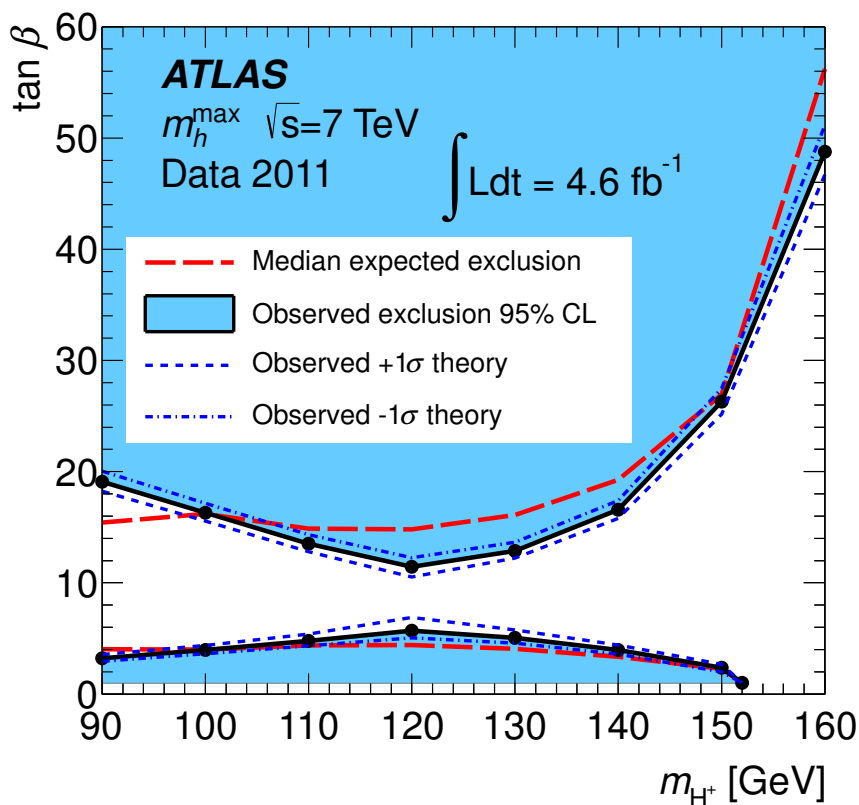


Figure 8. Combined 95% CL exclusion limits on $\tan \beta$ as a function of m_{H^+} . Results are shown in the context of the MSSM scenario m_h^{\max} for the region $1 < \tan \beta < 60$ in which reliable theoretical predictions exist. The theoretical uncertainties described in the text are shown as well.

We acknowledge the support of ANPCyT, Argentina; YerPhI, Armenia; ARC, Australia; BMWF, Austria; ANAS, Azerbaijan; SSTC, Belarus; CNPq and FAPESP, Brazil; NSERC, NRC and CFI, Canada; CERN; CONICYT, Chile; CAS, MOST and NSFC, China; COLCIENCIAS, Colombia; MSMT CR, MPO CR and VSC CR, Czech Republic; DNRF, DNSRC and Lundbeck Foundation, Denmark; EPLANET and ERC, European Union; IN2P3-CNRS, CEA-DSM/IRFU, France; GNAS, Georgia; BMBF, DFG, HGF, MPG and AvH Foundation, Germany; GSRT, Greece; ISF, MINERVA, GIF, DIP and Benoziyo Center, Israel; INFN, Italy; MEXT and JSPS, Japan; CNRST, Morocco; FOM and NWO, Netherlands; RCN, Norway; MNiSW, Poland; GRICES and FCT, Portugal; MERYS (MECTS), Romania; MES of Russia and ROSATOM, Russian Federation; JINR; MSTD, Serbia; MSSR, Slovakia; ARRS and MVZT, Slovenia; DST/NRF, South Africa; MICINN, Spain; SRC and Wallenberg Foundation, Sweden; SER, SNSF and Cantons of Bern and Geneva, Switzerland; NSC, Taiwan; TAEK, Turkey; STFC, the Royal Society and Leverhulme Trust, United Kingdom; DOE and NSF, United States of America.

The crucial computing support from all WLCG partners is acknowledged gratefully, in particular from CERN and the ATLAS Tier-1 facilities at TRIUMF (Canada), NDGF (Denmark, Norway, Sweden), CC-IN2P3 (France), KIT/GridKA (Germany), INFN-CNAF

(Italy), NL-T1 (Netherlands), PIC (Spain), ASGC (Taiwan), RAL (U.K.) and BNL (U.S.A.) and in the Tier-2 facilities worldwide.

Open Access. This article is distributed under the terms of the Creative Commons Attribution License which permits any use, distribution and reproduction in any medium, provided the original author(s) and source are credited.

References

- [1] T. Lee, *A theory of spontaneous T violation*, *Phys. Rev. D* **8** (1973) 1226 [INSPIRE].
- [2] T. Cheng and L.-F. Li, *Neutrino masses, mixings and oscillations in $SU(2) \times U(1)$ models of electroweak interactions*, *Phys. Rev. D* **22** (1980) 2860 [INSPIRE].
- [3] J. Schechter and J. Valle, *Neutrino masses in $SU(2) \times U(1)$ theories*, *Phys. Rev. D* **22** (1980) 2227 [INSPIRE].
- [4] G. Lazarides, Q. Shafi and C. Wetterich, *Proton lifetime and fermion masses in an $SO(10)$ model*, *Nucl. Phys. B* **181** (1981) 287 [INSPIRE].
- [5] R.N. Mohapatra and G. Senjanovic, *Neutrino masses and mixings in gauge models with spontaneous parity violation*, *Phys. Rev. D* **23** (1981) 165 [INSPIRE].
- [6] M. Magg and C. Wetterich, *Neutrino mass problem and gauge hierarchy*, *Phys. Lett. B* **94** (1980) 61 [INSPIRE].
- [7] P. Fayet, *Supersymmetry and weak, electromagnetic and strong interactions*, *Phys. Lett. B* **64** (1976) 159 [INSPIRE].
- [8] P. Fayet, *Spontaneously broken supersymmetric theories of weak, electromagnetic and strong interactions*, *Phys. Lett. B* **69** (1977) 489 [INSPIRE].
- [9] G.R. Farrar and P. Fayet, *Phenomenology of the production, decay and detection of new hadronic states associated with supersymmetry*, *Phys. Lett. B* **76** (1978) 575 [INSPIRE].
- [10] P. Fayet, *Relations between the masses of the superpartners of leptons and quarks, the goldstino couplings and the neutral currents*, *Phys. Lett. B* **84** (1979) 416 [INSPIRE].
- [11] S. Dimopoulos and H. Georgi, *Softly broken supersymmetry and $SU(5)$* , *Nucl. Phys. B* **193** (1981) 150 [INSPIRE].
- [12] LHC HIGGS CROSS SECTION WORKING GROUP collaboration, S. Dittmaier et al., *Handbook of LHC Higgs cross sections: 1. Inclusive observables*, CERN-2011-002, CERN, Geneva Switzerland (2011) [arXiv:1101.0593] [INSPIRE].
- [13] LEP HIGGS WORKING GROUP FOR HIGGS BOSON SEARCHES, ALEPH, DELPHI, L3 and OPAL collaborations, *Search for charged Higgs bosons: preliminary combined results using LEP data collected at energies up to 209 GeV*, hep-ex/0107031 [INSPIRE].
- [14] CDF collaboration, T. Aaltonen et al., *Search for charged Higgs bosons in decays of top quarks in $p\bar{p}$ collisions at $\sqrt{s} = 1.96$ TeV*, *Phys. Rev. Lett.* **103** (2009) 101803 [arXiv:0907.1269] [INSPIRE].
- [15] D0 collaboration, V. Abazov et al., *Search for charged Higgs bosons in top quark decays*, *Phys. Lett. B* **682** (2009) 278 [arXiv:0908.1811] [INSPIRE].

- [16] M.S. Carena, S. Heinemeyer, C. Wagner and G. Weiglein, *Suggestions for benchmark scenarios for MSSM Higgs boson searches at hadron colliders*, *Eur. Phys. J. C* **26** (2003) 601 [[hep-ph/0202167](#)] [[INSPIRE](#)].
- [17] ATLAS collaboration, G. Aad et al., *The ATLAS experiment at the CERN Large Hadron Collider*, *2008 JINST* **3** S08003 [[INSPIRE](#)].
- [18] ATLAS collaboration, *Luminosity determination in pp collisions at $\sqrt{s} = 7$ TeV using the ATLAS detector in 2011*, *ATLAS-CONF-2011-116*, CERN, Geneva Switzerland (2011).
- [19] ATLAS collaboration, G. Aad et al., *Luminosity determination in pp collisions at $\sqrt{s} = 7$ TeV using the ATLAS detector at the LHC*, *Eur. Phys. J. C* **71** (2011) 1630 [[arXiv:1101.2185](#)] [[INSPIRE](#)].
- [20] S. Frixione and B.R. Webber, *Matching NLO QCD computations and parton shower simulations*, *JHEP* **06** (2002) 029 [[hep-ph/0204244](#)] [[INSPIRE](#)].
- [21] B.P. Kersevan and E. Richter-Was, *The Monte Carlo event generator AcerMC version 2.0 with interfaces to PYTHIA 6.2 and HERWIG 6.5*, [hep-ph/0405247](#) [[INSPIRE](#)].
- [22] H.-L. Lai et al., *New parton distributions for collider physics*, *Phys. Rev. D* **82** (2010) 074024 [[arXiv:1007.2241](#)] [[INSPIRE](#)].
- [23] G. Corcella et al., *HERWIG 6: an event generator for hadron emission reactions with interfering gluons (including supersymmetric processes)*, *JHEP* **01** (2001) 010 [[hep-ph/0011363](#)] [[INSPIRE](#)].
- [24] J. Butterworth, J.R. Forshaw and M. Seymour, *Multiparton interactions in photoproduction at HERA*, *Z. Phys. C* **72** (1996) 637 [[hep-ph/9601371](#)] [[INSPIRE](#)].
- [25] T. Sjöstrand, S. Mrenna and P.Z. Skands, *PYTHIA 6.4 physics and manual*, *JHEP* **05** (2006) 026 [[hep-ph/0603175](#)] [[INSPIRE](#)].
- [26] M. Aliev et al., *HATHOR: HAdronic Top and Heavy quarks crOss section calculator*, *Comput. Phys. Commun.* **182** (2011) 1034 [[arXiv:1007.1327](#)] [[INSPIRE](#)].
- [27] N. Kidonakis, *Next-to-next-to-leading-order collinear and soft gluon corrections for t-channel single top quark production*, *Phys. Rev. D* **83** (2011) 091503 [[arXiv:1103.2792](#)] [[INSPIRE](#)].
- [28] N. Kidonakis, *NNLL resummation for s-channel single top quark production*, *Phys. Rev. D* **81** (2010) 054028 [[arXiv:1001.5034](#)] [[INSPIRE](#)].
- [29] N. Kidonakis, *Two-loop soft anomalous dimensions for single top quark associated production with a W^- or H^-* , *Phys. Rev. D* **82** (2010) 054018 [[arXiv:1005.4451](#)] [[INSPIRE](#)].
- [30] S. Frixione, E. Laenen, P. Motylinski and B.R. Webber, *Single-top production in MC@NLO*, *JHEP* **03** (2006) 092 [[hep-ph/0512250](#)] [[INSPIRE](#)].
- [31] M.L. Mangano, M. Moretti, F. Piccinini, R. Pittau and A.D. Polosa, *ALPGEN, a generator for hard multiparton processes in hadronic collisions*, *JHEP* **07** (2003) 001 [[hep-ph/0206293](#)] [[INSPIRE](#)].
- [32] J. Pumplin et al., *New generation of parton distributions with uncertainties from global QCD analysis*, *JHEP* **07** (2002) 012 [[hep-ph/0201195](#)] [[INSPIRE](#)].
- [33] R. Gavin, Y. Li, F. Petriello and S. Quackenbush, *W physics at the LHC with FEWZ 2.1*, [arXiv:1201.5896](#) [[INSPIRE](#)].

- [34] R. Gavin, Y. Li, F. Petriello and S. Quackenbush, *FEWZ 2.0: a code for hadronic Z production at next-to-next-to-leading order*, *Comput. Phys. Commun.* **182** (2011) 2388 [[arXiv:1011.3540](#)] [[INSPIRE](#)].
- [35] J.M. Campbell, R.K. Ellis and C. Williams, *Vector boson pair production at the LHC*, *JHEP* **07** (2011) 018 [[arXiv:1105.0020](#)] [[INSPIRE](#)].
- [36] Z. Was and P. Golonka, *TAUOLA as τ Monte Carlo for future applications*, *Nucl. Phys. Proc. Suppl.* **144** (2005) 88 [[hep-ph/0411377](#)] [[INSPIRE](#)].
- [37] E. Barberio, B. van Eijk and Z. Was, *PHOTOS: a universal Monte Carlo for QED radiative corrections in decays*, *Comput. Phys. Commun.* **66** (1991) 115 [[INSPIRE](#)].
- [38] ATLAS collaboration, *New ATLAS event generator tunes to 2010 data*, [ATL-PHYS-PUB-2011-008](#), CERN, Geneva Switzerland (2011).
- [39] ATLAS collaboration, *ATLAS tunes of PYTHIA 6 and PYTHIA 8 for MC11*, [ATL-PHYS-PUB-2011-009](#), CERN, Geneva Switzerland (2011).
- [40] GEANT4 collaboration, S. Agostinelli et al., *GEANT4: a simulation toolkit*, *Nucl. Instrum. Meth. A* **506** (2003) 250 [[INSPIRE](#)].
- [41] ATLAS collaboration, G. Aad et al., *The ATLAS simulation infrastructure*, *Eur. Phys. J. C* **70** (2010) 823 [[arXiv:1005.4568](#)] [[INSPIRE](#)].
- [42] ATLAS collaboration, G. Aad et al., *Electron performance measurements with the ATLAS detector using the 2010 LHC proton-proton collision data*, *Eur. Phys. J. C* **72** (2012) 1909 [[arXiv:1110.3174](#)] [[INSPIRE](#)].
- [43] ATLAS collaboration, *Muon reconstruction efficiency in reprocessed 2010 LHC proton-proton collision data recorded with the ATLAS detector*, [ATLAS-CONF-2011-063](#), CERN, Geneva Switzerland (2011).
- [44] M. Cacciari, G.P. Salam and G. Soyez, *The anti- k_t jet clustering algorithm*, *JHEP* **04** (2008) 063 [[arXiv:0802.1189](#)] [[INSPIRE](#)].
- [45] M. Cacciari and G.P. Salam, *Dispelling the N^3 myth for the k_t jet-finder*, *Phys. Lett. B* **641** (2006) 57 [[hep-ph/0512210](#)] [[INSPIRE](#)].
- [46] W. Lampl et al., *Calorimeter clustering algorithms: description and performance*, [ATL-LARG-PUB-2008-002](#), CERN, Geneva Switzerland (2008) [[INSPIRE](#)].
- [47] ATLAS collaboration, G. Aad et al., *Jet energy measurement with the ATLAS detector in proton-proton collisions at $\sqrt{s} = 7$ TeV*, [arXiv:1112.6426](#) [[INSPIRE](#)].
- [48] ATLAS collaboration, *Validating the measurement of jet energies with the ATLAS detector using Z + jet events from proton-proton collisions at $\sqrt{s} = 7$ TeV*, [ATLAS-CONF-2011-159](#), CERN, Geneva Switzerland (2011).
- [49] D0 collaboration, V. Abazov et al., *Measurement of the $p\bar{p} \rightarrow t\bar{t}$ production cross section at $\sqrt{s} = 1.96$ TeV in the fully hadronic decay channel*, *Phys. Rev. D* **76** (2007) 072007 [[hep-ex/0612040](#)] [[INSPIRE](#)].
- [50] ATLAS collaboration, *Commissioning of the ATLAS high-performance b-tagging algorithms in the 7 TeV collision data*, [ATLAS-CONF-2011-102](#), CERN, Geneva Switzerland (2011).
- [51] ATLAS collaboration, *Performance of the reconstruction and identification of hadronic tau decays with ATLAS*, [ATLAS-CONF-2011-152](#), CERN, Geneva Switzerland (2011).

- [52] ATLAS collaboration, G. Aad et al., *Performance of missing transverse momentum reconstruction in proton-proton collisions at 7 TeV with ATLAS*, *Eur. Phys. J. C* **72** (2012) 1844 [[arXiv:1108.5602](#)] [[INSPIRE](#)].
- [53] E. Gross and O. Vitells, *Transverse mass observables for charged Higgs boson searches at hadron colliders*, *Phys. Rev. D* **81** (2010) 055010 [[arXiv:0907.5367](#)] [[INSPIRE](#)].
- [54] ATLAS collaboration, G. Aad et al., *Search for neutral MSSM Higgs bosons decaying to $\tau^+\tau^-$ pairs in proton-proton collisions at $\sqrt{s} = 7$ TeV with the ATLAS detector*, *Phys. Lett. B* **705** (2011) 174 [[arXiv:1107.5003](#)] [[INSPIRE](#)].
- [55] ATLAS collaboration, *ATLAS muon momentum resolution in the first pass reconstruction of the 2010 pp collision data at $\sqrt{s} = 7$ TeV*, [ATLAS-CONF-2011-046](#), CERN, Geneva Switzerland (2011).
- [56] S. Frixione, P. Nason and C. Oleari, *Matching NLO QCD computations with parton shower simulations: the POWHEG method*, *JHEP* **11** (2007) 070 [[arXiv:0709.2092](#)] [[INSPIRE](#)].
- [57] P.Z. Skands, *Tuning Monte Carlo generators: the Perugia tunes*, *Phys. Rev. D* **82** (2010) 074018 [[arXiv:1005.3457](#)] [[INSPIRE](#)].
- [58] G. Cowan, K. Cranmer, E. Gross and O. Vitells, *Asymptotic formulae for likelihood-based tests of new physics*, *Eur. Phys. J. C* **71** (2011) 1554 [[arXiv:1007.1727](#)] [[INSPIRE](#)].
- [59] A.L. Read, *Presentation of search results: the CL_s technique*, *J. Phys. G* **28** (2002) 2693 [[INSPIRE](#)].
- [60] S. Heinemeyer, W. Hollik and G. Weiglein, *FeynHiggs: a program for the calculation of the masses of the neutral CP even Higgs bosons in the MSSM*, *Comput. Phys. Commun.* **124** (2000) 76 [[hep-ph/9812320](#)] [[INSPIRE](#)].
- [61] S. Dittmaier et al., *Handbook of LHC Higgs cross sections: 2. Differential distributions*, [CERN-2012-002](#), CERN, Geneva Switzerland (2012) [[arXiv:1201.3084](#)] [[INSPIRE](#)].
- [62] M.S. Carena, D. Garcia, U. Nierste and C.E. Wagner, *Effective Lagrangian for the $\bar{t}bH^+$ interaction in the MSSM and charged Higgs phenomenology*, *Nucl. Phys. B* **577** (2000) 88 [[hep-ph/9912516](#)] [[INSPIRE](#)].

The ATLAS collaboration

G. Aad⁴⁸, B. Abbott¹¹¹, J. Abdallah¹¹, S. Abdel Khalek¹¹⁵, A.A. Abdelalim⁴⁹, O. Abdinov¹⁰, B. Abi¹¹², M. Abolins⁸⁸, O.S. AbouZeid¹⁵⁸, H. Abramowicz¹⁵³, H. Abreu¹³⁶, E. Acerbi^{89a,89b}, B.S. Acharya^{164a,164b}, L. Adamczyk³⁷, D.L. Adams²⁴, T.N. Addy⁵⁶, J. Adelman¹⁷⁶, S. Adomeit⁹⁸, P. Adragna⁷⁵, T. Adye¹²⁹, S. Aefsky²², J.A. Aguilar-Saavedra^{124b,a}, M. Aharrouche⁸¹, S.P. Ahlen²¹, F. Ahles⁴⁸, A. Ahmad¹⁴⁸, M. Ahsan⁴⁰, G. Aielli^{133a,133b}, T. Akdogan^{18a}, T.P.A. Åkesson⁷⁹, G. Akimoto¹⁵⁵, A.V. Akimov⁹⁴, A. Akiyama⁶⁶, M.S. Alam¹, M.A. Alam⁷⁶, J. Albert¹⁶⁹, S. Albrand⁵⁵, M. Aleksa²⁹, I.N. Aleksandrov⁶⁴, F. Alessandria^{89a}, C. Alexa^{25a}, G. Alexander¹⁵³, G. Alexandre⁴⁹, T. Alexopoulos⁹, M. Alhroob^{164a,164c}, M. Aliev¹⁵, G. Alimonti^{89a}, J. Alison¹²⁰, B.M.M. Allbrooke¹⁷, P.P. Allport⁷³, S.E. Allwood-Spiers⁵³, J. Almond⁸², A. Aloisio^{102a,102b}, R. Alon¹⁷², A. Alonso⁷⁹, B. Alvarez Gonzalez⁸⁸, M.G. Alviggi^{102a,102b}, K. Amako⁶⁵, C. Amelung²², V.V. Ammosov¹²⁸, A. Amorim^{124a,b}, G. Amorós¹⁶⁷, N. Amram¹⁵³, C. Anastopoulos²⁹, L.S. Ancu¹⁶, N. Andari¹¹⁵, T. Andeen³⁴, C.F. Anders²⁰, G. Anders^{58a}, K.J. Anderson³⁰, A. Andreazza^{89a,89b}, V. Andrei^{58a}, X.S. Anduaga⁷⁰, A. Angerami³⁴, F. Anghinolfi²⁹, A. Anisenkov¹⁰⁷, N. Anjos^{124a}, A. Annovi⁴⁷, A. Antonaki⁸, M. Antonelli⁴⁷, A. Antonov⁹⁶, J. Antos^{144b}, F. Anulli^{132a}, S. Aoun⁸³, L. Aperio Bella⁴, R. Apolle^{118,c}, G. Arabidze⁸⁸, I. Aracena¹⁴³, Y. Arai⁶⁵, A.T.H. Arce⁴⁴, S. Arfaoui¹⁴⁸, J-F. Arguin¹⁴, E. Arik^{18a,*}, M. Arik^{18a}, A.J. Armbruster⁸⁷, O. Arnaez⁸¹, V. Arnal⁸⁰, C. Arnault¹¹⁵, A. Artamonov⁹⁵, G. Artoni^{132a,132b}, D. Arutinov²⁰, S. Asai¹⁵⁵, R. Asfandiyarov¹⁷³, S. Ask²⁷, B. Åsman^{146a,146b}, L. Asquith⁵, K. Assamagan²⁴, A. Astbury¹⁶⁹, B. Aubert⁴, E. Auge¹¹⁵, K. Augsten¹²⁷, M. Aurousseau^{145a}, G. Avolio¹⁶³, R. Avramidou⁹, D. Axen¹⁶⁸, G. Azuelos^{93,d}, Y. Azuma¹⁵⁵, M.A. Baak²⁹, G. Baccaglioni^{89a}, C. Bacci^{134a,134b}, A.M. Bach¹⁴, H. Bachacou¹³⁶, K. Bachas²⁹, M. Backes⁴⁹, M. Backhaus²⁰, E. Badescu^{25a}, P. Bagnaia^{132a,132b}, S. Bahinipati², Y. Bai^{32a}, D.C. Bailey¹⁵⁸, T. Bain¹⁵⁸, J.T. Baines¹²⁹, O.K. Baker¹⁷⁶, M.D. Baker²⁴, S. Baker⁷⁷, E. Banas³⁸, P. Banerjee⁹³, Sw. Banerjee¹⁷³, D. Banfi²⁹, A. Bangert¹⁵⁰, V. Bansal¹⁶⁹, H.S. Bansil¹⁷, L. Barak¹⁷², S.P. Baranov⁹⁴, A. Barbaro Galtieri¹⁴, T. Barber⁴⁸, E.L. Barberio⁸⁶, D. Barberis^{50a,50b}, M. Barbero²⁰, D.Y. Bardin⁶⁴, T. Barillari⁹⁹, M. Barisonzi¹⁷⁵, T. Barklow¹⁴³, N. Barlow²⁷, B.M. Barnett¹²⁹, R.M. Barnett¹⁴, A. Baroncelli^{134a}, G. Barone⁴⁹, A.J. Barr¹¹⁸, F. Barreiro⁸⁰, J. Barreiro Guimarães da Costa⁵⁷, P. Barrillon¹¹⁵, R. Bartoldus¹⁴³, A.E. Barton⁷¹, V. Bartsch¹⁴⁹, R.L. Bates⁵³, L. Batkova^{144a}, J.R. Batley²⁷, A. Battaglia¹⁶, M. Battistin²⁹, F. Bauer¹³⁶, H.S. Bawa^{143,e}, S. Beale⁹⁸, T. Beau⁷⁸, P.H. Beauchemin¹⁶¹, R. Beccherle^{50a}, P. Bechtel²⁰, H.P. Beck¹⁶, S. Becker⁹⁸, M. Beckingham¹³⁸, K.H. Becks¹⁷⁵, A.J. Beddall^{18c}, A. Beddall^{18c}, S. Bedikian¹⁷⁶, V.A. Bednyakov⁶⁴, C.P. Bee⁸³, M. Begel²⁴, S. Behar Harpaz¹⁵², P.K. Behera⁶², M. Beimforde⁹⁹, C. Belanger-Champagne⁸⁵, P.J. Bell⁴⁹, W.H. Bell⁴⁹, G. Bella¹⁵³, L. Bellagamba^{19a}, F. Bellina²⁹, M. Bellomo²⁹, A. Belloni⁵⁷, O. Beloborodova^{107,f}, K. Belotskiy⁹⁶, O. Beltramello²⁹, O. Benary¹⁵³, D. Benchekroun^{135a}, K. Bendtz^{146a,146b}, N. Benekos¹⁶⁵, Y. Benhammou¹⁵³, E. Benhar Noccioli⁴⁹, J.A. Benitez Garcia^{159b}, D.P. Benjamin⁴⁴, M. Benoit¹¹⁵, J.R. Bensinger²², K. Benslama¹³⁰, S. Bentvelsen¹⁰⁵, D. Berge²⁹, E. Bergeaas Kuutmann⁴¹, N. Berger⁴, F. Berghaus¹⁶⁹, E. Berglund¹⁰⁵, J. Beringer¹⁴, P. Bernat⁷⁷, R. Bernhard⁴⁸, C. Bernius²⁴,

T. Berry⁷⁶, C. Bertella⁸³, A. Bertin^{19a,19b}, F. Bertolucci^{122a,122b}, M.I. Besana^{89a,89b}, N. Besson¹³⁶, S. Bethke⁹⁹, W. Bhimji⁴⁵, R.M. Bianchi²⁹, M. Bianco^{72a,72b}, O. Biebel⁹⁸, S.P. Bieniek⁷⁷, K. Bierwagen⁵⁴, J. Biesiada¹⁴, M. Biglietti^{134a}, H. Bilokon⁴⁷, M. Bindi^{19a,19b}, S. Binet¹¹⁵, A. Bingul^{18c}, C. Bini^{132a,132b}, C. Biscarat¹⁷⁸, U. Bitenc⁴⁸, K.M. Black²¹, R.E. Blair⁵, J.-B. Blanchard¹³⁶, G. Blanchot²⁹, T. Blazek^{144a}, C. Blocker²², J. Blocki³⁸, A. Blondel⁴⁹, W. Blum⁸¹, U. Blumenschein⁵⁴, G.J. Bobbink¹⁰⁵, V.B. Bobrovnikov¹⁰⁷, S.S. Bocchetta⁷⁹, A. Bocci⁴⁴, C.R. Boddy¹¹⁸, M. Boehler⁴¹, J. Boek¹⁷⁵, N. Boelaert³⁵, J.A. Bogaerts²⁹, A. Bogdanchikov¹⁰⁷, A. Bogouch^{90,*}, C. Bohm^{146a}, J. Bohm¹²⁵, V. Boisvert⁷⁶, T. Bold³⁷, V. Boldea^{25a}, N.M. Bolnet¹³⁶, M. Bomben⁷⁸, M. Bona⁷⁵, M. Bondioli¹⁶³, M. Boonekamp¹³⁶, C.N. Booth¹³⁹, S. Bordoni⁷⁸, C. Borer¹⁶, A. Borisov¹²⁸, G. Borissov⁷¹, I. Borjanovic^{12a}, M. Borri⁸², S. Borroni⁸⁷, V. Bortolotto^{134a,134b}, K. Bos¹⁰⁵, D. Boscherini^{19a}, M. Bosman¹¹, H. Boterenbrood¹⁰⁵, D. Botterill¹²⁹, J. Bouchami⁹³, J. Boudreau¹²³, E.V. Bouhova-Thacker⁷¹, D. Boumediene³³, C. Bourdarios¹¹⁵, N. Bousson⁸³, A. Boveia³⁰, J. Boyd²⁹, I.R. Boyko⁶⁴, N.I. Bozhko¹²⁸, I. Bozovic-Jelisavcic^{12b}, J. Bracinik¹⁷, P. Branchini^{134a}, A. Brandt⁷, G. Brandt¹¹⁸, O. Brandt⁵⁴, U. Bratzler¹⁵⁶, B. Brau⁸⁴, J.E. Brau¹¹⁴, H.M. Braun¹⁷⁵, B. Brelier¹⁵⁸, J. Bremer²⁹, K. Brendlinger¹²⁰, R. Brenner¹⁶⁶, S. Bressler¹⁷², D. Britton⁵³, F.M. Brochu²⁷, I. Brock²⁰, R. Brock⁸⁸, E. Brodet¹⁵³, F. Broggi^{89a}, C. Bromberg⁸⁸, J. Bronner⁹⁹, G. Brooijmans³⁴, W.K. Brooks^{31b}, G. Brown⁸², H. Brown⁷, P.A. Bruckman de Renstrom³⁸, D. Bruncko^{144b}, R. Bruneliere⁴⁸, S. Brunet⁶⁰, A. Bruni^{19a}, G. Bruni^{19a}, M. Bruschi^{19a}, T. Buanes¹³, Q. Buat⁵⁵, F. Bucci⁴⁹, J. Buchanan¹¹⁸, P. Buchholz¹⁴¹, R.M. Buckingham¹¹⁸, A.G. Buckley⁴⁵, S.I. Buda^{25a}, I.A. Budagov⁶⁴, B. Budick¹⁰⁸, V. Büscher⁸¹, L. Bugge¹¹⁷, O. Bulekov⁹⁶, A.C. Bundock⁷³, M. Bunse⁴², T. Buran¹¹⁷, H. Burckhart²⁹, S. Burdin⁷³, T. Burgess¹³, S. Burke¹²⁹, E. Busato³³, P. Bussey⁵³, C.P. Buszello¹⁶⁶, B. Butler¹⁴³, J.M. Butler²¹, C.M. Buttar⁵³, J.M. Butterworth⁷⁷, W. Buttinger²⁷, S. Cabrera Urbán¹⁶⁷, D. Caforio^{19a,19b}, O. Cakir^{3a}, P. Calafura¹⁴, G. Calderini⁷⁸, P. Calfayan⁹⁸, R. Calkins¹⁰⁶, L.P. Caloba^{23a}, R. Caloi^{132a,132b}, D. Calvet³³, S. Calvet³³, R. Camacho Toro³³, P. Camarri^{133a,133b}, D. Cameron¹¹⁷, L.M. Caminada¹⁴, S. Campana²⁹, M. Campanelli⁷⁷, V. Canale^{102a,102b}, F. Canelli^{30,g}, A. Canepa^{159a}, J. Cantero⁸⁰, L. Capasso^{102a,102b}, M.D.M. Capeans Garrido²⁹, I. Caprini^{25a}, M. Caprini^{25a}, D. Capriotti⁹⁹, M. Capua^{36a,36b}, R. Caputo⁸¹, R. Cardarelli^{133a}, T. Carli²⁹, G. Carlino^{102a}, L. Carminati^{89a,89b}, B. Caron⁸⁵, S. Caron¹⁰⁴, E. Carquin^{31b}, G.D. Carrillo Montoya¹⁷³, A.A. Carter⁷⁵, J.R. Carter²⁷, J. Carvalho^{124a,h}, D. Casadei¹⁰⁸, M.P. Casado¹¹, M. Cascella^{122a,122b}, C. Caso^{50a,50b,*}, A.M. Castaneda Hernandez¹⁷³, E. Castaneda-Miranda¹⁷³, V. Castillo Gimenez¹⁶⁷, N.F. Castro^{124a}, G. Cataldi^{72a}, P. Catastini⁵⁷, A. Catinaccio²⁹, J.R. Catmore²⁹, A. Cattai²⁹, G. Cattani^{133a,133b}, S. Caughron⁸⁸, D. Cauz^{164a,164c}, P. Cavalleri⁷⁸, D. Cavalli^{89a}, M. Cavalli-Sforza¹¹, V. Cavasinni^{122a,122b}, F. Ceradini^{134a,134b}, A.S. Cerqueira^{23b}, A. Cerri²⁹, L. Cerrito⁷⁵, F. Cerutti⁴⁷, S.A. Cetin^{18b}, A. Chafaq^{135a}, D. Chakraborty¹⁰⁶, I. Chalupkova¹²⁶, K. Chan², B. Chapleau⁸⁵, J.D. Chapman²⁷, J.W. Chapman⁸⁷, E. Chareyre⁷⁸, D.G. Charlton¹⁷, V. Chavda⁸², C.A. Chavez Barajas²⁹, S. Cheatham⁸⁵, S. Chekanov⁵, S.V. Chekulaev^{159a}, G.A. Chelkov⁶⁴, M.A. Chelstowska¹⁰⁴, C. Chen⁶³, H. Chen²⁴, S. Chen^{32c}, X. Chen¹⁷³, A. Cheplakov⁶⁴, R. Cherkaoui El Moursli^{135e}, V. Chernyatin²⁴,

E. Cheu⁶, S.L. Cheung¹⁵⁸, L. Chevalier¹³⁶, G. Chiefari^{102a,102b}, L. Chikovani^{51a}, J.T. Childers²⁹, A. Chilingarov⁷¹, G. Chiodini^{72a}, A.S. Chisholm¹⁷, R.T. Chislett⁷⁷, M.V. Chizhov⁶⁴, G. Choudalakis³⁰, S. Chouridou¹³⁷, I.A. Christidi⁷⁷, A. Christov⁴⁸, D. Chromek-Burckhart²⁹, M.L. Chu¹⁵¹, J. Chudoba¹²⁵, G. Ciapetti^{132a,132b}, A.K. Ciftci^{3a}, R. Ciftci^{3a}, D. Cinca³³, V. Cindro⁷⁴, C. Ciocca^{19a}, A. Ciocio¹⁴, M. Cirilli⁸⁷, M. Citterio^{89a}, M. Ciubancan^{25a}, A. Clark⁴⁹, P.J. Clark⁴⁵, W. Cleland¹²³, J.C. Clemens⁸³, B. Clement⁵⁵, C. Clement^{146a,146b}, Y. Coadou⁸³, M. Cobal^{164a,164c}, A. Coccaro¹³⁸, J. Cochran⁶³, P. Coe¹¹⁸, J.G. Cogan¹⁴³, J. Coggeshall¹⁶⁵, E. Cogneras¹⁷⁸, J. Colas⁴, A.P. Colijn¹⁰⁵, N.J. Collins¹⁷, C. Collins-Tooth⁵³, J. Collot⁵⁵, G. Colon⁸⁴, P. Conde Muiño^{124a}, E. Coniavitis¹¹⁸, M.C. Conidi¹¹, S.M. Consonni^{89a,89b}, V. Consorti⁴⁸, S. Constantinescu^{25a}, C. Conta^{119a,119b}, G. Conti⁵⁷, F. Conventi^{102a,i}, M. Cooke¹⁴, B.D. Cooper⁷⁷, A.M. Cooper-Sarkar¹¹⁸, K. Copic¹⁴, T. Cornelissen¹⁷⁵, M. Corradi^{19a}, F. Corriveau^{85,j}, A. Cortes-Gonzalez¹⁶⁵, G. Cortiana⁹⁹, G. Costa^{89a}, M.J. Costa¹⁶⁷, D. Costanzo¹³⁹, T. Costin³⁰, D. Côté²⁹, L. Courneyea¹⁶⁹, G. Cowan⁷⁶, C. Cowden²⁷, B.E. Cox⁸², K. Cranmer¹⁰⁸, F. Crescioli^{122a,122b}, M. Cristinziani²⁰, G. Crosetti^{36a,36b}, R. Crupi^{72a,72b}, S. Crépe-Renaudin⁵⁵, C.-M. Cuciuc^{25a}, C. Cuenca Almenar¹⁷⁶, T. Cuhadar Donszelmann¹³⁹, M. Curatolo⁴⁷, C.J. Curtis¹⁷, C. Cuthbert¹⁵⁰, P. Cwetanski⁶⁰, H. Cziri¹⁴¹, P. Czodrowski⁴³, Z. Czyczula¹⁷⁶, S. D'Auria⁵³, M. D'Onofrio⁷³, A. D'Orazio^{132a,132b}, C. Da Via⁸², W. Dabrowski³⁷, A. Dafinca¹¹⁸, T. Dai⁸⁷, C. Dallapiccola⁸⁴, M. Dam³⁵, M. Dameri^{50a,50b}, D.S. Damiani¹³⁷, H.O. Danielsson²⁹, V. Dao⁴⁹, G. Darbo^{50a}, G.L. Darlea^{25b}, W. Davey²⁰, T. Davidek¹²⁶, N. Davidson⁸⁶, R. Davidson⁷¹, E. Davies^{118,c}, M. Davies⁹³, A.R. Davison⁷⁷, Y. Davygora^{58a}, E. Dawe¹⁴², I. Dawson¹³⁹, R.K. Daya-Ishmukhametova²², K. De⁷, R. de Asmundis^{102a}, S. De Castro^{19a,19b}, S. De Cecco⁷⁸, J. de Graat⁹⁸, N. De Groot¹⁰⁴, P. de Jong¹⁰⁵, C. De La Taille¹¹⁵, H. De la Torre⁸⁰, F. De Lorenzi⁶³, B. De Lotto^{164a,164c}, L. de Mora⁷¹, L. De Nooij¹⁰⁵, D. De Pedis^{132a}, A. De Salvo^{132a}, U. De Sanctis^{164a,164c}, A. De Santo¹⁴⁹, J.B. De Vivie De Regie¹¹⁵, G. De Zorzi^{132a,132b}, W.J. Dearnaley⁷¹, R. Debbé²⁴, C. Debenedetti⁴⁵, B. Dechenaux⁵⁵, D.V. Dedovich⁶⁴, J. Degenhardt¹²⁰, C. Del Papa^{164a,164c}, J. Del Peso⁸⁰, T. Del Prete^{122a,122b}, T. Delemontex⁵⁵, M. Deliyergiyev⁷⁴, A. Dell'Acqua²⁹, L. Dell'Asta²¹, M. Della Pietra^{102a,i}, D. della Volpe^{102a,102b}, M. Delmastro⁴, P.A. Delsart⁵⁵, C. Deluca¹⁴⁸, S. Demers¹⁷⁶, M. Demichev⁶⁴, B. Demirköz^{11,k}, J. Deng¹⁶³, S.P. Denisov¹²⁸, D. Derendarz³⁸, J.E. Derkaoui^{135d}, F. Derue⁷⁸, P. Dervan⁷³, K. Desch²⁰, E. Devetak¹⁴⁸, P.O. Deviveiros¹⁰⁵, A. Dewhurst¹²⁹, B. DeWilde¹⁴⁸, S. Dhaliwal¹⁵⁸, R. Dhullipudi^{24,l}, A. Di Ciaccio^{133a,133b}, L. Di Ciaccio⁴, A. Di Girolamo²⁹, B. Di Girolamo²⁹, S. Di Luise^{134a,134b}, A. Di Mattia¹⁷³, B. Di Micco²⁹, R. Di Nardo⁴⁷, A. Di Simone^{133a,133b}, R. Di Sipio^{19a,19b}, M.A. Diaz^{31a}, F. Diblen^{18c}, E.B. Diehl⁸⁷, J. Dietrich⁴¹, T.A. Dietzsch^{58a}, S. Diglio⁸⁶, K. Dindar Yagci³⁹, J. Dingfelder²⁰, C. Dionisi^{132a,132b}, P. Dita^{25a}, S. Dita^{25a}, F. Dittus²⁹, F. Djama⁸³, T. Djobava^{51b}, M.A.B. do Vale^{23c}, A. Do Valle Wemans^{124a}, T.K.O. Doan⁴, M. Dobbs⁸⁵, R. Dobinson^{29,*}, D. Dobos²⁹, E. Dobson^{29,m}, J. Dodd³⁴, C. Doglioni⁴⁹, T. Doherty⁵³, Y. Doi^{65,*}, J. Dolejsi¹²⁶, I. Dolenc⁷⁴, Z. Dolezal¹²⁶, B.A. Dolgoshein^{96,*}, T. Dohmae¹⁵⁵, M. Donadelli^{23d}, M. Donega¹²⁰, J. Donini³³, J. Dopke²⁹, A. Doria^{102a}, A. Dos Anjos¹⁷³, A. Dotti^{122a,122b}, M.T. Dova⁷⁰, A.D. Doxiadis¹⁰⁵, A.T. Doyle⁵³, M. Dris⁹, J. Dubbert⁹⁹, S. Dube¹⁴, E. Duchovni¹⁷², G. Duckeck⁹⁸, A. Dudarev²⁹,

F. Dudziak⁶³, M. Dührssen²⁹, I.P. Duerdoth⁸², L. Duflot¹¹⁵, M-A. Dufour⁸⁵, M. Dunford²⁹, H. Duran Yildiz^{3a}, R. Duxfield¹³⁹, M. Dwuznik³⁷, F. Dydak²⁹, M. Düren⁵², J. Ebke⁹⁸, S. Eckweiler⁸¹, K. Edmonds⁸¹, C.A. Edwards⁷⁶, N.C. Edwards⁵³, W. Ehrenfeld⁴¹, T. Eifert¹⁴³, G. Eigen¹³, K. Einsweiler¹⁴, E. Eisenhandler⁷⁵, T. Ekelof¹⁶⁶, M. El Kacimi^{135c}, M. Ellert¹⁶⁶, S. Elles⁴, F. Ellinghaus⁸¹, K. Ellis⁷⁵, N. Ellis²⁹, J. Elmsheuser⁹⁸, M. Elsing²⁹, D. Emelianov¹²⁹, R. Engelmann¹⁴⁸, A. Engl⁹⁸, B. Epp⁶¹, A. Eppig⁸⁷, J. Erdmann⁵⁴, A. Ereditato¹⁶, D. Eriksson^{146a}, J. Ernst¹, M. Ernst²⁴, J. Ernwein¹³⁶, D. Errede¹⁶⁵, S. Errede¹⁶⁵, E. Ertel⁸¹, M. Escalier¹¹⁵, C. Escobar¹²³, X. Espinal Curull¹¹, B. Esposito⁴⁷, F. Etienne⁸³, A.I. Etievre¹³⁶, E. Etzion¹⁵³, D. Evangelakou⁵⁴, H. Evans⁶⁰, L. Fabbri^{19a,19b}, C. Fabre²⁹, R.M. Fakhrutdinov¹²⁸, S. Falciano^{132a}, Y. Fang¹⁷³, M. Fanti^{89a,89b}, A. Farbin⁷, A. Farilla^{134a}, J. Farley¹⁴⁸, T. Farooque¹⁵⁸, S. Farrell¹⁶³, S.M. Farrington¹¹⁸, P. Farthouat²⁹, P. Fassnacht²⁹, D. Fassouliotis⁸, B. Fatholahzadeh¹⁵⁸, A. Favareto^{89a,89b}, L. Fayard¹¹⁵, S. Fazio^{36a,36b}, R. Febbraro³³, P. Federic^{144a}, O.L. Fedin¹²¹, W. Fedorko⁸⁸, M. Fehling-Kaschek⁴⁸, L. Felgioni⁸³, D. Fellmann⁵, C. Feng^{32d}, E.J. Feng³⁰, A.B. Fenyuk¹²⁸, J. Ferencei^{144b}, W. Fernando⁵, S. Ferrag⁵³, J. Ferrando⁵³, V. Ferrara⁴¹, A. Ferrari¹⁶⁶, P. Ferrari¹⁰⁵, R. Ferrari^{119a}, D.E. Ferreira de Lima⁵³, A. Ferrer¹⁶⁷, D. Ferrere⁴⁹, C. Ferretti⁸⁷, A. Ferretto Parodi^{50a,50b}, M. Fiascaris³⁰, F. Fiedler⁸¹, A. Filipčič⁷⁴, F. Filthaut¹⁰⁴, M. Fincke-Keeler¹⁶⁹, M.C.N. Fiolhais^{124a,h}, L. Fiorini¹⁶⁷, A. Firan³⁹, G. Fischer⁴¹, M.J. Fisher¹⁰⁹, M. Flechl⁴⁸, I. Fleck¹⁴¹, J. Fleckner⁸¹, P. Fleischmann¹⁷⁴, S. Fleischmann¹⁷⁵, T. Flick¹⁷⁵, A. Floderus⁷⁹, L.R. Flores Castillo¹⁷³, M.J. Flowerdew⁹⁹, T. Fonseca Martin¹⁶, D.A. Forbush¹³⁸, A. Formica¹³⁶, A. Forti⁸², D. Fortin^{159a}, D. Fournier¹¹⁵, H. Fox⁷¹, P. Francavilla¹¹, S. Franchino^{119a,119b}, D. Francis²⁹, T. Frank¹⁷², M. Franklin⁵⁷, S. Franz²⁹, M. Fraternali^{119a,119b}, S. Fratina¹²⁰, S.T. French²⁷, C. Friedrich⁴¹, F. Friedrich⁴³, R. Froeschl²⁹, D. Froidevaux²⁹, J.A. Frost²⁷, C. Fukunaga¹⁵⁶, E. Fullana Torregrosa²⁹, B.G. Fulson¹⁴³, J. Fuster¹⁶⁷, C. Gabaldon²⁹, O. Gabizon¹⁷², T. Gadfort²⁴, S. Gadomski⁴⁹, G. Gagliardi^{50a,50b}, P. Gagnon⁶⁰, C. Galea⁹⁸, E.J. Gallas¹¹⁸, V. Gallo¹⁶, B.J. Gallop¹²⁹, P. Gallus¹²⁵, K.K. Gan¹⁰⁹, Y.S. Gao^{143,e}, A. Gaponenko¹⁴, F. Garbersen¹⁷⁶, M. Garcia-Sciveres¹⁴, C. García¹⁶⁷, J.E. García Navarro¹⁶⁷, R.W. Gardner³⁰, N. Garelli²⁹, H. Garitaonandia¹⁰⁵, V. Garonne²⁹, J. Garvey¹⁷, C. Gatti⁴⁷, G. Gaudio^{119a}, B. Gaur¹⁴¹, L. Gauthier¹³⁶, P. Gauzzi^{132a,132b}, I.L. Gavrilenko⁹⁴, C. Gay¹⁶⁸, G. Gaycken²⁰, E.N. Gazis⁹, P. Ge^{32d}, Z. Gecse¹⁶⁸, C.N.P. Gee¹²⁹, D.A.A. Geerts¹⁰⁵, Ch. Geich-Gimbel²⁰, K. Gellerstedt^{146a,146b}, C. Gemme^{50a}, A. Gemmel⁵³, M.H. Genest⁵⁵, S. Gentile^{132a,132b}, M. George⁵⁴, S. George⁷⁶, P. Gerlach¹⁷⁵, A. Gershon¹⁵³, C. Geweniger^{58a}, H. Ghazlane^{135b}, N. Ghodbane³³, B. Giacobbe^{19a}, S. Giagu^{132a,132b}, V. Giakoumopoulou⁸, V. Giangiobbe¹¹, F. Gianotti²⁹, B. Gibbard²⁴, A. Gibson¹⁵⁸, S.M. Gibson²⁹, D. Gillberg²⁸, A.R. Gillman¹²⁹, D.M. Gingrich^{2,d}, J. Ginzburg¹⁵³, N. Giokaris⁸, M.P. Giordani^{164c}, R. Giordano^{102a,102b}, F.M. Giorgi¹⁵, P. Giovannini⁹⁹, P.F. Giraud¹³⁶, D. Giugni^{89a}, M. Giunta⁹³, P. Giusti^{19a}, B.K. Gjelsten¹¹⁷, L.K. Gladilin⁹⁷, C. Glasman⁸⁰, J. Glatzer⁴⁸, A. Glazov⁴¹, K.W. Glitza¹⁷⁵, G.L. Glonti⁶⁴, J.R. Goddard⁷⁵, J. Godfrey¹⁴², J. Godlewski²⁹, M. Goebel⁴¹, T. Göpfert⁴³, C. Goeringer⁸¹, C. Gössling⁴², T. Göttfert⁹⁹, S. Goldfarb⁸⁷, T. Golling¹⁷⁶, A. Gomes^{124a,b}, L.S. Gomez Fajardo⁴¹, R. Gonçalo⁷⁶, J. Goncalves Pinto Firmino Da Costa⁴¹, L. Gonella²⁰, S. Gonzalez¹⁷³, S. González de la Hoz¹⁶⁷, G. Gonzalez Parra¹¹, M.L. Gonzalez Silva²⁶,

S. Gonzalez-Sevilla⁴⁹, J.J. Goodson¹⁴⁸, L. Goossens²⁹, P.A. Gorbounov⁹⁵, H.A. Gordon²⁴, I. Gorelov¹⁰³, G. Gorfine¹⁷⁵, B. Gorini²⁹, E. Gorini^{72a,72b}, A. Gorišek⁷⁴, E. Gornicki³⁸, B. Gosdzik⁴¹, A.T. Goshaw⁵, M. Gosselink¹⁰⁵, M.I. Gostkin⁶⁴, I. Gough Eschrich¹⁶³, M. Gouighri^{135a}, D. Goujdami^{135c}, M.P. Goulette⁴⁹, A.G. Goussiou¹³⁸, C. Goy⁴, S. Gozpinar²², I. Grabowska-Bold³⁷, P. Grafström²⁹, K.-J. Grahm⁴¹, F. Grancagnolo^{72a}, S. Grancagnolo¹⁵, V. Grassi¹⁴⁸, V. Gratchev¹²¹, N. Grau³⁴, H.M. Gray²⁹, J.A. Gray¹⁴⁸, E. Graziani^{134a}, O.G. Grebenyuk¹²¹, T. Greenshaw⁷³, Z.D. Greenwood^{24,l}, K. Gregersen³⁵, I.M. Gregor⁴¹, P. Grenier¹⁴³, J. Griffiths¹³⁸, N. Grigalashvili⁶⁴, A.A. Grillo¹³⁷, S. Grinstein¹¹, Y.V. Grishkevich⁹⁷, J.-F. Grivaz¹¹⁵, E. Gross¹⁷², J. Grosse-Knetter⁵⁴, J. Groth-Jensen¹⁷², K. Grybel¹⁴¹, D. Guest¹⁷⁶, C. Guicheney³³, A. Guida^{72a,72b}, S. Guindon⁵⁴, H. Guler^{85,n}, J. Gunther¹²⁵, B. Guo¹⁵⁸, J. Guo³⁴, V.N. Gushchin¹²⁸, P. Gutierrez¹¹¹, N. Guttman¹⁵³, O. Gutzwiller¹⁷³, C. Guyot¹³⁶, C. Gwenlan¹¹⁸, C.B. Gwilliam⁷³, A. Haas¹⁴³, S. Haas²⁹, C. Haber¹⁴, H.K. Hadavand³⁹, D.R. Hadley¹⁷, P. Haefner⁹⁹, F. Hahn²⁹, S. Haider²⁹, Z. Hajduk³⁸, H. Hakobyan¹⁷⁷, D. Hall¹¹⁸, J. Haller⁵⁴, K. Hamacher¹⁷⁵, P. Hamal¹¹³, M. Hamer⁵⁴, A. Hamilton^{145b,o}, S. Hamilton¹⁶¹, L. Han^{32b}, K. Hanagaki¹¹⁶, K. Hanawa¹⁶⁰, M. Hance¹⁴, C. Handel⁸¹, P. Hanke^{58a}, J.R. Hansen³⁵, J.B. Hansen³⁵, J.D. Hansen³⁵, P.H. Hansen³⁵, P. Hansson¹⁴³, K. Hara¹⁶⁰, G.A. Hare¹³⁷, T. Harenberg¹⁷⁵, S. Harkusha⁹⁰, D. Harper⁸⁷, R.D. Harrington⁴⁵, O.M. Harris¹³⁸, K. Harrison¹⁷, J. Hartert⁴⁸, F. Hartjes¹⁰⁵, T. Haruyama⁶⁵, A. Harvey⁵⁶, S. Hasegawa¹⁰¹, Y. Hasegawa¹⁴⁰, S. Hassani¹³⁶, S. Haug¹⁶, M. Hauschild²⁹, R. Hauser⁸⁸, M. Havranek²⁰, C.M. Hawkes¹⁷, R.J. Hawkins²⁹, A.D. Hawkins⁷⁹, D. Hawkins¹⁶³, T. Hayakawa⁶⁶, T. Hayashi¹⁶⁰, D. Hayden⁷⁶, H.S. Hayward⁷³, S.J. Haywood¹²⁹, M. He^{32d}, S.J. Head¹⁷, V. Hedberg⁷⁹, L. Heelan⁷, S. Heim⁸⁸, B. Heinemann¹⁴, S. Heisterkamp³⁵, L. Helary⁴, C. Heller⁹⁸, M. Heller²⁹, S. Hellman^{146a,146b}, D. Hellmich²⁰, C. Helsen¹¹, R.C.W. Henderson⁷¹, M. Henke^{58a}, A. Henrichs⁵⁴, A.M. Henriques Correia²⁹, S. Henrot-Versille¹¹⁵, F. Henry-Couannier⁸³, C. Hensel⁵⁴, T. Henß¹⁷⁵, C.M. Hernandez⁷, Y. Hernández Jiménez¹⁶⁷, R. Herrberg¹⁵, G. Herten⁴⁸, R. Hertenberger⁹⁸, L. Hervas²⁹, G.G. Hesketh⁷⁷, N.P. Hessey¹⁰⁵, E. Higón-Rodriguez¹⁶⁷, J.C. Hill²⁷, K.H. Hiller⁴¹, S. Hillert²⁰, S.J. Hillier¹⁷, I. Hinchliffe¹⁴, E. Hines¹²⁰, M. Hirose¹¹⁶, F. Hirsch⁴², D. Hirschbuehl¹⁷⁵, J. Hobbs¹⁴⁸, N. Hod¹⁵³, M.C. Hodgkinson¹³⁹, P. Hodgson¹³⁹, A. Hoecker²⁹, M.R. Hoferkamp¹⁰³, J. Hoffman³⁹, D. Hoffmann⁸³, M. Hohlfeld⁸¹, M. Holder¹⁴¹, S.O. Holmgren^{146a}, T. Holy¹²⁷, J.L. Holzbauer⁸⁸, T.M. Hong¹²⁰, L. Hooft van Huysduynen¹⁰⁸, C. Horn¹⁴³, S. Horner⁴⁸, J.-Y. Hostachy⁵⁵, S. Hou¹⁵¹, A. Hoummada^{135a}, J. Howarth⁸², I. Hristova¹⁵, J. Hrivnac¹¹⁵, I. Hruska¹²⁵, T. Hryn'ova⁴, P.J. Hsu⁸¹, S.-C. Hsu¹⁴, Z. Hubacek¹²⁷, F. Hubaut⁸³, F. Huegging²⁰, A. Huettmann⁴¹, T.B. Huffman¹¹⁸, E.W. Hughes³⁴, G. Hughes⁷¹, M. Huhtinen²⁹, M. Hurwitz¹⁴, U. Husemann⁴¹, N. Huseynov^{64,p}, J. Huston⁸⁸, J. Huth⁵⁷, G. Iacobucci⁴⁹, G. Iakovidis⁹, M. Ibbotson⁸², I. Ibragimov¹⁴¹, L. Iconomidou-Fayard¹¹⁵, J. Idarraga¹¹⁵, P. Iengo^{102a}, O. Igonkina¹⁰⁵, Y. Ikegami⁶⁵, M. Ikeno⁶⁵, D. Iliadis¹⁵⁴, N. Ilic¹⁵⁸, M. Imori¹⁵⁵, T. Ince²⁰, J. Inigo-Golfín²⁹, P. Ioannou⁸, M. Iodice^{134a}, K. Iordanidou⁸, V. Ippolito^{132a,132b}, A. Irles Quiles¹⁶⁷, C. Isaksson¹⁶⁶, A. Ishikawa⁶⁶, M. Ishino⁶⁷, R. Ishmukhametov³⁹, C. Issever¹¹⁸, S. Istin^{18a}, A.V. Ivashin¹²⁸, W. Iwanski³⁸, H. Iwasaki⁶⁵, J.M. Izen⁴⁰, V. Izzo^{102a}, B. Jackson¹²⁰, J.N. Jackson⁷³, P. Jackson¹⁴³, M.R. Jaekel²⁹, V. Jain⁶⁰,

K. Jakobs⁴⁸, S. Jakobsen³⁵, J. Jakubek¹²⁷, D.K. Jana¹¹¹, E. Jansen⁷⁷, H. Jansen²⁹,
 A. Jantsch⁹⁹, M. Janus⁴⁸, G. Jarlskog⁷⁹, L. Jeanty⁵⁷, I. Jen-La Plante³⁰, P. Jenni²⁹,
 A. Jeremie⁴, P. Jež³⁵, S. Jézéquel⁴, M.K. Jha^{19a}, H. Ji¹⁷³, W. Ji⁸¹, J. Jia¹⁴⁸,
 Y. Jiang^{32b}, M. Jimenez Belenguer⁴¹, S. Jin^{32a}, O. Jinnouchi¹⁵⁷, M.D. Joergensen³⁵,
 D. Joffe³⁹, L.G. Johansen¹³, M. Johansen^{146a,146b}, K.E. Johansson^{146a}, P. Johansson¹³⁹,
 S. Johnert⁴¹, K.A. Johns⁶, K. Jon-And^{146a,146b}, G. Jones¹¹⁸, R.W.L. Jones⁷¹, T.J. Jones⁷³,
 C. Joram²⁹, P.M. Jorge^{124a}, K.D. Joshi⁸², J. Jovicevic¹⁴⁷, T. Jovin^{12b}, X. Ju¹⁷³,
 C.A. Jung⁴², R.M. Jungst²⁹, V. Juranek¹²⁵, P. Jussel⁶¹, A. Juste Rozas¹¹, S. Kabana¹⁶,
 M. Kaci¹⁶⁷, A. Kaczmarska³⁸, P. Kadlecik³⁵, M. Kado¹¹⁵, H. Kagan¹⁰⁹, M. Kagan⁵⁷,
 E. Kajomovitz¹⁵², S. Kalinin¹⁷⁵, L.V. Kalinovskaya⁶⁴, S. Kama³⁹, N. Kanaya¹⁵⁵,
 M. Kaneda²⁹, S. Kaneti²⁷, T. Kanno¹⁵⁷, V.A. Kantserov⁹⁶, J. Kanzaki⁶⁵, B. Kaplan¹⁷⁶,
 A. Kapliy³⁰, J. Kaplon²⁹, D. Kar⁵³, M. Karagounis²⁰, M. Karnevskiy⁴¹, V. Kartvelishvili⁷¹,
 A.N. Karyukhin¹²⁸, L. Kashif¹⁷³, G. Kasieczka^{58b}, R.D. Kass¹⁰⁹, A. Kastanas¹³,
 M. Kataoka⁴, Y. Kataoka¹⁵⁵, E. Katsoufis⁹, J. Katzy⁴¹, V. Kaushik⁶, K. Kawagoe⁶⁹,
 T. Kawamoto¹⁵⁵, G. Kawamura⁸¹, M.S. Kayl¹⁰⁵, V.A. Kazanin¹⁰⁷, M.Y. Kazarinov⁶⁴,
 R. Keeler¹⁶⁹, R. Kehoe³⁹, M. Keil⁵⁴, G.D. Kekelidze⁶⁴, J.S. Keller¹³⁸, J. Kennedy⁹⁸,
 M. Kenyon⁵³, O. Kepka¹²⁵, N. Kerschen²⁹, B.P. Kerševan⁷⁴, S. Kersten¹⁷⁵, K. Kessoku¹⁵⁵,
 J. Keung¹⁵⁸, F. Khalil-zada¹⁰, H. Khandanyan¹⁶⁵, A. Khanov¹¹², D. Kharchenko⁶⁴,
 A. Khodinov⁹⁶, A. Khomich^{58a}, T.J. Khoo²⁷, G. Khoriauli²⁰, A. Khoroshilov¹⁷⁵,
 V. Khovanskiy⁹⁵, E. Khramov⁶⁴, J. Khubua^{51b}, H. Kim^{146a,146b}, M.S. Kim², S.H. Kim¹⁶⁰,
 N. Kimura¹⁷¹, O. Kind¹⁵, B.T. King⁷³, M. King⁶⁶, R.S.B. King¹¹⁸, J. Kirk¹²⁹,
 A.E. Kiryunin⁹⁹, T. Kishimoto⁶⁶, D. Kisielewska³⁷, T. Kittelmann¹²³, A.M. Kiver¹²⁸,
 E. Kladiva^{144b}, M. Klein⁷³, U. Klein⁷³, K. Kleinknecht⁸¹, M. Klemetti⁸⁵, A. Klier¹⁷²,
 P. Klimek^{146a,146b}, A. Klimentov²⁴, R. Klingenberg⁴², J.A. Klinger⁸², E.B. Klinkby³⁵,
 T. Klioutchnikova²⁹, P.F. Klok¹⁰⁴, S. Klous¹⁰⁵, E.-E. Kluge^{58a}, T. Kluge⁷³, P. Kluit¹⁰⁵,
 S. Kluth⁹⁹, N.S. Knecht¹⁵⁸, E. Kneringer⁶¹, E.B.F.G. Knoops⁸³, A. Knue⁵⁴, B.R. Ko⁴⁴,
 T. Kobayashi¹⁵⁵, M. Kobel⁴³, M. Kocian¹⁴³, P. Kodys¹²⁶, K. Köneke²⁹, A.C. König¹⁰⁴,
 S. Koenig⁸¹, L. Köpke⁸¹, F. Koetsveld¹⁰⁴, P. Koevesarki²⁰, T. Koffas²⁸, E. Koffeman¹⁰⁵,
 L.A. Kogan¹¹⁸, S. Kohlmann¹⁷⁵, F. Kohn⁵⁴, Z. Kohout¹²⁷, T. Kohriki⁶⁵, T. Koi¹⁴³,
 G.M. Kolachev¹⁰⁷, H. Kolanoski¹⁵, V. Kolesnikov⁶⁴, I. Koletsou^{89a}, J. Koll⁸⁸,
 M. Kollfrath⁴⁸, A.A. Komar⁹⁴, Y. Komori¹⁵⁵, T. Kondo⁶⁵, T. Kono^{41,q}, A.I. Kononov⁴⁸,
 R. Konoplich^{108,r}, N. Konstantinidis⁷⁷, A. Kootz¹⁷⁵, S. Koperny³⁷, A.K. Kopp⁴⁸,
 K. Korcyl³⁸, K. Kordas¹⁵⁴, A. Korn¹¹⁸, A. Korol¹⁰⁷, I. Korolkov¹¹, E.V. Korolkova¹³⁹,
 V.A. Korotkov¹²⁸, O. Kortner⁹⁹, S. Kortner⁹⁹, V.V. Kostyukhin²⁰, S. Kotov⁹⁹,
 V.M. Kotov⁶⁴, A. Kotwal⁴⁴, C. Kourkouvelis⁸, V. Kouskoura¹⁵⁴, A. Koutsman^{159a},
 R. Kowalewski¹⁶⁹, T.Z. Kowalski³⁷, W. Kozanecki¹³⁶, A.S. Kozhin¹²⁸, V. Kral¹²⁷,
 V.A. Kramarenko⁹⁷, G. Kramberger⁷⁴, M.W. Krasny⁷⁸, A. Krasznahorkay¹⁰⁸, J. Kraus⁸⁸,
 J.K. Kraus²⁰, F. Krejci¹²⁷, J. Kretzschmar⁷³, N. Krieger⁵⁴, P. Krieger¹⁵⁸, K. Kroeninger⁵⁴,
 H. Kroha⁹⁹, J. Kroll¹²⁰, J. Kroseberg²⁰, J. Krstic^{12a}, U. Kruchonak⁶⁴, H. Krüger²⁰,
 T. Kruker¹⁶, N. Krumnack⁶³, Z.V. Krumshteyn⁶⁴, A. Kruth²⁰, T. Kubota⁸⁶, S. Kuday^{3a},
 S. Kuehn⁴⁸, A. Kugel^{58c}, T. Kuhl⁴¹, D. Kuhn⁶¹, V. Kukhtin⁶⁴, Y. Kulchitsky⁹⁰,
 S. Kuleshov^{31b}, C. Kummer⁹⁸, M. Kuna⁷⁸, J. Kunkle¹²⁰, A. Kupco¹²⁵, H. Kurashige⁶⁶,
 M. Kurata¹⁶⁰, Y.A. Kurochkin⁹⁰, V. Kus¹²⁵, E.S. Kuwertz¹⁴⁷, M. Kuze¹⁵⁷, J. Kvita¹⁴²,

R. Kwee¹⁵, A. La Rosa⁴⁹, L. La Rotonda^{36a,36b}, L. Labarga⁸⁰, J. Labbe⁴, S. Lablak^{135a}, C. Lacasta¹⁶⁷, F. Lacava^{132a,132b}, H. Lacker¹⁵, D. Lacour⁷⁸, V.R. Lacuesta¹⁶⁷, E. Ladygin⁶⁴, R. Lafaye⁴, B. Laforge⁷⁸, T. Lagouri⁸⁰, S. Lai⁴⁸, E. Laisne⁵⁵, M. Lamanna²⁹, L. Lambourne⁷⁷, C.L. Lampen⁶, W. Lampl⁶, E. Lancon¹³⁶, U. Landgraf⁴⁸, M.P.J. Landon⁷⁵, J.L. Lane⁸², C. Lange⁴¹, A.J. Lankford¹⁶³, F. Lanni²⁴, K. Lantzsch¹⁷⁵, S. Laplace⁷⁸, C. Lapoire²⁰, J.F. Laporte¹³⁶, T. Lari^{89a}, A. Lerner¹¹⁸, M. Lassnig²⁹, P. Laurelli⁴⁷, V. Lavorini^{36a,36b}, W. Lavrijsen¹⁴, P. Laycock⁷³, O. Le Dortz⁷⁸, E. Le Guirriec⁸³, C. Le Maner¹⁵⁸, E. Le Menedeu¹¹, T. LeCompte⁵, F. Ledroit-Guillon⁵⁵, H. Lee¹⁰⁵, J.S.H. Lee¹¹⁶, S.C. Lee¹⁵¹, L. Lee¹⁷⁶, M. Lefebvre¹⁶⁹, M. Legendre¹³⁶, B.C. LeGeyt¹²⁰, F. Legger⁹⁸, C. Leggett¹⁴, M. Lehmacher²⁰, G. Lehmann Miotto²⁹, X. Lei⁶, M.A.L. Leite^{23d}, R. Leitner¹²⁶, D. Lellouch¹⁷², B. Lemmer⁵⁴, V. Lendermann^{58a}, K.J.C. Leney^{145b}, T. Lenz¹⁰⁵, G. Lenzen¹⁷⁵, B. Lenzi²⁹, K. Leonhardt⁴³, S. Leontsinis⁹, F. Lepold^{58a}, C. Leroy⁹³, J-R. Lessard¹⁶⁹, C.G. Lester²⁷, C.M. Lester¹²⁰, J. Levêque⁴, D. Levin⁸⁷, L.J. Levinson¹⁷², A. Lewis¹¹⁸, G.H. Lewis¹⁰⁸, A.M. Leyko²⁰, M. Leyton¹⁵, B. Li⁸³, H. Li^{173,s}, S. Li^{32b,t}, X. Li⁸⁷, Z. Liang^{118,u}, H. Liao³³, B. Liberti^{133a}, P. Lichard²⁹, M. Lichtnecker⁹⁸, K. Lie¹⁶⁵, W. Liebig¹³, C. Limbach²⁰, A. Limosani⁸⁶, M. Limper⁶², S.C. Lin^{151,v}, F. Linde¹⁰⁵, J.T. Linnemann⁸⁸, E. Lipeles¹²⁰, A. Lipniacka¹³, T.M. Liss¹⁶⁵, D. Lissauer²⁴, A. Lister⁴⁹, A.M. Litke¹³⁷, C. Liu²⁸, D. Liu¹⁵¹, H. Liu⁸⁷, J.B. Liu⁸⁷, M. Liu^{32b}, Y. Liu^{32b}, M. Livan^{119a,119b}, S.S.A. Livermore¹¹⁸, A. Lleres⁵⁵, J. Llorente Merino⁸⁰, S.L. Lloyd⁷⁵, E. Lobodzinska⁴¹, P. Loch⁶, W.S. Lockman¹³⁷, T. Loddenkoetter²⁰, F.K. Loebinger⁸², A. Loginov¹⁷⁶, C.W. Loh¹⁶⁸, T. Lohse¹⁵, K. Lohwasser⁴⁸, M. Lokajicek¹²⁵, V.P. Lombardo⁴, R.E. Long⁷¹, L. Lopes^{124a}, D. Lopez Mateos⁵⁷, J. Lorenz⁹⁸, N. Lorenzo Martinez¹¹⁵, M. Losada¹⁶², P. Loscutoff¹⁴, F. Lo Sterzo^{132a,132b}, M.J. Losty^{159a}, X. Lou⁴⁰, A. Lounis¹¹⁵, K.F. Loureiro¹⁶², J. Love²¹, P.A. Love⁷¹, A.J. Lowe^{143,e}, F. Lu^{32a}, H.J. Lubatti¹³⁸, C. Luci^{132a,132b}, A. Lucotte⁵⁵, A. Ludwig⁴³, D. Ludwig⁴¹, I. Ludwig⁴⁸, J. Ludwig⁴⁸, F. Luehring⁶⁰, G. Luijckx¹⁰⁵, W. Lukas⁶¹, D. Lumb⁴⁸, L. Luminari^{132a}, E. Lund¹¹⁷, B. Lund-Jensen¹⁴⁷, B. Lundberg⁷⁹, J. Lundberg^{146a,146b}, J. Lundquist³⁵, M. Lungwitz⁸¹, D. Lynn²⁴, J. Lys¹⁴, E. Lytken⁷⁹, H. Ma²⁴, L.L. Ma¹⁷³, J.A. Macana Goia⁹³, G. Maccarrone⁴⁷, A. Macchiolo⁹⁹, B. Maček⁷⁴, J. Machado Miguens^{124a}, R. Mackeprang³⁵, R.J. Madaras¹⁴, W.F. Mader⁴³, A.K. Madsen¹⁶⁶, R. Maenner^{58c}, T. Maeno²⁴, P. Mättig¹⁷⁵, S. Mättig⁴¹, L. Magnoni²⁹, E. Magradze⁵⁴, K. Mahboubi⁴⁸, S. Mahmoud⁷³, G. Mahout¹⁷, C. Maiani^{132a,132b}, C. Maidantchik^{23a}, A. Maio^{124a,b}, S. Majewski²⁴, Y. Makida⁶⁵, N. Makovec¹¹⁵, P. Mal¹³⁶, B. Malaescu²⁹, Pa. Malecki³⁸, P. Malecki³⁸, V.P. Maleev¹²¹, F. Malek⁵⁵, U. Mallik⁶², D. Malon⁵, C. Malone¹⁴³, S. Maltezos⁹, V. Malyshev¹⁰⁷, S. Malyukov²⁹, R. Mameghani⁹⁸, J. Mamuzic^{12b}, A. Manabe⁶⁵, L. Mandelli^{89a}, I. Mandić⁷⁴, R. Mandrysch¹⁵, J. Maneira^{124a}, P.S. Mangear⁸⁸, L. Manhaes de Andrade Filho^{23a}, A. Mann⁵⁴, P.M. Manning¹³⁷, A. Manousakis-Katsikakis⁸, B. Mansoulie¹³⁶, A. Mapelli²⁹, L. Mapelli²⁹, L. March⁸⁰, J.F. Marchand²⁸, F. Marchese^{133a,133b}, G. Marchiori⁷⁸, M. Marcisovsky¹²⁵, C.P. Marino¹⁶⁹, F. Marroquim^{23a}, Z. Marshall²⁹, F.K. Martens¹⁵⁸, S. Marti-Garcia¹⁶⁷, B. Martin²⁹, B. Martin⁸⁸, J.P. Martin⁹³, T.A. Martin¹⁷, V.J. Martin⁴⁵, B. Martin dit Latour⁴⁹, S. Martin-Haugh¹⁴⁹, M. Martinez¹¹, V. Martinez Outschoorn⁵⁷, A.C. Martyniuk¹⁶⁹, M. Marx⁸², F. Marzano^{132a}, A. Marzin¹¹¹, L. Masetti⁸¹, T. Mashimo¹⁵⁵, R. Mashinistov⁹⁴,

J. Masik⁸², A.L. Maslennikov¹⁰⁷, I. Massa^{19a,19b}, G. Massaro¹⁰⁵, N. Massol⁴, P. Mastrandrea^{132a,132b}, A. Mastroberardino^{36a,36b}, T. Masubuchi¹⁵⁵, P. Matricon¹¹⁵, H. Matsunaga¹⁵⁵, T. Matsushita⁶⁶, C. Mattravers^{118,c}, J. Maurer⁸³, S.J. Maxfield⁷³, A. Mayne¹³⁹, R. Mazini¹⁵¹, M. Mazur²⁰, L. Mazzaferro^{133a,133b}, M. Mazzanti^{89a}, S.P. Mc Kee⁸⁷, A. McCarn¹⁶⁵, R.L. McCarthy¹⁴⁸, T.G. McCarthy²⁸, N.A. McCubbin¹²⁹, K.W. McFarlane⁵⁶, J.A. Mcfayden¹³⁹, H. McGlone⁵³, G. Mchedlidze^{51b}, T. McLaughlan¹⁷, S.J. McMahan¹²⁹, R.A. McPherson^{169,j}, A. Meade⁸⁴, J. Mechnich¹⁰⁵, M. Mechtel¹⁷⁵, M. Medinnis⁴¹, R. Meera-Lebbai¹¹¹, T. Meguro¹¹⁶, S. Mehlhase³⁵, A. Mehta⁷³, K. Meier^{58a}, B. Meirose⁷⁹, C. Melachrinou³⁰, B.R. Mellado Garcia¹⁷³, F. Meloni^{89a,89b}, L. Mendoza Navas¹⁶², Z. Meng^{151,s}, A. Mengarelli^{19a,19b}, S. Menke⁹⁹, E. Meoni¹¹, K.M. Mercurio⁵⁷, P. Mermod⁴⁹, L. Merola^{102a,102b}, C. Meroni^{89a}, F.S. Merritt³⁰, H. Merritt¹⁰⁹, A. Messina^{29,w}, J. Metcalfe¹⁰³, A.S. Mete⁶³, C. Meyer⁸¹, C. Meyer³⁰, J-P. Meyer¹³⁶, J. Meyer¹⁷⁴, J. Meyer⁵⁴, T.C. Meyer²⁹, W.T. Meyer⁶³, J. Miao^{32d}, S. Michal²⁹, L. Micu^{25a}, R.P. Middleton¹²⁹, S. Migas⁷³, L. Mijović⁴¹, G. Mikenberg¹⁷², M. Mikestikova¹²⁵, M. Mikuž⁷⁴, D.W. Miller³⁰, R.J. Miller⁸⁸, W.J. Mills¹⁶⁸, C. Mills⁵⁷, A. Milov¹⁷², D.A. Milstead^{146a,146b}, D. Milstein¹⁷², A.A. Minaenko¹²⁸, M. Miñano Moya¹⁶⁷, I.A. Minashvili⁶⁴, A.I. Mincer¹⁰⁸, B. Mindur³⁷, M. Mineev⁶⁴, Y. Ming¹⁷³, L.M. Mir¹¹, G. Mirabelli^{132a}, A. Misiejuk⁷⁶, J. Mitrevski¹³⁷, V.A. Mitsou¹⁶⁷, S. Mitsui⁶⁵, P.S. Miyagawa¹³⁹, K. Miyazaki⁶⁶, J.U. Mjörnmark⁷⁹, T. Moa^{146a,146b}, P. Mockett¹³⁸, S. Moed⁵⁷, V. Moeller²⁷, K. Mönig⁴¹, N. Möser²⁰, S. Mohapatra¹⁴⁸, W. Mohr⁴⁸, R. Moles-Valls¹⁶⁷, J. Molina-Perez²⁹, J. Monk⁷⁷, E. Monnier⁸³, S. Montesano^{89a,89b}, F. Monticelli⁷⁰, S. Monzani^{19a,19b}, R.W. Moore², G.F. Moorhead⁸⁶, C. Mora Herrera⁴⁹, A. Moraes⁵³, N. Morange¹³⁶, J. Morel⁵⁴, G. Morello^{36a,36b}, D. Moreno⁸¹, M. Moreno Llacer¹⁶⁷, P. Morettini^{50a}, M. Morgenstern⁴³, M. Morii⁵⁷, J. Morin⁷⁵, A.K. Morley²⁹, G. Mornacchi²⁹, J.D. Morris⁷⁵, L. Morvaj¹⁰¹, H.G. Moser⁹⁹, M. Mosidze^{51b}, J. Moss¹⁰⁹, R. Mount¹⁴³, E. Mountricha^{9,x}, S.V. Mouraviev⁹⁴, E.J.W. Moyse⁸⁴, F. Mueller^{58a}, J. Mueller¹²³, K. Mueller²⁰, T.A. Müller⁹⁸, T. Mueller⁸¹, D. Muenstermann²⁹, Y. Munwes¹⁵³, W.J. Murray¹²⁹, I. Mussche¹⁰⁵, E. Musto^{102a,102b}, A.G. Myagkov¹²⁸, M. Myska¹²⁵, J. Nadal¹¹, K. Nagai¹⁶⁰, K. Nagano⁶⁵, A. Nagarkar¹⁰⁹, Y. Nagasaka⁵⁹, M. Nagel⁹⁹, A.M. Nairz²⁹, Y. Nakahama²⁹, K. Nakamura¹⁵⁵, T. Nakamura¹⁵⁵, I. Nakano¹¹⁰, G. Nanava²⁰, A. Napier¹⁶¹, R. Narayan^{58b}, M. Nash^{77,c}, T. Nattermann²⁰, T. Naumann⁴¹, G. Navarro¹⁶², H.A. Neal⁸⁷, P.Yu. Nechaeva⁹⁴, T.J. Neep⁸², A. Negri^{119a,119b}, G. Negri²⁹, S. Nektarijevic⁴⁹, A. Nelson¹⁶³, T.K. Nelson¹⁴³, S. Nemecek¹²⁵, P. Nemethy¹⁰⁸, A.A. Nepomuceno^{23a}, M. Nessi^{29,y}, M.S. Neubauer¹⁶⁵, A. Neusiedl⁸¹, R.M. Neves¹⁰⁸, P. Nevski²⁴, P.R. Newman¹⁷, V. Nguyen Thi Hong¹³⁶, R.B. Nickerson¹¹⁸, R. Nicolaidou¹³⁶, L. Nicolas¹³⁹, B. Nicquevert²⁹, F. Niedercorn¹¹⁵, J. Nielsen¹³⁷, N. Nikiforou³⁴, A. Nikiforov¹⁵, V. Nikolaenko¹²⁸, I. Nikolic-Audit⁷⁸, K. Nikolics⁴⁹, K. Nikolopoulos²⁴, H. Nilsen⁴⁸, P. Nilsson⁷, Y. Ninomiya¹⁵⁵, A. Nisati^{132a}, T. Nishiyama⁶⁶, R. Nisius⁹⁹, L. Nodulman⁵, M. Nomachi¹¹⁶, I. Nomidis¹⁵⁴, M. Nordberg²⁹, P.R. Norton¹²⁹, J. Novakova¹²⁶, M. Nozaki⁶⁵, L. Nozka¹¹³, I.M. Nugent^{159a}, A.-E. Nuncio-Quiroz²⁰, G. Nunes Hanninger⁸⁶, T. Nunnemann⁹⁸, E. Nurse⁷⁷, B.J. O'Brien⁴⁵, S.W. O'Neale^{17,*}, D.C. O'Neil¹⁴², V. O'Shea⁵³, L.B. Oakes⁹⁸, F.G. Oakham^{28,d}, H. Oberlack⁹⁹, J. Ocariz⁷⁸, A. Ochi⁶⁶, S. Oda¹⁵⁵, S. Odaka⁶⁵, J. Odier⁸³, H. Ogren⁶⁰,

A. Oh⁸², S.H. Oh⁴⁴, C.C. Ohm^{146a,146b}, T. Ohshima¹⁰¹, S. Okada⁶⁶, H. Okawa¹⁶³, Y. Okumura¹⁰¹, T. Okuyama¹⁵⁵, A. Olariu^{25a}, A.G. Olchevski⁶⁴, S.A. Olivares Pino^{31a}, M. Oliveira^{124a,h}, D. Oliveira Damazio²⁴, E. Oliver Garcia¹⁶⁷, D. Olivito¹²⁰, A. Olszewski³⁸, J. Olszowska³⁸, A. Onofre^{124a,z}, P.U.E. Onyisi³⁰, C.J. Oram^{159a}, M.J. Oreglia³⁰, Y. Oren¹⁵³, D. Orestano^{134a,134b}, N. Orlando^{72a,72b}, I. Orlov¹⁰⁷, C. Oropeza Barrera⁵³, R.S. Orr¹⁵⁸, B. Osculati^{50a,50b}, R. Ospanov¹²⁰, C. Osuna¹¹, G. Otero y Garzon²⁶, J.P. Ottersbach¹⁰⁵, M. Ouchrif^{135d}, E.A. Ouellette¹⁶⁹, F. Ould-Saada¹¹⁷, A. Ouraou¹³⁶, Q. Ouyang^{32a}, A. Ovcharova¹⁴, M. Owen⁸², S. Owen¹³⁹, V.E. Ozcan^{18a}, N. Ozturk⁷, A. Pacheco Pages¹¹, C. Padilla Aranda¹¹, S. Pagan Griso¹⁴, E. Paganis¹³⁹, F. Paige²⁴, P. Pais⁸⁴, K. Pajchel¹¹⁷, G. Palacino^{159b}, C.P. Paleari⁶, S. Palestini²⁹, D. Pallin³³, A. Palma^{124a}, J.D. Palmer¹⁷, Y.B. Pan¹⁷³, E. Panagiotopoulou⁹, N. Panikashvili⁸⁷, S. Panitkin²⁴, D. Pantea^{25a}, A. Papadelis^{146a}, Th.D. Papadopoulos⁹, A. Paramonov⁵, D. Paredes Hernandez³³, W. Park^{24,aa}, M.A. Parker²⁷, F. Parodi^{50a,50b}, J.A. Parsons³⁴, U. Parzefall⁴⁸, S. Pashapour⁵⁴, E. Pasqualucci^{132a}, S. Passaggio^{50a}, A. Passeri^{134a}, F. Pastore^{134a,134b}, Fr. Pastore⁷⁶, G. Pásztor^{49,ab}, S. Pataraiia¹⁷⁵, N. Patel¹⁵⁰, J.R. Pater⁸², S. Patricelli^{102a,102b}, T. Pauly²⁹, M. Pecsý^{144a}, M.I. Pedraza Morales¹⁷³, S.V. Peleganchuk¹⁰⁷, D. Pelikan¹⁶⁶, H. Peng^{32b}, B. Penning³⁰, A. Penson³⁴, J. Penwell⁶⁰, M. Perantoni^{23a}, K. Perez^{34,ac}, T. Perez Cavalcanti⁴¹, E. Perez Codina^{159a}, M.T. Pérez García-Estañ¹⁶⁷, V. Perez Reale³⁴, L. Perini^{89a,89b}, H. Pernegger²⁹, R. Perrino^{72a}, P. Perrodo⁴, S. Persebe^{3a}, V.D. Peshekhonov⁶⁴, K. Peters²⁹, B.A. Petersen²⁹, J. Petersen²⁹, T.C. Petersen³⁵, E. Petit⁴, A. Petridis¹⁵⁴, C. Petridou¹⁵⁴, E. Petrolu^{132a}, F. Petrucci^{134a,134b}, D. Petschull⁴¹, M. Petteni¹⁴², R. Pezoa^{31b}, A. Phan⁸⁶, P.W. Phillips¹²⁹, G. Piacquadio²⁹, A. Picazio⁴⁹, E. Piccaro⁷⁵, M. Piccinini^{19a,19b}, S.M. Piec⁴¹, R. Piegaiia²⁶, D.T. Pignotti¹⁰⁹, J.E. Pilcher³⁰, A.D. Pilkington⁸², J. Pina^{124a,b}, M. Pinamonti^{164a,164c}, A. Pinder¹¹⁸, J.L. Pinfold², B. Pinto^{124a}, C. Pizio^{89a,89b}, M. Plamondon¹⁶⁹, M.-A. Pleier²⁴, E. Plotnikova⁶⁴, A. Poblaguev²⁴, S. Poddar^{58a}, F. Podlyski³³, L. Poggioli¹¹⁵, T. Poghosyan²⁰, M. Pohl⁴⁹, F. Polci⁵⁵, G. Polesello^{119a}, A. Policicchio^{36a,36b}, A. Polini^{19a}, J. Poll⁷⁵, V. Polychronakos²⁴, D.M. Pomarede¹³⁶, D. Pomeroy²², K. Pommès²⁹, L. Pontecorvo^{132a}, B.G. Pope⁸⁸, G.A. Popeneciu^{25a}, D.S. Popovic^{12a}, A. Poppleton²⁹, X. Portell Bueso²⁹, G.E. Pospelov⁹⁹, S. Pospisil¹²⁷, I.N. Potrap⁹⁹, C.J. Potter¹⁴⁹, C.T. Potter¹¹⁴, G. Poulard²⁹, J. Poveda¹⁷³, V. Pozdnyakov⁶⁴, R. Prabhu⁷⁷, P. Pralavorio⁸³, A. Pranko¹⁴, S. Prasad²⁹, R. Pravahan²⁴, S. Prell⁶³, K. Pretzl¹⁶, D. Price⁶⁰, J. Price⁷³, L.E. Price⁵, D. Prieur¹²³, M. Primavera^{72a}, K. Prokofiev¹⁰⁸, F. Prokoshin^{31b}, S. Protopopescu²⁴, J. Proudfoot⁵, X. Prudent⁴³, M. Przybycien³⁷, H. Przysiezniak⁴, S. Psoroulas²⁰, E. Ptacek¹¹⁴, E. Pueschel⁸⁴, J. Purdham⁸⁷, M. Purohit^{24,aa}, P. Puzo¹¹⁵, Y. Pylypchenko⁶², J. Qian⁸⁷, Z. Qin⁴¹, A. Quadt⁵⁴, D.R. Quarrie¹⁴, W.B. Quayle¹⁷³, F. Quinonez^{31a}, M. Raas¹⁰⁴, V. Radescu⁴¹, P. Radloff¹¹⁴, T. Rador^{18a}, F. Ragusa^{89a,89b}, G. Rahal¹⁷⁸, A.M. Rahimi¹⁰⁹, D. Rahm²⁴, S. Rajagopalan²⁴, M. Rammensee⁴⁸, M. Rammes¹⁴¹, A.S. Randle-Conde³⁹, K. Randrianarivony²⁸, F. Rauscher⁹⁸, T.C. Rave⁴⁸, M. Raymond²⁹, A.L. Read¹¹⁷, D.M. Rebutzi^{119a,119b}, A. Redelbach¹⁷⁴, G. Redlinger²⁴, R. Reece¹²⁰, K. Reeves⁴⁰, E. Reinherz-Aronis¹⁵³, A. Reinsch¹¹⁴, I. Reisinger⁴², C. Rembser²⁹, Z.L. Ren¹⁵¹, A. Renaud¹¹⁵, M. Rescigno^{132a}, S. Resconi^{89a}, B. Resende¹³⁶, P. Reznicek⁹⁸, R. Rezvani¹⁵⁸, R. Richter⁹⁹, E. Richter-

Was^{4,ad}, M. Ridel⁷⁸, M. Rijpstra¹⁰⁵, M. Rijssenbeek¹⁴⁸, A. Rimoldi^{119a,119b}, L. Rinaldi^{19a}, R.R. Rios³⁹, I. Riu¹¹, G. Rivoltella^{89a,89b}, F. Rizatdinova¹¹², E. Rizvi⁷⁵, S.H. Robertson^{85,j}, A. Robichaud-Veronneau¹¹⁸, D. Robinson²⁷, J.E.M. Robinson⁷⁷, A. Robson⁵³, J.G. Rocha de Lima¹⁰⁶, C. Roda^{122a,122b}, D. Roda Dos Santos²⁹, D. Rodriguez¹⁶², A. Roe⁵⁴, S. Roe²⁹, O. Røhne¹¹⁷, S. Rolli¹⁶¹, A. Romaniouk⁹⁶, M. Romano^{19a,19b}, G. Romeo²⁶, E. Romero Adam¹⁶⁷, L. Roos⁷⁸, E. Ros¹⁶⁷, S. Rosati^{132a}, K. Rosbach⁴⁹, A. Rose¹⁴⁹, M. Rose⁷⁶, G.A. Rosenbaum¹⁵⁸, E.I. Rosenberg⁶³, P.L. Rosendahl¹³, O. Rosenthal¹⁴¹, L. Rossetlet⁴⁹, V. Rossetti¹¹, E. Rossi^{132a,132b}, L.P. Rossi^{50a}, M. Rotaru^{25a}, I. Roth¹⁷², J. Rothberg¹³⁸, D. Rousseau¹¹⁵, C.R. Royon¹³⁶, A. Rozanov⁸³, Y. Rozen¹⁵², X. Ruan^{32a,ae}, F. Rubbo¹¹, I. Rubinskiy⁴¹, B. Ruckert⁹⁸, N. Ruckstuhl¹⁰⁵, V.I. Rud⁹⁷, C. Rudolph⁴³, G. Rudolph⁶¹, F. Rühr⁶, F. Ruggieri^{134a,134b}, A. Ruiz-Martinez⁶³, L. Rumyantsev⁶⁴, K. Runge⁴⁸, Z. Rurikova⁴⁸, N.A. Rusakovich⁶⁴, J.P. Rutherford⁶, C. Ruwiedel¹⁴, P. Ruzicka¹²⁵, Y.F. Ryabov¹²¹, P. Ryan⁸⁸, M. Rybar¹²⁶, G. Rybkin¹¹⁵, N.C. Ryder¹¹⁸, A.F. Saavedra¹⁵⁰, I. Sadeh¹⁵³, H.F-W. Sadrozinski¹³⁷, R. Sadykov⁶⁴, F. Safai Tehrani^{132a}, H. Sakamoto¹⁵⁵, G. Salamanna⁷⁵, A. Salamon^{133a}, M. Saleem¹¹¹, D. Salek²⁹, D. Salihagic⁹⁹, A. Salnikov¹⁴³, J. Salt¹⁶⁷, B.M. Salvachua Ferrando⁵, D. Salvatore^{36a,36b}, F. Salvatore¹⁴⁹, A. Salvucci¹⁰⁴, A. Salzburger²⁹, D. Sampsonidis¹⁵⁴, B.H. Samset¹¹⁷, A. Sanchez^{102a,102b}, V. Sanchez Martinez¹⁶⁷, H. Sandaker¹³, H.G. Sander⁸¹, M.P. Sanders⁹⁸, M. Sandhoff¹⁷⁵, T. Sandoval²⁷, C. Sandoval¹⁶², R. Sandstroem⁹⁹, D.P.C. Sankey¹²⁹, A. Sansoni⁴⁷, C. Santamarina Rios⁸⁵, C. Santoni³³, R. Santonico^{133a,133b}, H. Santos^{124a}, J.G. Saraiva^{124a}, T. Sarangi¹⁷³, E. Sarkisyan-Grinbaum⁷, F. Sarri^{122a,122b}, G. Sartisohn¹⁷⁵, O. Sasaki⁶⁵, N. Sasao⁶⁷, I. Satsounkevitch⁹⁰, G. Sauvage⁴, E. Sauvan⁴, J.B. Sauvan¹¹⁵, P. Savard^{158,d}, V. Savinov¹²³, D.O. Savu²⁹, L. Sawyer^{24,l}, D.H. Saxon⁵³, J. Saxon¹²⁰, C. Sbarra^{19a}, A. Sbrizzi^{19a,19b}, O. Scallon⁹³, D.A. Scannicchio¹⁶³, M. Scarcella¹⁵⁰, J. Schaarschmidt¹¹⁵, P. Schacht⁹⁹, D. Schaefer¹²⁰, U. Schäfer⁸¹, S. Schaepe²⁰, S. Schaetzel^{58b}, A.C. Schaffer¹¹⁵, D. Schaile⁹⁸, R.D. Schamberger¹⁴⁸, A.G. Schamov¹⁰⁷, V. Scharf^{58a}, V.A. Schegelsky¹²¹, D. Scheirich⁸⁷, M. Schernau¹⁶³, M.I. Scherzer³⁴, C. Schiavi^{50a,50b}, J. Schieck⁹⁸, M. Schioppa^{36a,36b}, S. Schlenker²⁹, E. Schmidt⁴⁸, K. Schmieden²⁰, C. Schmitt⁸¹, S. Schmitt^{58b}, M. Schmitz²⁰, A. Schöning^{58b}, M. Schott²⁹, D. Schouten^{159a}, J. Schovancova¹²⁵, M. Schram⁸⁵, C. Schroeder⁸¹, N. Schroer^{58c}, M.J. Schultens²⁰, J. Schultes¹⁷⁵, H.-C. Schultz-Coulon^{58a}, H. Schulz¹⁵, J.W. Schumacher²⁰, M. Schumacher⁴⁸, B.A. Schumm¹³⁷, Ph. Schune¹³⁶, C. Schwanenberger⁸², A. Schwartzman¹⁴³, Ph. Schwemling⁷⁸, R. Schwienhorst⁸⁸, R. Schwierz⁴³, J. Schwindling¹³⁶, T. Schwindt²⁰, M. Schwoerer⁴, G. Sciolla²², W.G. Scott¹²⁹, J. Searcy¹¹⁴, G. Sedov⁴¹, E. Sedykh¹²¹, S.C. Seidel¹⁰³, A. Seiden¹³⁷, F. Seifert⁴³, J.M. Seixas^{23a}, G. Sekhniaidze^{102a}, S.J. Sekula³⁹, K.E. Selbach⁴⁵, D.M. Seliverstov¹²¹, B. Sellden^{146a}, G. Sellers⁷³, M. Seman^{144b}, N. Semprini-Cesari^{19a,19b}, C. Serfon⁹⁸, L. Serin¹¹⁵, L. Serkin⁵⁴, R. Seuster⁹⁹, H. Severini¹¹¹, A. Sfyrla²⁹, E. Shabalina⁵⁴, M. Shamim¹¹⁴, L.Y. Shan^{32a}, J.T. Shank²¹, Q.T. Shao⁸⁶, M. Shapiro¹⁴, P.B. Shatalov⁹⁵, K. Shaw^{164a,164c}, D. Sherman¹⁷⁶, P. Sherwood⁷⁷, A. Shibata¹⁰⁸, H. Shichi¹⁰¹, S. Shimizu²⁹, M. Shimojima¹⁰⁰, T. Shin⁵⁶, M. Shiyakova⁶⁴, A. Shmeleva⁹⁴, M.J. Shochet³⁰, D. Short¹¹⁸, S. Shrestha⁶³, E. Shulga⁹⁶, M.A. Shupe⁶, P. Sicho¹²⁵, A. Sidoti^{132a}, F. Siegert⁴⁸, Dj. Sijacki^{12a}, O. Silbert¹⁷², J. Silva^{124a}, Y. Silver¹⁵³,

D. Silverstein¹⁴³, S.B. Silverstein^{146a}, V. Simak¹²⁷, O. Simard¹³⁶, Lj. Simic^{12a}, S. Simion¹¹⁵, B. Simmons⁷⁷, R. Simoniello^{89a,89b}, M. Simonyan³⁵, P. Sinervo¹⁵⁸, N.B. Sinev¹¹⁴, V. Sipica¹⁴¹, G. Siragusa¹⁷⁴, A. Sircar²⁴, A.N. Sisakyan⁶⁴, S.Yu. Sivoklov⁹⁷, J. Sjölin^{146a,146b}, T.B. Sjursen¹³, L.A. Skinnari¹⁴, H.P. Skottowe⁵⁷, K. Skovpen¹⁰⁷, P. Skubic¹¹¹, M. Slater¹⁷, T. Slavicek¹²⁷, K. Sliwa¹⁶¹, V. Smakhtin¹⁷², B.H. Smart⁴⁵, S.Yu. Smirnov⁹⁶, Y. Smirnov⁹⁶, L.N. Smirnova⁹⁷, O. Smirnova⁷⁹, B.C. Smith⁵⁷, D. Smith¹⁴³, K.M. Smith⁵³, M. Smizanska⁷¹, K. Smolek¹²⁷, A.A. Snesarev⁹⁴, S.W. Snow⁸², J. Snow¹¹¹, S. Snyder²⁴, R. Sobie^{169,j}, J. Sodomka¹²⁷, A. Soffer¹⁵³, C.A. Solans¹⁶⁷, M. Solar¹²⁷, J. Solc¹²⁷, E. Soldatov⁹⁶, U. Soldevila¹⁶⁷, E. Solfaroli Camillocci^{132a,132b}, A.A. Solodkov¹²⁸, O.V. Solovyanov¹²⁸, N. Soni², V. Sopko¹²⁷, B. Sopko¹²⁷, M. Sosebee⁷, R. Soualah^{164a,164c}, A. Soukharev¹⁰⁷, S. Spagnolo^{72a,72b}, F. Spanò⁷⁶, R. Spighi^{19a}, G. Spigo²⁹, F. Spila^{132a,132b}, R. Spiwox²⁹, M. Spousta¹²⁶, T. Spreitzer¹⁵⁸, B. Spurlock⁷, R.D. St. Denis⁵³, J. Stahlman¹²⁰, R. Stamen^{58a}, E. Stanecka³⁸, R.W. Stanek⁵, C. Stanescu^{134a}, M. Stanescu-Bellu⁴¹, S. Stapnes¹¹⁷, E.A. Starchenko¹²⁸, J. Stark⁵⁵, P. Staroba¹²⁵, P. Starovoitov⁴¹, A. Staude⁹⁸, P. Stavina^{144a}, G. Steele⁵³, P. Steinbach⁴³, P. Steinberg²⁴, I. Stekl¹²⁷, B. Stelzer¹⁴², H.J. Stelzer⁸⁸, O. Stelzer-Chilton^{159a}, H. Stenzel⁵², S. Stern⁹⁹, G.A. Stewart²⁹, J.A. Stillings²⁰, M.C. Stockton⁸⁵, K. Stoerig⁴⁸, G. Stoica^{25a}, S. Stonjek⁹⁹, P. Strachota¹²⁶, A.R. Stradling⁷, A. Straessner⁴³, J. Strandberg¹⁴⁷, S. Strandberg^{146a,146b}, A. Strandlie¹¹⁷, M. Strang¹⁰⁹, E. Strauss¹⁴³, M. Strauss¹¹¹, P. Strizenec^{144b}, R. Ströhmer¹⁷⁴, D.M. Strom¹¹⁴, J.A. Strong^{76,*}, R. Stroynowski³⁹, J. Strube¹²⁹, B. Stugu¹³, I. Stumer^{24,*}, J. Stupak¹⁴⁸, P. Sturm¹⁷⁵, N.A. Styles⁴¹, D.A. Soh^{151,u}, D. Su¹⁴³, HS. Subramania², A. Succurro¹¹, Y. Sugaya¹¹⁶, C. Suhr¹⁰⁶, K. Suita⁶⁶, M. Suk¹²⁶, V.V. Sulin⁹⁴, S. Sultansoy^{3d}, T. Sumida⁶⁷, X. Sun⁵⁵, J.E. Sundermann⁴⁸, K. Suruliz¹³⁹, G. Susinno^{36a,36b}, M.R. Sutton¹⁴⁹, Y. Suzuki⁶⁵, Y. Suzuki⁶⁶, M. Svatos¹²⁵, S. Swedish¹⁶⁸, I. Sykora^{144a}, T. Sykora¹²⁶, J. Sánchez¹⁶⁷, D. Ta¹⁰⁵, K. Tackmann⁴¹, A. Taffard¹⁶³, R. Tafirout^{159a}, N. Taiblum¹⁵³, Y. Takahashi¹⁰¹, H. Takai²⁴, R. Takashima⁶⁸, H. Takeda⁶⁶, T. Takeshita¹⁴⁰, Y. Takubo⁶⁵, M. Talby⁸³, A. Talyshev^{107,f}, M.C. Tamsett²⁴, J. Tanaka¹⁵⁵, R. Tanaka¹¹⁵, S. Tanaka¹³¹, S. Tanaka⁶⁵, A.J. Tanasijczuk¹⁴², K. Tani⁶⁶, N. Tannoury⁸³, S. Tapprogge⁸¹, D. Tardif¹⁵⁸, S. Tarem¹⁵², F. Tarrade²⁸, G.F. Tartarelli^{89a}, P. Tas¹²⁶, M. Tasevsky¹²⁵, E. Tassi^{36a,36b}, M. Tatarkhanov¹⁴, Y. Tayalati^{135d}, C. Taylor⁷⁷, F.E. Taylor⁹², G.N. Taylor⁸⁶, W. Taylor^{159b}, M. Teinturier¹¹⁵, M. Teixeira Dias Castanheira⁷⁵, P. Teixeira-Dias⁷⁶, K.K. Temming⁴⁸, H. Ten Kate²⁹, P.K. Teng¹⁵¹, S. Terada⁶⁵, K. Terashi¹⁵⁵, J. Terron⁸⁰, M. Testa⁴⁷, R.J. Teuscher^{158,j}, J. Therhaag²⁰, T. Theveneaux-Pelzer⁷⁸, M. Thioye¹⁷⁶, S. Thoma⁴⁸, J.P. Thomas¹⁷, E.N. Thompson³⁴, P.D. Thompson¹⁷, P.D. Thompson¹⁵⁸, A.S. Thompson⁵³, L.A. Thomsen³⁵, E. Thomson¹²⁰, M. Thomson²⁷, R.P. Thun⁸⁷, F. Tian³⁴, M.J. Tibbetts¹⁴, T. Tic¹²⁵, V.O. Tikhomirov⁹⁴, Y.A. Tikhonov^{107,f}, S. Timoshenko⁹⁶, P. Tipton¹⁷⁶, F.J. Tique Aires Viegas²⁹, S. Tisserant⁸³, T. Todorov⁴, S. Todorova-Nova¹⁶¹, B. Toggerson¹⁶³, J. Tojo⁶⁹, S. Tokár^{144a}, K. Tokunaga⁶⁶, K. Tokushuku⁶⁵, K. Tollefson⁸⁸, M. Tomoto¹⁰¹, L. Tompkins³⁰, K. Toms¹⁰³, A. Tonoyan¹³, C. Topfel¹⁶, N.D. Topilin⁶⁴, I. Torchiani²⁹, E. Torrence¹¹⁴, H. Torres⁷⁸, E. Torró Pastor¹⁶⁷, J. Toth^{83,ab}, F. Touchard⁸³, D.R. Tovey¹³⁹, T. Trefzger¹⁷⁴, L. Tremblet²⁹, A. Tricoli²⁹, I.M. Trigger^{159a}, S. Trincaz-Duvoid⁷⁸, M.F. Tripiana⁷⁰, W. Trischuk¹⁵⁸,

B. Trocmé⁵⁵, C. Troncon^{89a}, M. Trottier-McDonald¹⁴², M. Trzebinski³⁸, A. Trzupek³⁸, C. Tsarouchas²⁹, J.C-L. Tseng¹¹⁸, M. Tsiakiris¹⁰⁵, P.V. Tsiareshka⁹⁰, D. Tsionou^{4,af}, G. Tsipolitis⁹, V. Tsiskaridze⁴⁸, E.G. Tskhadadze^{51a}, I.I. Tsukerman⁹⁵, V. Tsulaia¹⁴, J.-W. Tsung²⁰, S. Tsuno⁶⁵, D. Tsybychev¹⁴⁸, A. Tua¹³⁹, A. Tudorache^{25a}, V. Tudorache^{25a}, J.M. Tuggle³⁰, M. Turala³⁸, D. Turecek¹²⁷, I. Turk Cakir^{3e}, E. Turlay¹⁰⁵, R. Turra^{89a,89b}, P.M. Tuts³⁴, A. Tykhonov⁷⁴, M. Tylmad^{146a,146b}, M. Tyndel¹²⁹, G. Tzanakos⁸, K. Uchida²⁰, I. Ueda¹⁵⁵, R. Ueno²⁸, M. Ugland¹³, M. Uhlenbrock²⁰, M. Uhrmacher⁵⁴, F. Ukegawa¹⁶⁰, G. Unal²⁹, A. Undrus²⁴, G. Unel¹⁶³, Y. Unno⁶⁵, D. Urbaniec³⁴, G. Usai⁷, M. Uslenghi^{119a,119b}, L. Vacavant⁸³, V. Vacek¹²⁷, B. Vachon⁸⁵, S. Vahsen¹⁴, J. Valenta¹²⁵, P. Valente^{132a}, S. Valentinetti^{19a,19b}, S. Valkar¹²⁶, E. Valladolid Gallego¹⁶⁷, S. Vallecorsa¹⁵², J.A. Valls Ferrer¹⁶⁷, H. van der Graaf¹⁰⁵, E. van der Kraaij¹⁰⁵, R. Van Der Leeuw¹⁰⁵, E. van der Poel¹⁰⁵, D. van der Ster²⁹, N. van Eldik⁸⁴, P. van Gemmeren⁵, I. van Vulpen¹⁰⁵, M. Vanadia⁹⁹, W. Vandelli²⁹, A. Vaniachine⁵, P. Vankov⁴¹, F. Vannucci⁷⁸, R. Vari^{132a}, T. Varol⁸⁴, D. Varouchas¹⁴, A. Vartapetian⁷, K.E. Varvell¹⁵⁰, V.I. Vassilakopoulos⁵⁶, F. Vazeille³³, T. Vazquez Schroeder⁵⁴, G. Vegni^{89a,89b}, J.J. Veillet¹¹⁵, F. Veloso^{124a}, R. Veness²⁹, S. Veneziano^{132a}, A. Ventura^{72a,72b}, D. Ventura⁸⁴, M. Venturi⁴⁸, N. Venturi¹⁵⁸, V. Vercesi^{119a}, M. Verducci¹³⁸, W. Verkerke¹⁰⁵, J.C. Vermeulen¹⁰⁵, A. Vest⁴³, M.C. Vetterli^{142,d}, I. Vichou¹⁶⁵, T. Vickey^{145b,ag}, O.E. Vickey Boeriu^{145b}, G.H.A. Viehhauser¹¹⁸, S. Viel¹⁶⁸, M. Villa^{19a,19b}, M. Villaplana Perez¹⁶⁷, E. Vilucchi⁴⁷, M.G. Vincter²⁸, E. Vinek²⁹, V.B. Vinogradov⁶⁴, M. Virchaux^{136,*}, J. Virzi¹⁴, O. Vitells¹⁷², M. Viti⁴¹, I. Vivarelli⁴⁸, F. Vives Vaque², S. Vlachos⁹, D. Vladoiu⁹⁸, M. Vlasak¹²⁷, A. Vogel²⁰, P. Vokac¹²⁷, G. Volpi⁴⁷, M. Volpi⁸⁶, G. Volpini^{89a}, H. von der Schmitt⁹⁹, J. von Loeben⁹⁹, H. von Radziewski⁴⁸, E. von Toerne²⁰, V. Vorobel¹²⁶, V. Vorwerk¹¹, M. Vos¹⁶⁷, R. Voss²⁹, T.T. Voss¹⁷⁵, J.H. Vossebeld⁷³, N. Vranjes¹³⁶, M. Vranjes Milosavljevic¹⁰⁵, V. Vrba¹²⁵, M. Vreeswijk¹⁰⁵, T. Vu Anh⁴⁸, R. Vuillermet²⁹, I. Vukotic¹¹⁵, W. Wagner¹⁷⁵, P. Wagner¹²⁰, H. Wahlen¹⁷⁵, S. Wahrmund⁴³, J. Wakabayashi¹⁰¹, S. Walch⁸⁷, J. Walder⁷¹, R. Walker⁹⁸, W. Walkowiak¹⁴¹, R. Wall¹⁷⁶, P. Waller⁷³, C. Wang⁴⁴, H. Wang¹⁷³, H. Wang^{32b,ah}, J. Wang¹⁵¹, J. Wang⁵⁵, J.C. Wang¹³⁸, R. Wang¹⁰³, S.M. Wang¹⁵¹, T. Wang²⁰, A. Warburton⁸⁵, C.P. Ward²⁷, M. Warsinsky⁴⁸, A. Washbrook⁴⁵, C. Wasicki⁴¹, P.M. Watkins¹⁷, A.T. Watson¹⁷, I.J. Watson¹⁵⁰, M.F. Watson¹⁷, G. Watts¹³⁸, S. Watts⁸², A.T. Waugh¹⁵⁰, B.M. Waugh⁷⁷, M. Weber¹²⁹, M.S. Weber¹⁶, P. Weber⁵⁴, A.R. Weidberg¹¹⁸, P. Weigell⁹⁹, J. Weingarten⁵⁴, C. Weiser⁴⁸, H. Wellenstein²², P.S. Wells²⁹, T. Wenaus²⁴, D. Wendland¹⁵, Z. Weng^{151,u}, T. Wengler²⁹, S. Wenig²⁹, N. Wermes²⁰, M. Werner⁴⁸, P. Werner²⁹, M. Werth¹⁶³, M. Wessels^{58a}, J. Wetter¹⁶¹, C. Weydert⁵⁵, K. Whalen²⁸, S.J. Wheeler-Ellis¹⁶³, A. White⁷, M.J. White⁸⁶, S. White^{122a,122b}, S.R. Whitehead¹¹⁸, D. Whiteson¹⁶³, D. Whittington⁶⁰, F. Wicke¹¹⁵, D. Wicke¹⁷⁵, F.J. Wickens¹²⁹, W. Wiedenmann¹⁷³, M. Wielers¹²⁹, P. Wienemann²⁰, C. Wiglesworth⁷⁵, L.A.M. Wiik-Fuchs⁴⁸, P.A. Wijeratne⁷⁷, A. Wildauer¹⁶⁷, M.A. Wildt^{41,q}, I. Wilhelm¹²⁶, H.G. Wilkens²⁹, J.Z. Will⁹⁸, E. Williams³⁴, H.H. Williams¹²⁰, W. Willis³⁴, S. Willocq⁸⁴, J.A. Wilson¹⁷, M.G. Wilson¹⁴³, A. Wilson⁸⁷, I. Wingerter-Seez⁴, S. Winkelmann⁴⁸, F. Winklmeier²⁹, M. Wittgen¹⁴³, M.W. Wolter³⁸, H. Wolters^{124a,h}, W.C. Wong⁴⁰, G. Wooden⁸⁷, B.K. Wosiek³⁸, J. Wotschack²⁹, M.J. Woudstra⁸⁴, K.W. Wozniak³⁸, K. Wraight⁵³, C. Wright⁵³, M. Wright⁵³, B. Wrona⁷³, S.L. Wu¹⁷³,

X. Wu⁴⁹, Y. Wu^{32b,ai}, E. Wulf³⁴, B.M. Wynne⁴⁵, S. Xella³⁵, M. Xiao¹³⁶, S. Xie⁴⁸, C. Xu^{32b,x}, D. Xu¹³⁹, B. Yabsley¹⁵⁰, S. Yacoob^{145b}, M. Yamada⁶⁵, H. Yamaguchi¹⁵⁵, A. Yamamoto⁶⁵, K. Yamamoto⁶³, S. Yamamoto¹⁵⁵, T. Yamamura¹⁵⁵, T. Yamanaka¹⁵⁵, J. Yamaoka⁴⁴, T. Yamazaki¹⁵⁵, Y. Yamazaki⁶⁶, Z. Yan²¹, H. Yang⁸⁷, U.K. Yang⁸², Y. Yang⁶⁰, Z. Yang^{146a,146b}, S. Yanush⁹¹, L. Yao^{32a}, Y. Yao¹⁴, Y. Yasu⁶⁵, G.V. Ybels Smit¹³⁰, J. Ye³⁹, S. Ye²⁴, M. Yilmaz^{3c}, R. Yoosoofmiya¹²³, K. Yorita¹⁷¹, R. Yoshida⁵, C. Young¹⁴³, C.J. Young¹¹⁸, S. Youssef²¹, D. Yu²⁴, J. Yu⁷, J. Yu¹¹², L. Yuan⁶⁶, A. Yurkewicz¹⁰⁶, B. Zabinski³⁸, R. Zaidan⁶², A.M. Zaitsev¹²⁸, Z. Zajacova²⁹, L. Zanello^{132a,132b}, A. Zaytsev¹⁰⁷, C. Zeitnitz¹⁷⁵, M. Zeller¹⁷⁶, M. Zeman¹²⁵, A. Zemla³⁸, C. Zender²⁰, O. Zenin¹²⁸, T. Ženiš^{144a}, Z. Zinonos^{122a,122b}, S. Zenz¹⁴, D. Zerwas¹¹⁵, G. Zevi della Porta⁵⁷, Z. Zhan^{32d}, D. Zhang^{32b,ah}, H. Zhang⁸⁸, J. Zhang⁵, X. Zhang^{32d}, Z. Zhang¹¹⁵, L. Zhao¹⁰⁸, T. Zhao¹³⁸, Z. Zhao^{32b}, A. Zhemchugov⁶⁴, J. Zhong¹¹⁸, B. Zhou⁸⁷, N. Zhou¹⁶³, Y. Zhou¹⁵¹, C.G. Zhu^{32d}, H. Zhu⁴¹, J. Zhu⁸⁷, Y. Zhu^{32b}, X. Zhuang⁹⁸, V. Zhuravlov⁹⁹, D. Zieminska⁶⁰, R. Zimmermann²⁰, S. Zimmermann²⁰, S. Zimmermann⁴⁸, M. Ziolkowski¹⁴¹, R. Zitoun⁴, L. Živković³⁴, V.V. Zmouchko^{128,*}, G. Zobernig¹⁷³, A. Zoccoli^{19a,19b}, M. zur Nedden¹⁵, V. Zutshi¹⁰⁶ and L. Zwalinski²⁹.

- 1: University at Albany, Albany NY, United States of America
- 2: Department of Physics, University of Alberta, Edmonton AB, Canada
- 3: ^(a)Department of Physics, Ankara University, Ankara; ^(b)Department of Physics, Dumlupinar University, Kutahya; ^(c)Department of Physics, Gazi University, Ankara; ^(d)Division of Physics, TOBB University of Economics and Technology, Ankara; ^(e)Turkish Atomic Energy Authority, Ankara, Turkey
- 4: LAPP, CNRS/IN2P3 and Université de Savoie, Annecy-le-Vieux, France
- 5: High Energy Physics Division, Argonne National Laboratory, Argonne IL, United States of America
- 6: Department of Physics, University of Arizona, Tucson AZ, United States of America
- 7: Department of Physics, The University of Texas at Arlington, Arlington TX, United States of America
- 8: Physics Department, University of Athens, Athens, Greece
- 9: Physics Department, National Technical University of Athens, Zografou, Greece
- 10: Institute of Physics, Azerbaijan Academy of Sciences, Baku, Azerbaijan
- 11: Institut de Física d'Altes Energies and Departament de Física de la Universitat Autònoma de Barcelona and ICREA, Barcelona, Spain
- 12: ^(a)Institute of Physics, University of Belgrade, Belgrade; ^(b)Vinca Institute of Nuclear Sciences, University of Belgrade, Belgrade, Serbia
- 13: Department for Physics and Technology, University of Bergen, Bergen, Norway
- 14: Physics Division, Lawrence Berkeley National Laboratory and University of California, Berkeley CA, United States of America
- 15: Department of Physics, Humboldt University, Berlin, Germany
- 16: Albert Einstein Center for Fundamental Physics and Laboratory for High Energy Physics, University of Bern, Bern, Switzerland

- 17: School of Physics and Astronomy, University of Birmingham, Birmingham, United Kingdom
- 18: ^(a)Department of Physics, Bogazici University, Istanbul; ^(b)Division of Physics, Dogus University, Istanbul; ^(c)Department of Physics Engineering, Gaziantep University, Gaziantep; ^(d)Department of Physics, Istanbul Technical University, Istanbul, Turkey
- 19: ^(a)INFN Sezione di Bologna; ^(b)Dipartimento di Fisica, Università di Bologna, Bologna, Italy
- 20: Physikalisches Institut, University of Bonn, Bonn, Germany
- 21: Department of Physics, Boston University, Boston MA, United States of America
- 22: Department of Physics, Brandeis University, Waltham MA, United States of America
- 23: ^(a)Universidade Federal do Rio De Janeiro COPPE/EE/IF, Rio de Janeiro; ^(b)Federal University of Juiz de Fora (UFJF), Juiz de Fora; ^(c)Federal University of Sao Joao del Rei (UFSJ), Sao Joao del Rei; ^(d)Instituto de Fisica, Universidade de Sao Paulo, Sao Paulo, Brazil
- 24: Physics Department, Brookhaven National Laboratory, Upton NY, United States of America
- 25: ^(a)National Institute of Physics and Nuclear Engineering, Bucharest; ^(b)University Politehnica Bucharest, Bucharest; ^(c)West University in Timisoara, Timisoara, Romania
- 26: Departamento de Física, Universidad de Buenos Aires, Buenos Aires, Argentina
- 27: Cavendish Laboratory, University of Cambridge, Cambridge, United Kingdom
- 28: Department of Physics, Carleton University, Ottawa ON, Canada
- 29: CERN, Geneva, Switzerland
- 30: Enrico Fermi Institute, University of Chicago, Chicago IL, United States of America
- 31: ^(a)Departamento de Física, Pontificia Universidad Católica de Chile, Santiago; ^(b)Departamento de Física, Universidad Técnica Federico Santa María, Valparaíso, Chile
- 32: ^(a)Institute of High Energy Physics, Chinese Academy of Sciences, Beijing; ^(b)Department of Modern Physics, University of Science and Technology of China, Anhui; ^(c)Department of Physics, Nanjing University, Jiangsu; ^(d)School of Physics, Shandong University, Shandong, China
- 33: Laboratoire de Physique Corpusculaire, Clermont Université and Université Blaise Pascal and CNRS/IN2P3, Aubiere Cedex, France
- 34: Nevis Laboratory, Columbia University, Irvington NY, United States of America
- 35: Niels Bohr Institute, University of Copenhagen, Kobenhavn, Denmark
- 36: ^(a)INFN Gruppo Collegato di Cosenza; ^(b)Dipartimento di Fisica, Università della Calabria, Arcavata di Rende, Italy
- 37: AGH University of Science and Technology, Faculty of Physics and Applied Computer Science, Krakow, Poland
- 38: The Henryk Niewodniczanski Institute of Nuclear Physics, Polish Academy of Sciences, Krakow, Poland
- 39: Physics Department, Southern Methodist University, Dallas TX, United States of America

- 40: Physics Department, University of Texas at Dallas, Richardson TX, United States of America
- 41: DESY, Hamburg and Zeuthen, Germany
- 42: Institut für Experimentelle Physik IV, Technische Universität Dortmund, Dortmund, Germany
- 43: Institut für Kern- und Teilchenphysik, Technical University Dresden, Dresden, Germany
- 44: Department of Physics, Duke University, Durham NC, United States of America
- 45: SUPA - School of Physics and Astronomy, University of Edinburgh, Edinburgh, United Kingdom
- 46: Fachhochschule Wiener Neustadt, Johannes Gutenbergstrasse 3 2700 Wiener Neustadt, Austria
- 47: INFN Laboratori Nazionali di Frascati, Frascati, Italy
- 48: Fakultät für Mathematik und Physik, Albert-Ludwigs-Universität, Freiburg i.Br., Germany
- 49: Section de Physique, Université de Genève, Geneva, Switzerland
- 50: ^(a)INFN Sezione di Genova; ^(b)Dipartimento di Fisica, Università di Genova, Genova, Italy
- 51: ^(a)E.Andronikashvili Institute of Physics, Tbilisi State University, Tbilisi; ^(b)High Energy Physics Institute, Tbilisi State University, Tbilisi, Georgia
- 52: II Physikalisches Institut, Justus-Liebig-Universität Giessen, Giessen, Germany
- 53: SUPA - School of Physics and Astronomy, University of Glasgow, Glasgow, United Kingdom
- 54: II Physikalisches Institut, Georg-August-Universität, Göttingen, Germany
- 55: Laboratoire de Physique Subatomique et de Cosmologie, Université Joseph Fourier and CNRS/IN2P3 and Institut National Polytechnique de Grenoble, Grenoble, France
- 56: Department of Physics, Hampton University, Hampton VA, United States of America
- 57: Laboratory for Particle Physics and Cosmology, Harvard University, Cambridge MA, United States of America
- 58: ^(a)Kirchhoff-Institut für Physik, Ruprecht-Karls-Universität Heidelberg, Heidelberg; ^(b)Physikalisches Institut, Ruprecht-Karls-Universität Heidelberg, Heidelberg; ^(c)ZITI Institut für technische Informatik, Ruprecht-Karls-Universität Heidelberg, Mannheim, Germany
- 59: Faculty of Applied Information Science, Hiroshima Institute of Technology, Hiroshima, Japan
- 60: Department of Physics, Indiana University, Bloomington IN, United States of America
- 61: Institut für Astro- und Teilchenphysik, Leopold-Franzens-Universität, Innsbruck, Austria
- 62: University of Iowa, Iowa City IA, United States of America
- 63: Department of Physics and Astronomy, Iowa State University, Ames IA, United States of America

- 64: Joint Institute for Nuclear Research, JINR Dubna, Dubna, Russia
- 65: KEK, High Energy Accelerator Research Organization, Tsukuba, Japan
- 66: Graduate School of Science, Kobe University, Kobe, Japan
- 67: Faculty of Science, Kyoto University, Kyoto, Japan
- 68: Kyoto University of Education, Kyoto, Japan
- 69: Department of Physics, Kyushu University, Fukuoka, Japan
- 70: Instituto de Física La Plata, Universidad Nacional de La Plata and CONICET, La Plata, Argentina
- 71: Physics Department, Lancaster University, Lancaster, United Kingdom
- 72: ^(a)INFN Sezione di Lecce; ^(b)Dipartimento di Matematica e Fisica, Università del Salento, Lecce, Italy
- 73: Oliver Lodge Laboratory, University of Liverpool, Liverpool, United Kingdom
- 74: Department of Physics, Jožef Stefan Institute and University of Ljubljana, Ljubljana, Slovenia
- 75: School of Physics and Astronomy, Queen Mary University of London, London, United Kingdom
- 76: Department of Physics, Royal Holloway University of London, Surrey, United Kingdom
- 77: Department of Physics and Astronomy, University College London, London, United Kingdom
- 78: Laboratoire de Physique Nucléaire et de Hautes Energies, UPMC and Université Paris-Diderot and CNRS/IN2P3, Paris, France
- 79: Fysiska institutionen, Lunds universitet, Lund, Sweden
- 80: Departamento de Física Teórica C-15, Universidad Autónoma de Madrid, Madrid, Spain
- 81: Institut für Physik, Universität Mainz, Mainz, Germany
- 82: School of Physics and Astronomy, University of Manchester, Manchester, United Kingdom
- 83: CPPM, Aix-Marseille Université and CNRS/IN2P3, Marseille, France
- 84: Department of Physics, University of Massachusetts, Amherst MA, United States of America
- 85: Department of Physics, McGill University, Montreal QC, Canada
- 86: School of Physics, University of Melbourne, Victoria, Australia
- 87: Department of Physics, The University of Michigan, Ann Arbor MI, United States of America
- 88: Department of Physics and Astronomy, Michigan State University, East Lansing MI, United States of America
- 89: ^(a)INFN Sezione di Milano; ^(b)Dipartimento di Fisica, Università di Milano, Milano, Italy
- 90: B.I. Stepanov Institute of Physics, National Academy of Sciences of Belarus, Minsk, Republic of Belarus
- 91: National Scientific and Educational Centre for Particle and High Energy Physics, Minsk, Republic of Belarus

- 92: Department of Physics, Massachusetts Institute of Technology, Cambridge MA, United States of America
- 93: Group of Particle Physics, University of Montreal, Montreal QC, Canada
- 94: P.N. Lebedev Institute of Physics, Academy of Sciences, Moscow, Russia
- 95: Institute for Theoretical and Experimental Physics (ITEP), Moscow, Russia
- 96: Moscow Engineering and Physics Institute (MEPhI), Moscow, Russia
- 97: Skobeltsyn Institute of Nuclear Physics, Lomonosov Moscow State University, Moscow, Russia
- 98: Fakultät für Physik, Ludwig-Maximilians-Universität München, München, Germany
- 99: Max-Planck-Institut für Physik (Werner-Heisenberg-Institut), München, Germany
- 100: Nagasaki Institute of Applied Science, Nagasaki, Japan
- 101: Graduate School of Science, Nagoya University, Nagoya, Japan
- 102: ^(a)INFN Sezione di Napoli; ^(b)Dipartimento di Scienze Fisiche, Università di Napoli, Napoli, Italy
- 103: Department of Physics and Astronomy, University of New Mexico, Albuquerque NM, United States of America
- 104: Institute for Mathematics, Astrophysics and Particle Physics, Radboud University Nijmegen/Nikhef, Nijmegen, Netherlands
- 105: Nikhef National Institute for Subatomic Physics and University of Amsterdam, Amsterdam, Netherlands
- 106: Department of Physics, Northern Illinois University, DeKalb IL, United States of America
- 107: Budker Institute of Nuclear Physics, SB RAS, Novosibirsk, Russia
- 108: Department of Physics, New York University, New York NY, United States of America
- 109: Ohio State University, Columbus OH, United States of America
- 110: Faculty of Science, Okayama University, Okayama, Japan
- 111: Homer L. Dodge Department of Physics and Astronomy, University of Oklahoma, Norman OK, United States of America
- 112: Department of Physics, Oklahoma State University, Stillwater OK, United States of America
- 113: Palacký University, RCPTM, Olomouc, Czech Republic
- 114: Center for High Energy Physics, University of Oregon, Eugene OR, United States of America
- 115: LAL, Univ. Paris-Sud and CNRS/IN2P3, Orsay, France
- 116: Graduate School of Science, Osaka University, Osaka, Japan
- 117: Department of Physics, University of Oslo, Oslo, Norway
- 118: Department of Physics, Oxford University, Oxford, United Kingdom
- 119: ^(a)INFN Sezione di Pavia; ^(b)Dipartimento di Fisica, Università di Pavia, Pavia, Italy
- 120: Department of Physics, University of Pennsylvania, Philadelphia PA, United States of America
- 121: Petersburg Nuclear Physics Institute, Gatchina, Russia
- 122: ^(a)INFN Sezione di Pisa; ^(b)Dipartimento di Fisica E. Fermi, Università di Pisa, Pisa, Italy

- 123: Department of Physics and Astronomy, University of Pittsburgh, Pittsburgh PA, United States of America
- 124: ^(a)Laboratorio de Instrumentacao e Fisica Experimental de Particulas - LIP, Lisboa, Portugal; ^(b)Departamento de Fisica Teorica y del Cosmos and CAFPE, Universidad de Granada, Granada, Spain
- 125: Institute of Physics, Academy of Sciences of the Czech Republic, Praha, Czech Republic
- 126: Faculty of Mathematics and Physics, Charles University in Prague, Praha, Czech Republic
- 127: Czech Technical University in Prague, Praha, Czech Republic
- 128: State Research Center Institute for High Energy Physics, Protvino, Russia
- 129: Particle Physics Department, Rutherford Appleton Laboratory, Didcot, United Kingdom
- 130: Physics Department, University of Regina, Regina SK, Canada
- 131: Ritsumeikan University, Kusatsu, Shiga, Japan
- 132: ^(a)INFN Sezione di Roma I; ^(b)Dipartimento di Fisica, Università La Sapienza, Roma, Italy
- 133: ^(a)INFN Sezione di Roma Tor Vergata; ^(b)Dipartimento di Fisica, Università di Roma Tor Vergata, Roma, Italy
- 134: ^(a)INFN Sezione di Roma Tre; ^(b)Dipartimento di Fisica, Università Roma Tre, Roma, Italy
- 135: ^(a)Faculté des Sciences Ain Chock, Réseau Universitaire de Physique des Hautes Energies - Université Hassan II, Casablanca; ^(b)Centre National de l'Energie des Sciences Techniques Nucleaires, Rabat; ^(c)Faculté des Sciences Semlalia, Université Cadi Ayyad, LPHEA-Marrakech; ^(d)Faculté des Sciences, Université Mohamed Premier and LPTPM, Oujda; ^(e)Faculty of sciences, Mohammed V-Agdal University, Rabat, Morocco
- 136: DSM/IRFU (Institut de Recherches sur les Lois Fondamentales de l'Univers), CEA Saclay (Commissariat a l'Energie Atomique), Gif-sur-Yvette, France
- 137: Santa Cruz Institute for Particle Physics, University of California Santa Cruz, Santa Cruz CA, United States of America
- 138: Department of Physics, University of Washington, Seattle WA, United States of America
- 139: Department of Physics and Astronomy, University of Sheffield, Sheffield, United Kingdom
- 140: Department of Physics, Shinshu University, Nagano, Japan
- 141: Fachbereich Physik, Universität Siegen, Siegen, Germany
- 142: Department of Physics, Simon Fraser University, Burnaby BC, Canada
- 143: SLAC National Accelerator Laboratory, Stanford CA, United States of America
- 144: ^(a)Faculty of Mathematics, Physics & Informatics, Comenius University, Bratislava; ^(b)Department of Subnuclear Physics, Institute of Experimental Physics of the Slovak Academy of Sciences, Kosice, Slovak Republic

- 145: ^(a)Department of Physics, University of Johannesburg, Johannesburg; ^(b)School of Physics, University of the Witwatersrand, Johannesburg, South Africa
- 146: ^(a)Department of Physics, Stockholm University; ^(b)The Oskar Klein Centre, Stockholm, Sweden
- 147: Physics Department, Royal Institute of Technology, Stockholm, Sweden
- 148: Departments of Physics & Astronomy and Chemistry, Stony Brook University, Stony Brook NY, United States of America
- 149: Department of Physics and Astronomy, University of Sussex, Brighton, United Kingdom
- 150: School of Physics, University of Sydney, Sydney, Australia
- 151: Institute of Physics, Academia Sinica, Taipei, Taiwan
- 152: Department of Physics, Technion: Israel Inst. of Technology, Haifa, Israel
- 153: Raymond and Beverly Sackler School of Physics and Astronomy, Tel Aviv University, Tel Aviv, Israel
- 154: Department of Physics, Aristotle University of Thessaloniki, Thessaloniki, Greece
- 155: International Center for Elementary Particle Physics and Department of Physics, The University of Tokyo, Tokyo, Japan
- 156: Graduate School of Science and Technology, Tokyo Metropolitan University, Tokyo, Japan
- 157: Department of Physics, Tokyo Institute of Technology, Tokyo, Japan
- 158: Department of Physics, University of Toronto, Toronto ON, Canada
- 159: ^(a)TRIUMF, Vancouver BC; ^(b)Department of Physics and Astronomy, York University, Toronto ON, Canada
- 160: Institute of Pure and Applied Sciences, University of Tsukuba, 1-1-1 Tennodai, Tsukuba, Ibaraki 305-8571, Japan
- 161: Science and Technology Center, Tufts University, Medford MA, United States of America
- 162: Centro de Investigaciones, Universidad Antonio Narino, Bogota, Colombia
- 163: Department of Physics and Astronomy, University of California Irvine, Irvine CA, United States of America
- 164: ^(a)INFN Gruppo Collegato di Udine; ^(b)ICTP, Trieste; ^(c)Dipartimento di Chimica, Fisica e Ambiente, Università di Udine, Udine, Italy
- 165: Department of Physics, University of Illinois, Urbana IL, United States of America
- 166: Department of Physics and Astronomy, University of Uppsala, Uppsala, Sweden
- 167: Instituto de Física Corpuscular (IFIC) and Departamento de Física Atómica, Molecular y Nuclear and Departamento de Ingeniería Electrónica and Instituto de Microelectrónica de Barcelona (IMB-CNM), University of Valencia and CSIC, Valencia, Spain
- 168: Department of Physics, University of British Columbia, Vancouver BC, Canada
- 169: Department of Physics and Astronomy, University of Victoria, Victoria BC, Canada
- 170: Department of Physics, University of Warwick, Coventry, United Kingdom
- 171: Waseda University, Tokyo, Japan
- 172: Department of Particle Physics, The Weizmann Institute of Science, Rehovot, Israel

- 173: Department of Physics, University of Wisconsin, Madison WI, United States of America
- 174: Fakultät für Physik und Astronomie, Julius-Maximilians-Universität, Würzburg, Germany
- 175: Fachbereich C Physik, Bergische Universität Wuppertal, Wuppertal, Germany
- 176: Department of Physics, Yale University, New Haven CT, United States of America
- 177: Yerevan Physics Institute, Yerevan, Armenia
- 178: Domaine scientifique de la Doua, Centre de Calcul CNRS/IN2P3, Villeurbanne Cedex, France
- a*: Also at Laboratório de Instrumentação e Física Experimental de Partículas - LIP, Lisboa, Portugal
- b*: Also at Faculdade de Ciências and CFNUL, Universidade de Lisboa, Lisboa, Portugal
- c*: Also at Particle Physics Department, Rutherford Appleton Laboratory, Didcot, United Kingdom
- d*: Also at TRIUMF, Vancouver BC, Canada
- e*: Also at Department of Physics, California State University, Fresno CA, United States of America
- f*: Also at Novosibirsk State University, Novosibirsk, Russia
- g*: Also at Fermilab, Batavia IL, United States of America
- h*: Also at Department of Physics, University of Coimbra, Coimbra, Portugal
- i*: Also at Università di Napoli Parthenope, Napoli, Italy
- j*: Also at Institute of Particle Physics (IPP), Canada
- k*: Also at Department of Physics, Middle East Technical University, Ankara, Turkey
- l*: Also at Louisiana Tech University, Ruston LA, United States of America
- m*: Also at Department of Physics and Astronomy, University College London, London, United Kingdom
- n*: Also at Group of Particle Physics, University of Montreal, Montreal QC, Canada
- o*: Also at Department of Physics, University of Cape Town, Cape Town, South Africa
- p*: Also at Institute of Physics, Azerbaijan Academy of Sciences, Baku, Azerbaijan
- q*: Also at Institut für Experimentalphysik, Universität Hamburg, Hamburg, Germany
- r*: Also at Manhattan College, New York NY, United States of America
- s*: Also at School of Physics, Shandong University, Shandong, China
- t*: Also at CPPM, Aix-Marseille Université and CNRS/IN2P3, Marseille, France
- u*: Also at School of Physics and Engineering, Sun Yat-sen University, Guanzhou, China
- v*: Also at Academia Sinica Grid Computing, Institute of Physics, Academia Sinica, Taipei, Taiwan
- w*: Also at Dipartimento di Fisica, Università La Sapienza, Roma, Italy
- x*: Also at DSM/IRFU (Institut de Recherches sur les Lois Fondamentales de l'Univers), CEA Saclay (Commissariat à l'Énergie Atomique), Gif-sur-Yvette, France
- y*: Also at Section de Physique, Université de Genève, Geneva, Switzerland
- z*: Also at Departamento de Física, Universidade de Minho, Braga, Portugal
- aa*: Also at Department of Physics and Astronomy, University of South Carolina, Columbia SC, United States of America

- ab*: Also at Institute for Particle and Nuclear Physics, Wigner Research Centre for Physics, Budapest, Hungary
- ac*: Also at California Institute of Technology, Pasadena CA, United States of America
- ad*: Also at Institute of Physics, Jagiellonian University, Krakow, Poland
- ae*: Also at LAL, Univ. Paris-Sud and CNRS/IN2P3, Orsay, France
- af*: Also at Department of Physics and Astronomy, University of Sheffield, Sheffield, United Kingdom
- ag*: Also at Department of Physics, Oxford University, Oxford, United Kingdom
- ah*: Also at Institute of Physics, Academia Sinica, Taipei, Taiwan
- ai*: Also at Department of Physics, The University of Michigan, Ann Arbor MI, United States of America
- *: Deceased